



Serial: NPD-NRC-2009-006

10CFR52.79

February 27, 2009

U.S. Nuclear Regulatory Commission
Attention: Document Control Desk
Washington, D.C. 20555-0001

**SHEARON HARRIS NUCLEAR POWER PLANT, UNITS 2 AND 3
DOCKET NOS. 52-022 AND 52-023
RESPONSE TO REQUEST FOR ADDITIONAL INFORMATION LETTER NO. 020 RELATED TO
STABILITY OF SUBSURFACE MATERIALS AND FOUNDATIONS – SUPPLEMENT 2**

- References:
1. Letter from Manny Comar (NRC) to James Scarola (PEC), dated September 26, 2008, "Request for Additional Information Letter No. 020 Related to SRP Section 02.05.04 for the Harris Units 2 and 3 Combined License Application"
 2. Letter from Garry D. Miller (PEC) to U.S. Nuclear Regulatory Commission, dated November 24, 2008, "Response to Request for Additional information Letter No. 020 Related to Stability of Subsurface Materials and Foundations"; Serial NPD-NRC-2008-51
 3. Letter from Garry D. Miller (PEC) to U.S. Nuclear Regulatory Commission, dated December 3, 2008, "Response to Request for Additional information Letter No. 020 Related to Stability of Subsurface Materials and Foundations – Supplement 1"; Serial NPD-NRC-2008-082

Ladies and Gentlemen:

Progress Energy Carolinas, Inc. (PEC) hereby submits a supplemental response to the Nuclear Regulatory Commission's (NRC) request for additional information provided in Reference 1. A partial response to the NRC request was provided in References 2 and 3.

Enclosure 1 to this letter provides supplemental information and completes our response to NRC's Request for Additional Information Letter No. 020. Enclosure 1 also identifies changes that will be made in a future revision of the Shearon Harris Nuclear Power Plant Units 2 and 3 (HAR) application. Enclosure 2 lists attachments provided with this response.

If you have any further questions, or need additional information, please contact Bob Kitchen at (919) 546-6992, or me at (919) 546-6107.

I declare under penalty of perjury that the foregoing is true and correct.

Executed on February 27, 2009.

Sincerely,



Garry D. Miller
General Manager
Nuclear Plant Development

Enclosures/Attachments

cc : U.S. NRC Director, Office of New Reactors/NRLPO
U.S. NRC Office of Nuclear Reactor Regulation/NRLPO
U.S. NRC Region II, Regional Administrator
U.S. NRC Resident Inspector, SHNPP Unit 1
Mr. Manny Comar, U.S. NRC Project Manager

**Shearon Harris Nuclear Power Plant Units 2 and 3
Supplement 2 to Response to NRC Request for Additional Information Letter No. 020
Related to SRP Section 02.05.04 for the Combined License Application,
dated September 26, 2008**

<u>NRC RAI #</u>	<u>Progress Energy RAI #</u>	<u>Progress Energy Response</u>
02.05.04-3	H-0117 & H-0389	NPD-NRC-2008-082 dated 12/3/08, with supplemental information enclosed
02.05.04-4	H-0118	NPD-NRC-2008-051 dated 11/24/08
02.05.04-5	H-0119	NPD-NRC-2008-051 dated 11/24/08
02.05.04-6	H-0120	NPD-NRC-2008-082 dated 12/3/08
02.05.04-7	H-0121	NPD-NRC-2008-051 dated 11/24/08
02.05.04-8	H-0122 & H-0390	NPD-NRC-2008-082 dated 12/3/08, with supplemental information enclosed
02.05.04-9	H-0123	NPD-NRC-2008-051 dated 11/24/08
02.05.04-10	H-0124	NPD-NRC-2008-051 dated 11/24/08
02.05.04-11	H-0125 & H-0443	NPD-NRC-2008-051 dated 11/24/08, with supplemental information enclosed
02.05.04-12	H-0126 & H-0444	NPD-NRC-2008-051 dated 11/24/08, with supplemental information enclosed
02.05.04-13	H-0127 & H-0391	NPD-NRC-2008-082 dated 12/3/08, with supplemental information enclosed
02.05.04-14	H-0128 & H-0392	NPD-NRC-2008-082 dated 12/3/08, with supplemental information enclosed

NRC Letter No.: HAR-NRC-LTR-020

NRC Letter Date: September 26, 2008

NRC Review of Final Safety Analysis Report

NRC RAI #: 02.05.04-3

Text of NRC RAI:

Technical Memorandum (NPD-NRC-2008-014), "Supplemental Liquefaction Evaluation – HAR Site Backfill and Native Soil"; Section 1.0 "Site Specific Ground Motion Parameters, CSR, and FS Criteria", states that a site factor of 1.2 was assigned to "convert the PGA at top of sound rock to a ground surface motion" based on IBC 2006.

Please clarify whether IBC 2006 or a site-specific response was used for the liquefaction analysis. The report indicates a factor of 1.2 was applied, however, the plant grade peak ground acceleration could not be found in the report. Please provide the value of the peak ground acceleration at the surface, a sample liquefaction calculation using SPT N-values, and document how you determined N equals 30 for the sand backfill.

PGN RAI ID #: H-0389

PGN Response to NRC RAI:

PEC response was provided in Reference 3 (PGN-RAI ID # H-0117). Supplemental information is provided in response to NRC RAI #02.05.04-8 (PGN-RAI ID # H-0390) included in this letter.

Associated HAR COL Application Revisions:

See NRC RAI #02.05.04-8 (PGN-RAI ID # H-0390) for proposed COLA revisions.

Attachments/Enclosures:

None.

NRC Letter No.: HAR-NRC-LTR-020

NRC Letter Date: September 26, 2008

NRC Review of Final Safety Analysis Report

NRC RAI #: 02.05.04-8

Text of NRC RAI:

FSAR 2.5.4.10.4, "Lateral Earth Pressures", states "The resulting at-rest lateral earth pressure profiles for the two soil backfill types are presented for representative sidewall elevations in Table 2.5.4-217."

Please provide all the lateral earth pressures required by AP1000 DCD, Tier 2, and Section 2.5.4.6.7. Provide sample calculations showing the assumptions and methods used in the calculation of the dynamic active and passive lateral earth pressures.

PGN RAI ID #: H-0390

Initial PGN Response to NRC RAI (provided in Reference 3 as H-0122):

AP1000 DCD, Tier 2, Section 2.5.4.6.7 states:

"Earth Pressures – The combined License applicant will describe the design for static and dynamic lateral earth pressures and hydrostatic groundwater pressures acting on plant safety-related facilities using soil parameters as evaluated in previous subsections."

As discussed in the response to NRC RAI # 02.05.04-12, the HAR FSAR was prepared with consideration that the nuclear island design did not take credit for lateral support from backfill materials (reference PEC letter to NRC dated November 24, 2008, Serial NPD-NRC-2008-051). Therefore, only the at-rest static lateral earth pressures were calculated and presented in the HAR FSAR. Dynamic active and passive earth pressures were not calculated nor presented in the HAR FSAR.

Information now available from WEC indicates that under some loading conditions, passive lateral forces must be considered in the nuclear island design, including the dynamic passive forces considered in the sliding resistance evaluations. Based on this more recent documentation, modified lateral earth pressure evaluations are currently being prepared to assess and document the magnitude of seismic active and passive earth pressures, as well as the need to rely on passive earth pressures for sliding stability. These evaluations include the following:

- Determination of dynamic active and passive forces related to various native rock, soil, and backfill conditions on the different sides of the HAR 2 and HAR 3 nuclear islands. The rock embedment depth will be considered in this determination;
- Additional determination of the effects of surcharge loads from adjacent structures on the nuclear island lateral earth pressures (see response to NRC RAI # 02.05.04-11; reference PEC letter to NRC dated November 24, 2008, Serial NPD-NRC-2008-051); and
- Comparison of the calculated dynamic active and passive forces with values considered in the nuclear island sliding evaluation and documentation of adequate factor of safety against sliding.

If necessary based on the above evaluations, revised or additional backfill engineering property requirements may be proposed in a revised FSAR Table 2.5.4-212. A technical memorandum will be prepared to document the methodology used for these evaluations, including sample calculations. Associated proposed revisions to the HAR FSAR will also be presented in the technical memorandum. It is anticipated that this technical memorandum will be provided to the NRC for review by January 2009.

Supplemental PGN Response to NRC RAI:

Technical Memorandum 338884-TMEM-081, Rev. 0 (TMEM-081), titled "Supplemental Evaluations of Sliding Resistance, Bearing Capacity, and Dynamic Passive and Active Lateral Forces Associated with Rock Discontinuities at the HAR Nuclear Islands" is attached.

TMEM-081 provides the supplemental information referenced in the initial response to this RAI. One of the references cited in TMEM-081 is WEC Report TR-85 (APP-GLR-GW-044), Rev. 0, specifically Figure 2.4-2 of that report. This figure is used to establish distribution of bearing pressure under the nuclear island. Rev. 1 of Report TR-85 has now been submitted by WEC, and no longer includes an equivalent representation of bearing pressure distribution. PGN is currently requesting a replacement figure from WEC and does not anticipate the conclusions to be significantly impacted.

Associated HAR COL Application Revisions:

The following changes will be made to HAR FSAR Chapter 2 in a future revision:

1. Revise FSAR Subsection 2.5.4.5.3 to read:

"2.5.4.5.3 Properties of Backfill Adjacent to Nuclear Islands

Backfill materials will be placed adjacent to the sidewalls of the nuclear islands. The backfill material adjacent to the nuclear island sidewalls will consist of concrete fill and compacted backfill. Concrete fill will be placed as backfill between rock excavations and the sidewalls of the nuclear islands below elevation 69.3 m (227.5 ft), and at other select locations. Backfill soil will be placed above the concrete fill. Anticipated properties of the concrete fill and soil backfill are summarized herein. Final selection and testing of soil backfill sources will be performed prior to construction.

The characteristics and use of the materials described in Table 2.5.4-212 are as follows:

- Concrete fill. This will consist of structural (mass) concrete with no reinforcing. The concrete fill is required below elevation 69.3 m (227.5 ft) to transfer passive resistance from adjacent rock to prevent sliding during the SSE. The concrete fill will have a minimum unconfined compressive strength of 363 kPa (2500 psi). Concrete fill will also be used above elevation 69.3 m (227.5 ft) at other select locations such as under the Annex Building foundations. It will also be used to fill and smooth excavated rock surfaces below the nuclear island subgrade.
- Compacted granular fill. This will consist of granular, well-graded sand and gravel. This material may include select material segregated during excavation of on-site sandy or gravelly soils, but will more likely be imported from off-site sources. Sources of off-site granular fill are plentiful in the site vicinity. Compacted granular fill

may be placed between excavation sideslopes and the sidewalls of the nuclear islands above elevation 69.3 m (227.5 ft.).

- Compacted cohesive fill. This will consist of cohesive soils present at the HAR 2 and HAR 3 sites, with USCS classifications of lean clay (CL), silt (ML), clayey sand (SC), or silty sand (SM). Compacted cohesive fill may be placed between excavation sideslopes and the sidewalls of the nuclear islands above elevation 69.3 m (227.5 ft.), in areas where the backfill will not support overlying structures adjacent to the nuclear island.

Figures 2.5.4-211A, 2.5.4-211B, 2.5.4-212A, and 2.5.4-212B show the approximate planned limits of backfill adjacent to nuclear island structures at HAR 2 and HAR 3, respectively. Table 2.5.4-212 is a summary of the anticipated engineering properties for each type of backfill. The engineering properties listed in Table 2.5.4-212 will be included in the construction specifications. Backfill material sources, once identified, will be tested to demonstrate that they are consistent with the properties in Table 2.5.4-212. The development of the backfill specification, and associated testing and approval of backfill sources, will occur prior to construction. "

2. Revise FSAR Subsection 2.5.4.10.1 to read:

"2.5.4.10.1 Bearing Capacity

The allowable bearing pressures at the HAR nuclear island subgrades under static and dynamic loading conditions have been evaluated, as presented in this subsection. The resulting allowable bearing pressures exceed the bearing pressure requirements for the AP1000 nuclear islands, as listed in the DCD, and therefore satisfy safety requirements. Conservative methods and rock mass strength parameters were used in these analyses, and appropriate FS values for static and dynamic loading conditions were considered, as summarized in Subsection 2.5.4.10.1.3.

2.5.4.10.1.1 Bearing Capacity Analysis Methodology

The ultimate bearing capacities of the rock mass at the HAR 2 and HAR 3 nuclear island basemat subgrades was calculated for static and dynamic loading using multiple methods:

- The primary method was based on classic bearing capacity equations adopted for rock foundations (Reference 2.5.4-231).
- The second method involved the use of two simple empirical methods as a secondary check of the primary method results (Reference 2.5.4-232, Reference 2.5.4-233).
- The third method involved the use of the finite element modeling software package Plaxis as an alternate method to evaluate foundation stability based on rock mass strength conditions at HAR 2 and HAR 3, and to conservatively evaluate potential effects of thin soil intervals within rock at Borehole BPA-6 near the HAR 2 nuclear island.
- The final method involved an evaluation of dynamic bearing capacity provided by the specific oriented rock discontinuity sets at HAR 2 and HAR 3. This evaluation was based on the force equilibrium of rock and soil wedges under and adjacent to the Plant West sides of the nuclear islands.

Details of these methods are described in the following Subsections 2.5.4.10.1.1.1, 2.5.4.10.1.1.2, 2.5.4.10.1.1.3, and 2.5.4.10.1.1.4.

2.5.4.10.1.1.1 General Bearing Capacity Equation

The general bearing capacity equation is commonly used to calculate the ultimate bearing capacity under both static and dynamic loading conditions, as shown in Equation 2.5.4-1 (Reference 2.5.4-231):

$$q_{ult} = c(N_c C_c) + 0.5\gamma' B(N_\gamma C_\gamma) + \gamma' D N_q \quad (2.5.4-1)$$

In Equation 2.5.4-1, q_{ult} is the ultimate bearing capacity, c is the cohesion, $\gamma'D$ is the effective surcharge pressure at the foundation depth, γ' is the effective unit weight of foundation media, and B is the foundation width in the least direction. For foundations located below the groundwater elevation, such as occurs at the HAR sites, the effective unit weight of the foundation media is used. C_c and C_γ are shape correction factors to account for a rectangular footing. The factors N_c , N_q , and N_γ in the bearing capacity equation are based on empirical relationships with the foundation media strength properties (friction angle, ϕ), as follows:

$$N_c = 2N_\phi^{0.5}(N_\phi + 1) \quad (2.5.4-2)$$

$$N_\gamma = N_\phi^{0.5}(N_\phi^2 - 1) \quad (2.5.4-3)$$

$$N_q = N_\phi^2 \quad (2.5.4-4)$$

$$N_\phi = \tan^2\left(45 + \frac{\phi}{2}\right) \quad (2.5.4-5)$$

The local shear failure condition was also analyzed. For this condition, q_{ult} is calculated as in Equation 2.5.4-1, except that the third term " $\gamma'DN_q$ " is excluded, as follows:

$$q_{ult} = c(N_c C_c) + 0.5\gamma' B(N_\gamma C_\gamma) \quad (2.5.4-6)$$

By definition, ultimate bearing capacity calculated using the local shear failure condition is less than using the general condition, and is considered the controlling value of q_{ult} .

Use of the bearing capacity equations required determination of an apparent cohesion and effective friction angle for the rock mass. The strength of the rock mass was defined as a function of the intact rock strength and condition of discontinuities using the Hoek-Brown method (Reference 2.5.4-225). In this method, a set of strength parameters (c and ϕ) was calculated to represent the rock mass based on the intact rock UCS and condition of discontinuities, as represented by the geologic strength index (GSI). Conservative values of UCS and GSI were used for rock beneath the nuclear islands in this calculation, as described in Subsection 2.5.4.10.1.2.

Equation 2.5.4-6 and the Hoek-Brown strength parameters were used to calculate the ultimate bearing capacities under static and dynamic loads, as follows:

- The static ultimate bearing capacity was calculated using an equivalent foundation width B , representative of the width of the nuclear island basemat. Equivalent width B was reduced to approximately 37.8 m (124 ft.), from the maximum width of approximately 48.8 m (160 ft.) in the Plant east-west direction through the

containment structure, to account for the variable Plant east-west width of the nuclear island. The reduced width represented a weighed average of the variable width of the nuclear island.

- The method for calculating dynamic bearing capacity considered the overturning moment that would occur from the inertial response of the nuclear island during seismic loading, in addition to the vertical gravity load from the structure. The overturning moment was represented by an equivalent transient bearing pressure subgrade loading profile, as presented in Figure 2.4-2 of report APP-GW-GLR-044 (Reference 2.5.4-234). The critical loading profile has a peak load near the edge of the nuclear island basemat, which decreases rapidly with distance from the edge of the basemat. This loading profile was used in the dynamic bearing capacity analyses as follows:
 1. The asymmetrical load profile was converted to an equivalent vertical load and moment, and a corresponding load eccentricity (e) was calculated.
 2. The reduced effective foundation width ($B' = B - 2e$) was calculated, based on the eccentricity.
 3. The local bearing capacity equation (Equation 2.5.4-6) was then used to calculate the ultimate bearing capacity under static loading using the effective width, B' , rather than the total width of the island (Reference 2.5.4-231, Reference 2.5.4-235).

The allowable bearing pressure (P) was determined from the ultimate bearing capacity of the rock (q_{ult}) by dividing the ultimate bearing capacity by an appropriate FS, as in Equation 2.5.4-7:

$$P = q_{ult}/FS \quad (2.5.4-7)$$

Appropriate FS under static and dynamic loading are discussed in Subsection 2.5.4.10.1.3.

2.5.4.10.1.1.2 Empirical Methods

Two alternate empirical methods were used to confirm the results from the general bearing capacity method:

1. The first alternate method was presented in American Association of State Highway and Transportation Officials' (AASHTO) (Reference 2.5.4-233). This method estimates the bearing capacity of rock by modifying the UCS of intact rock using a reduction factor, which is correlated to the RQD of the rock mass. The most conservative scenario of assuming jointed or broken rock was considered in this calculation.
2. The second alternative was based on the Hoek-Brown rock strength criterion (Reference 2.5.4-232). The main inputs were the UCS of intact rock and the Hoek-Brown strength criterion constants, which were determined from the type and quality of rock.

Like the general bearing capacity evaluations, this approach considers the mass properties for the rock without specific reference to the location and orientation of discontinuities.

2.5.4.10.1.1.3 Two-Dimensional Finite Element Modeling

As a supplemental method, two-dimensional (2-D) finite-element modeling using the software package Plaxis version 8.5 was performed as an alternate calculation of the static

and dynamic (seismic) bearing capacity of the HAR 2 and HAR 3 nuclear islands. The modeling was also performed to conservatively evaluate the potential effects of thin soil intervals within rock at Borehole BPA-6 near the HAR 2 nuclear island. Two-dimensional models cut in the north-south direction ("Plant West" to "Plant East") at the HAR 2 and HAR 3 nuclear islands were developed. The resulting section represented a unit width strip through the structure.

In the 2-D models, the spatial variations of the subsurface stratigraphy, material properties, and pore pressure distribution, as well as the approximate excavation extents and backfill material properties, were considered. The stiffness of the below-grade structures (for example, the basemat and wall of the nuclear islands) was modeled using the elastic property and thickness of these structures. Because the above-grade structures were not considered in the 2-D models discussed herein, relatively rigid fixed-end anchors were used to laterally brace the top of the walls.

The following three cases were modeled to evaluate a range of subsurface conditions:

- **Case 1: HAR 2 Lower-Bound Properties.** The lower-bound material parameters of the rock below HAR 2 were used in this model, as described in Subsection 2.5.4.10.1.2.
- **Case 2: HAR 3 Lower-Bound Properties.** The lower-bound material parameters of the layered shallow and deep rock below HAR 3 were used in this model.
- **Case 3: Potential Influence of Borehole BPA-6 Conditions.** In this model, the HAR 2 lower-bound rock properties were assigned, except for inclusion of a 1.5-m- (5-ft.-) thick soil seam where it was encountered at Borehole BPA-6. This seam was assumed to dip to the south ("Plant East") towards the HAR 2 nuclear island, passing just under the bottom depth of Borehole BPA-7 and continuing along dip to under HAR 2. Two different strength values were considered for this seam (ϕ' of 33 degrees and 10 degrees) in different model runs to evaluate the sensitivity of bearing capacity to this seam.

To model static loading, a uniform bearing pressure of 0.43 MPa (8900 psf) was applied. To model dynamic conditions, the variable bearing pressure distribution shown on Figure 2.4-2 of report APP-GW-GLR-044 (Reference 2.5.4-234) was applied as a pseudo-static loading. The ϕ/c reduction procedure in Plaxis was utilized to calculate the FS under static and seismic loading conditions.

2.5.4.10.1.1.4 Oriented Rock Discontinuity Model

As a supplemental method, the FS against dynamic bearing loads along the Plant West sides of HAR 2 and HAR 3 were evaluated based on the specific orientations and engineering properties of the rock discontinuity sets present at the HAR sites. These analyses were performed to show that structure loads would not result in failure along discontinuities located beneath and adjacent to the nuclear island, as a supplement to the global bearing capacity analyses. The Plant West side was evaluated in this method because the peak site parameter for dynamic bearing demand (35 ksf) occurs at this location.

Bedding-oriented discontinuities (denoted discontinuity Set A herein) and high-angle joints (denoted discontinuity Set B herein) are oriented as summarized in Table 2.5.4-202. For these evaluations, the upper-bound estimate of the dip angle of bedding discontinuity Set A at HAR 3, based on the acoustic televiewer surveys (23.2 degrees from horizontal), was used to provide a conservatively low estimate of bearing capacity. In addition, approximately

vertical joint sets are present as summarized in Subsection 2.5.1 (denoted discontinuity Sets C and D herein), which strike roughly parallel to the HAR Plant North-South and East-West orthogonal axes, respectively. These discontinuity sets represent oriented planes of weakness relative to the strength of intact rock. Interface strength properties that represent these discontinuity sets are summarized in Subsection 2.5.4.10.1.2.2.

In this supplemental assessment of bearing stability, the force equilibrium of two rock and soil wedges under applied peak seismic bearing and lateral loads was calculated. The wedges were defined as follows:

- Wedge I represents rock underneath the Plant West side of the nuclear island, extending from the Plant West edge of the nuclear island to a distance B_1 from the Plant West edge under the nuclear island. The base of Wedge I is defined by discontinuity Set B, which dips down in the general Plant West direction. The Plant West side of Wedge I is vertical, located at the Plant West side of the nuclear island.
- Wedge II represents rock and soil adjacent and Plant West of Wedge I. This wedge resists lateral loads from Wedge I. The base of Wedge II is defined by discontinuity Set A, which dips down in the general Plant East direction. The Plant East edge of Wedge II is vertical, adjacent to Wedge I.
- The sidewalls of both wedges, and the interface between Wedge I and II, are represented by discontinuity Sets C and D. In this way, Wedges I and II are defined as rectangular prisms, which are each rectangular in plan view and triangular in profile. Wedges I and II are similar in orientation to Wedges 1 and 3 considered in the sliding evaluation described in Subsection 2.5.4.10.2, and as shown in Figure RAI 02.05.04-8-001. Both the true dips angles of discontinuity Sets A and B, and the apparent dips of these sets in the Plant East-West directions, were evaluated as separate cases for HAR 2 and HAR 3.

Forces acting on Wedges I and II were modeled as follows:

- The peak vertical load acting at any under the foundation over Wedge I (σ_{peak}) was assigned, and the corresponding average pressure acting over Wedge I within distance B_1 was calculated based on the dynamic bearing pressure distribution shown on Figure 2.4-2 of report APP-GW-GLR-044.
- A lateral inertial structure force was applied at the top of Wedge I. This force is proportional to the total nuclear island inertial sliding force under seismic loads ($F_{\text{lat.struct}}$) as defined in Subsection 2.5.4.10.2, multiplied by the fraction of the total nuclear island weight applied with distance B_1 , which is a function of σ_{peak} described above.
- Horizontal and vertical accelerations were also modeled for Wedges I and II rock and soil. These accelerations were conservatively assigned as the GMRS PGA values for HAR 3, as defined in Subsection 2.5.2. The directions of the horizontal and vertical rock and soil accelerations were specified in the direction that resulted in a conservative estimate of bearing capacity (Plant West direction and upwards, respectively).

The trial value of σ_{peak} was iterated until wedge force equilibrium was obtained for the corresponding trial value of B_1 . The corresponding FS_b was calculated as $\sigma_{\text{peak}} / \sigma_{\text{demand}}$ of 35 ksf. FS_b values were calculated for various distances B_1 , until the critical distance B_1 corresponding to the lowest overall FS_b was determined.

Four cases were evaluated, one each based on the true dip and apparent dip values at HAR 2 and HAR 3.

This approach required conservative simplifications, resulting in low estimates of the resulting FS_b . For example, the strike of the bedding features (discontinuity Set A) and high-angle joints (discontinuity Set B) are oriented at a skew of approximately 20 to 40 degrees from the nuclear island orthogonal axes and to the vertical joint Sets C and D. Based on this true configuration, as load is applied down- or up-dip along these dipping discontinuities, a high normal force will develop along at least one vertical joint interface (Sets C or D) that forms a "sidewall" of the loaded wedge. Due to the very tight nature of Sets C and D and high interface friction angle (see Subsection 2.5.4.10.1.2.2), a corresponding high frictional resistance will develop along this discontinuity. In the two-dimensional model, no such normal force increase is considered to develop on the vertical sidewalls – they are conservatively modeled as parallel to the direction of seismic loading (perpendicular to strike Sets A and B), and only at-rest normal forces are considered for the friction resistance along the vertical wedge sidewalls.

A secondary method by Landanyi and Roy, 1971 as presented in Wyllie 1999 (Reference 2.5.4-232), was also used to evaluate bearing capacity, as an order-of-magnitude confirmation of the oriented rock discontinuity evaluations described above.

2.5.4.10.1.2 Rock Mass and Rock Discontinuity Strength Parameters for Bearing Capacity Analyses

This subsection defines the rock mass strength parameters used in the general and finite element bearing capacity evaluations described in Subsections 2.5.4.10.1.1.1, 2.5.4.10.1.1.2, and 2.5.4.10.1.1.3, and the rock discontinuity strength parameters used in the oriented rock discontinuity bearing capacity evaluations described in Subsection 2.5.4.10.1.1.4.

2.5.4.10.1.2.1 Rock Mass Strength Parameters

Rock mass strength parameters were used to represent the global characteristics of the rock mass. In this approach the strength and quality of the rock is considered by defining reduced strength parameters for the rock mass rather than explicitly modeling strength along discontinuities. The rock mass strength parameters were selected for the bearing capacity evaluations described in Subsections 2.5.4.10.1.1.1, 2.5.4.10.1.1.2, and 2.5.4.10.1.1.3 using the following steps:

1. The mean and standard deviation of rock UCS were calculated from the laboratory UCS test results under and near each nuclear island. These test results are for samples collected within one foundation width B of the nuclear island basemat elevation. Table 2.5.4-206 summarizes the results.
2. The GSI was calculated for each rock core run at boreholes under and near each nuclear island. Statistics on the GSI (mean and standard deviation) for rock under each nuclear island subgrade elevation were then calculated to develop mean and lower-bound values, as summarized in Table 2.5.4-213.
3. "Mean" Hoek-Brown strength parameters were calculated for the rock mass (equivalent c and ϕ) using the average values of rock UCS and GSI for rock below the nuclear island subgrade elevations of 67.1 m (220 ft.) at HAR 2 and HAR 3.

4. "Lower-Bound" Hoek-Brown strength parameters were then calculated for the rock mass. Lower-bound values of rock UCS and GSI were selected as one standard deviation below the mean for rock below elevation 67.1 m (220 ft.). Subsection 2.5.4.10.1.3 describes the rationale for use of this criterion to select "lower-bound" values for analyses.
5. "Worst-Case" Hoek-Brown strength parameters were also calculated using the lowest UCS laboratory test result from any intact rock sample collected from below elevation 67.1 m (220 ft.), along with the lower-bound GSI. The lowest UCS test result is 9.57 MPa (1388 psi), encountered at BPA-6 at HAR 2.

Table 2.5.4-213 summarizes the various values of rock UCS and GSI and resulting Hoek-Brown strength parameters used for the bearing capacity analyses. The following trends in rock mass quality and strength are indicated by Table 2.5.4-213:

- The lower-bound UCS within one foundation width below the nuclear island under HAR 2 is higher than at HAR 3.
- Rock at HAR 3 exhibits more strength variation with depth within one foundation width below the nuclear island than at HAR 2. This is related to the larger depth of soil and underlying weathered rock at HAR 3.

The subsurface profile under the nuclear island at HAR 3 was divided into two elevation ranges for bearing capacity analyses — a shallow layer between elevation 51.8 and 67.1 m (170 and 220 ft.) and a deeper layer below elevation 51.8 m (170 ft.). The GSI and UCS results at HAR 2 were more consistent with depth below the nuclear island than at HAR 3; therefore, one rock layer with lower-bound strength properties was modeled for HAR 2.

2.5.4.10.1.2.2 Rock Discontinuity Strength Parameters

The following rock discontinuity strength parameters were determined for discontinuity Sets A through D, and were applied in the bearing capacity evaluations described in Subsection 2.5.4.10.1.1.4:

- **Discontinuity Set A (bedding features):** Undrained shear strength (S_u) = 0.072 MPa (1500 psf) above the nuclear island subgrade elevation, and S_u = 0.105 MPa (2200 psf) below the subgrade elevation. This is based on the strength of bedding-related clay seams present within otherwise sound rock, which have similar index properties as soil samples collected above rock as summarized in Table 2.5.4-208. These S_u values are significantly less than average S_u from UU triaxial tests performed on soil samples collected near the ground surface with similar index properties. Use of this value conservatively assumes that the clay seams are fully continuous and planar within the extents of the rock wedges considered in the evaluations.
- **Discontinuity Set B (high-angle joints):** Interface friction angle (ϕ_i) = 45 degrees below top of sound rock, with no cohesion. This is based on the typically rough and tight conditions of high-angle discontinuities observed in the HAR rock cores, and observations presented in the HNP foundation conditions report (Reference RAI 02.05.04-8-001). At the HNP, the high-angle and vertical joints were observed to be tight and to often undulate a meter or more (several feet) from planar over the mapping extent with significant asperities. The joints were also reported to be vertically discontinuous, often initiating and terminating at parallel bedding planes a few meters (several feet) apart.

The value of ϕ_r was calculated as follows (Reference 2.5.4-232):

$$\phi_r = \phi_b + JRC \log_{10} \frac{JCS}{\sigma'} \quad (2.5.4-14)$$

Where ϕ_b is the base friction angle for a planar rock surface (27 to 34 degrees for siltstone), JRC is the joint roughness coefficient (20 for rough tensional joints), JCS is the compressive strength of rock at the joint surface, and σ' is the applied normal stress. For the HAR site conditions and observed high-angle joint conditions, the resulting ϕ_r is calculated to be greater than 60 degrees. Use of $\phi_r = 45$ degrees without cohesion is therefore considered conservative to characterize such joints. For discontinuities above the top of sound rock, a lower $\phi_r = 30$ degrees was conservatively applied, which is the approximate base friction angle without asperities (ϕ_b).

- **Discontinuity Sets C and D (vertical joints):** The same properties applied to discontinuity Set B were assigned to Sets C and D, because the discontinuity conditions are similar.

2.5.4.10.1.3 Bearing Capacity Results and Design Criteria

The bearing capacity results corresponding to the four methods described in Subsections 2.5.4.10.1.1.1, 2.5.4.10.1.1.2, 2.5.4.10.1.1.3, and 2.5.4.10.1.1.4 are presented below. Design criteria, including minimum acceptable FS values against static and dynamic bearing loads, are then presented.

2.5.4.10.1.3.1 General Bearing Capacity Method Results

Table 2.5.4-214 presents the ultimate bearing capacities calculated using the general bearing capacity method described in Subsection 2.5.4.10.1.1.1. The resulting FS based on the ratio of the ultimate bearing capacities to design static bearing demand of 0.43 MPa (8900 psf) and peak dynamic bearing demand of 1.68 MPa (35,000 psf) are also presented for each result.

2.5.4.10.1.3.2 Empirical Method Results

Table 2.5.4-214 presents the ultimate bearing capacity results for the two alternative empirical methods described in Subsection 2.5.4.10.1.1.2. As shown, these are similar to and confirm the results from the general bearing capacity method.

2.5.4.10.1.3.3 Two-Dimensional Finite Element Modeling Results

The two-dimensional finite element analyses described in Subsection 2.5.4.10.1.1.3 each result in FS greater than the corresponding cases presented in Table 2.5.4-214. This is in part because the shear strength of the soil and rock materials above the basemat of the nuclear islands was ignored in the general bearing capacity method, while the finite-element models inherently considered the shear strength of the materials above the basemat. The finite element analyses also indicate that soil conditions postulated on the basis of a 1.5-m- (5-ft) thick soil seam present at Borehole BPA-6 do not affect foundation performance of the HAR 2 nuclear island. For these analyses the resulting FS was 4 or greater for each analyzed static and dynamic condition.

2.5.4.10.1.3.4 Oriented Rock Discontinuity Model Results

The evaluations based on the oriented rock discontinuity model described in Subsection 2.5.4.10.1.1.4 result in minimum FS_b against dynamic bearing loads of 5.4 at HAR 2, and 2.6 at HAR 3. These results are associated with the true dip values for

discontinuity Sets A and B, including the conservatively high estimate of Set A true dip of 23.2 degrees at HAR 3; the resulting FS_b corresponding to the apparent dip values are greater than for the true dip values.

The results of the secondary method by Landanyi and Roy, 1971 as presented in Wyllie 1999 (Reference 2.5.4-232), also each result in FS_b greater than 2.0 for each case evaluated. These results provide an order-of-magnitude confirmation of the results from the oriented rock discontinuity evaluations presented above.

2.5.4.10.1.3.5 Bearing Capacity Design Criteria

Minimum FS of 3.0 for static loads (dead plus live loads) and 2.0 for dynamic or seismic loads are commonly considered acceptable (Reference 2.5.4-237). A lower minimum FS of 1.5 against the peak seismic bearing loads has been applied for safety-related structures (e.g., Reference RAI 02.05.04-8-002). As shown in Table 2.5.4-214 and described in the preceding subsections, the minimum FS of 3.0 (static) and 2.0 (dynamic) are satisfied by each of the presented cases for HAR 2 and HAR 3, including those based on the lower-bound rock mass strength parameters.

Allowable bearing pressures are calculated based on the ultimate bearing capacities calculated using the lower-bound strength parameters at HAR 2 and HAR 3, and using FS of 3.0 and 2.0 for static and dynamic loading, respectively.

Allowable bearing pressures are designated as follows:

- HAR 2 – Static Loading: 2.59 MPa (54 ksf)
- HAR 2 – Dynamic Loading: 3.26 MPa (68 ksf)
- HAR 3 – Static Loading: 1.39 MPa (29 ksf)
- HAR 3 – Dynamic Loading: 1.77 MPa (37 ksf)

The FS values in Table 2.5.4-214 and allowable bearing pressure values are considered very conservative for the following reasons:

- They are based on the lower-bound rock mass strength parameters based on rock UCS and GSI values corresponding to one-standard deviation below the mean. This is equivalent to the 16th percentile value – such that 84 percent of the rock has strength higher than this value. In addition, use of these lower-bound strength values provides very high confidence that the mean values of UCS and GSI for rock under the nuclear island subgrades are greater than these values. Further, these strength values are considered highly conservative because only thin zones will be represented by these lower-bound rock mass strength parameters, and bearing capacity will be more closely represented by the average within the zone of influence beneath the foundation. As shown in Table 2.5.4-214, FS based on mean rock mass strength (best estimate) are significantly higher than those based on lower-bound strength values.
- Results of the finite element analyses in Subsection 2.5.4.10.1.3.3 indicate that the FS results from the general and empirical methods are conservative. The oriented rock discontinuity evaluations in Subsection 2.5.4.10.1.3.4 also result in FS greater than those obtained from the general bearing capacity method in Subsection 2.5.4.10.1.1.1 using the lower-bound rock mass strength properties.
- Each of the site-specific FS against dynamic bearing demand presented in this subsection is based on a peak dynamic bearing demand of 1.68 MPa (35 ksf),

consistent with the AP1000 design parameter corresponding to the 0.3g SSE design event. However, this peak bearing pressure corresponds to hard-rock site conditions. For a firm-rock site (such as HAR), the peak bearing pressure is 1.34 MPa (27.9 ksf) for the 0.3g SSE design event. The HAR-specific bearing pressure will be significantly less than this lower value because the HAR GMRS and FIRS are bounded by the 0.3g SSE design spectra. For these reasons, the FS against dynamic bearing demand at HAR 2 and 3 are greater than those presented herein.”

2.5.4.10.1.4 Annex Building Bearing Capacity

The bearing capacities of the HAR 2 and HAR 3 Annex Buildings (Seismic Category 2 structures) have been evaluated based on the preliminary static bearing pressure of 0.070 MPa (1460 psf) provided by Westinghouse. For building foundations on compacted granular fill, concrete, or rock, the static FS are significantly greater than 3.0. Confirmation of final static and dynamic allowable bearing pressures for the Annex Buildings will be completed upon final determination of the Annex Building bearing pressures.

3. Revise FSAR Subsection 2.5.4.10.2 to read:

“2.5.4.10.2 Resistance to Sliding

The HAR 2 and HAR 3 nuclear islands will each be founded on sound rock. During excavation, loose material at the subgrade elevation will be removed, resulting in a relatively clean, exposed rock, as discussed in Subsection 2.5.4.5.2. The concrete mudmat, geomembrane, and nuclear island foundation will be constructed over the exposed rock. The mudmat and any underlying concrete fill will interlock with the rock subgrade and create a stronger bond than the overlying waterproofing membrane interface. As described in Subsection 2.5.4.5.3, concrete fill will also be placed within the space between the excavated rock and the nuclear island sidewall below elevation 69.3 m (227.5 ft.). These construction plans were used to evaluate sliding stability of the nuclear islands under peak seismic design loads. Subsection 2.5.4.10.2.1 provides a summary of the evaluation methodology, and Subsection 2.5.4.10.2.2 presents the results.

2.5.4.10.2.1 Sliding Evaluation Methodology

The sliding stability evaluations were based on the force equilibrium of five wedges representing soil and rock below and on the active and passive sides of the nuclear island. Figure RAI 02.05.04-8-001 shows the configuration of the nuclear island and associated rock and soil wedges considered in the sliding stability evaluations. Conservative assumptions were applied to convert the three-dimensional nuclear island and subsurface configuration to an equivalent limited-width two-dimensional model. Two-dimensional profiles associated with each of the four orthogonal directions at HAR 2 and HAR 3 (total of eight profiles) were evaluated. The resulting FS against sliding in each direction were then compared to minimum required value (FS_s) of 1.1.

The orientations and conditions of rock discontinuity sets were conservatively modeled as described for the bearing capacity evaluations in Subsections 2.5.4.10.1.1.4 and 2.5.4.10.1.2.2. Driving forces included the inertial lateral and vertical forces of the nuclear island due to the SSE and the external lateral forces on the active side of the nuclear island. Dynamic forces were represented by equivalent static loads. These loads represented instantaneous peak forces computed on the basis of spectral accelerations from the FIRS and GMRS for the HAR 2 and HAR 3 site. In Figure RAI 02.05.04-8-001, SSE seismic forces are directed to the left, with concentration of bearing load near the left side of the

nuclear island. Vertical forces associated with SSE loading were assumed to occur in the direction that results in the lowest FS against sliding.

Two sets of dipping discontinuities were considered in the model, denoted as Set 1 (apparent dip down in the direction of seismic loading) and Set 2 (apparent dip in opposite direction). The dip angles from horizontal (β_1 and β_2) and strength properties in rock (ϕ_{1r} , ϕ_{2r} and c_{1r} , c_{2r}) were assigned based on the orthogonal direction under consideration; Set 1 was assigned properties consistent with the discontinuity Set (A or B) which dips down in the modeled direction of SSE loading. Set 2 was assigned properties of either discontinuity Set B or A that were not assigned to Set 1. Depth to sound rock was modeled separately on either side of the nuclear island (D_{s1} and D_{s2}).

Five rock and soil wedges are considered in the model. Three of the wedges contribute net driving forces (Wedges 1, 4, and 5) that must be resisted for stability, and two provide net resisting forces (Wedges 2 and 3). For each wedge, driving and/or resisting forces are contributed by the wedge self-weight and lateral inertial force; whether these act as driving or resisting forces depends on the dip direction of the base of the wedge. Resisting forces are provided by friction and cohesion along the base and the sidewalls of each wedge. Groundwater table is conservatively modeled at site grade for all calculations.

Two separate methods are used to calculate the driving force on the active side of the nuclear island. The first method is based on wedge force equilibrium (the resulting force is $F_{lat5.wedge}$). The second is based on the force from compacted backfill, based on the elastic method presented in ASCE 4-98 (Reference RAI 02.05.04-8-003) (the resulting force is $F_{lat5.backfill}$). This second method conservatively considers that the granular backfill is present from site grade to the nuclear island subgrade elevation, without reduction for the concrete fill below elevation 69.3 m (227.5 ft). The net lateral force on the active NI endwall (F_{active}) is assigned as the greater of the two forces $F_{lat5.wedge}$ or $F_{lat5.backfill}$.

Based on the input parameters, the stability of each wedge was calculated sequentially starting with Wedge 1. For Wedges 1, 4, and 5, the separate external lateral forces required for wedge stability (denoted F_{lat1} , F_{lat4} , and F_{active} , respectively) were calculated, which act as driving forces in the overall NI stability calculation. For Wedges 2 and 3, the additional external lateral forces that can be resisted while maintaining stability (denoted R_{lat2} and R_{lat3} , respectively) were calculated, which act as resisting forces in the overall stability calculation.

The peak inertial driving force from the nuclear island during seismic loading ($F_{lat.struct}$) was calculated based on a HAR site-specific SSI bounding study by WEC (Reference RAI 02.05.04-8-004). The FS against sliding (FS_{slide}) was calculated directly as the ratio of the sum of lateral resisting forces to the sum of lateral driving forces, as follows:

$$FS_{slide} = (R_{passive} + R_{base}) / (F_{active} + F_{lat.struct}) \quad (2.5.4-15)$$

In this equation, $R_{passive}$ is the net passive resistance provided between Wedges 1 and 3 ($R_{lat3} - F_{lat1}$). R_{base} is the net resistance provided by Wedges 2 and 4 ($R_{lat2} - F_{lat4}$), or the available friction resistance at the waterproofing membrane interface, whichever is lower. F_{active} and $F_{lat.struct}$ are as defined previously.

The resulting FS_{slide} was then compared to the minimum allowable sliding FS of 1.1 for evaluation of acceptable stability.

2.5.4.10.2.2 Sliding Evaluation Results

Table RAI 02.05.04-8-001 presents the key input parameters used in the sliding stability evaluations, the net driving (lateral) forces $F_{lat.struct}$ and F_{active} , the net resisting forces R_{base}

and R_{passive} , and the resulting FS against sliding (FS_{slide}) for each of the orthogonal directions of nuclear islands at HAR 2 and HAR 3.

For each orthogonal direction, multiple iterations were performed to identify the critical value of B_1 that results in the lowest FS_{slide} . Two results are presented for each NI orthogonal direction: (1) the first result corresponds to the distance B_1 that resulted in the lowest FS_{slide} ; and (2) the second result corresponds to B_1 of zero, such that bearing pressures did not contribute to the lateral sliding forces. This second result represents a typical sliding evaluation decoupled from the bearing capacity evaluation.

As shown in Table RAI 02.05.04-8-001, FS_{slide} is 1.75 or greater for each case evaluated; therefore, each of these results satisfies the minimum FS of 1.1 required against sliding with significant margin. The resulting FS_{slide} for each of the Plant North and Plant East profiles at HAR 2 and HAR 3 were very high, with FS_{slide} greater than 12 for each case. This is due in part to the steep dip angle and high friction angle of discontinuity Set B, which is oriented to resist sliding in the Plant North and Plant East directions.

Table RAI 02.05.04-8-001 also lists the passive force required to provide a minimum FS_{slide} of 1.1 for each profile. As shown, for six of the eight profiles, no passive force is required. For the Plant West profiles at HAR 2 and HAR 3, only 17 and 22 percent of the available net passive resistances are needed to provide the minimum FS_{slide} of 1.1, respectively.

As indicated by the sliding evaluations, the concrete fill below elevation 69.3 m (227.5 ft.) will sufficiently transfer the required passive resistance to the adjacent rock to prevent sliding. Fill above elevation 69.3 m (227.5 ft.), consisting of concrete, compacted cohesive fill, or compacted granular fill, is not required to prevent sliding. "

4. Revise FSAR Subsection 2.5.4.10.4 to read:

"2.5.4.10.4 Lateral Earth Pressures

Lateral earth pressures will develop against below-grade nuclear island sidewalls due to placement and compaction of soil backfill materials. At-rest earth pressures will act on the sidewalls after construction and are considered appropriate values for wall design during static loading, and are presented in Subsection 2.5.4.10.4.1. The maximum forces that could develop along the active nuclear island sidewalls during dynamic loading, and the passive forces available to resist sliding; are presented in Subsection 2.5.4.10.4.2.

2.5.4.10.4.1 At-Rest Lateral Earth Pressures

Equations for calculation of lateral earth pressures are presented in this subsection. The compacted granular and compacted cohesive backfill types described in Subsection 2.5.4.5.3 are considered in the calculation of lateral earth pressures, with the following effective stress parameters:

- Compacted granular backfill: $\phi' = 35$ degrees, $c = 0$ psf
- Compacted cohesive backfill: $\phi' = 20$ degrees, $c = 400$ psf

It was assumed that backfill adjacent to the nuclear island sidewalls will be compacted as described in Subsection 2.5.4.5.3 for calculation of lateral earth pressures. In addition, light, hand-operated compaction equipment will be used to compact the soil adjacent to the nuclear island sidewalls. This will minimize compaction-induced soil stresses against the sidewalls, rendering them small and insignificant. The nuclear island sidewalls will not yield to the lateral earth pressures; therefore, the at-rest pressure condition is appropriate for use in wall design under static loads.

The at-rest earth pressure coefficient (K_o) is calculated as follows (Reference 2.5.4-238):

$$K_o = 1 - \sin(\phi') \text{OCR}^{\sin(\phi')} \quad (2.5.4-10)$$

where OCR is the overconsolidation ratio, which is considered to be 1.0 for fill compacted with hand-guided equipment adjacent to the sidewalls.

The at-rest pressure, $P_{(\text{at-rest})}$, against the nuclear island sidewalls at any depth z bgs can be calculated as follows:

$$P_{(\text{at-rest})} = \sigma'_v * K_o + P_h + S_s * K_o \quad (2.5.4-12)$$

where σ'_v is the effective overburden pressure at the depth z , P_h is the groundwater pressure, and S_s is the surface surcharge due to surface loads, such as adjacent buildings, and other terms are as defined previously.

Hydrostatic pressures (P_h) have been considered in the calculation of lateral at-rest pressures. A groundwater elevation of 78.6 m (258 ft.), the maximum estimated post-construction groundwater elevation at the HAR sites, was conservatively considered in the calculation of hydrostatic pressures. Hydrostatic pressures will act simultaneously on all sides of the nuclear islands.

The resulting at-rest lateral earth pressure profiles for the two soil backfill types are presented for representative sidewall elevations in Table 2.5.4-217. The actual depth of soil backfill against the nuclear island sidewalls will vary by location. Concrete backfill will be placed between the nuclear island sidewalls and rock excavation slopes below elevation 69.3 m (227.5 ft.) around the perimeter of each nuclear island and at select locations above this elevation, as discussed in Subsection 2.5.4.5.3. Once the concrete fill solidifies, the at-rest pressure from the concrete fill will be less than the at-rest pressure from compacted backfill, such that the at-rest pressures listed in Table 2.5.4-217 are considered a conservative envelope of the at-rest lateral earth pressures. The pressures presented in Table 2.5.4-217 include hydrostatic pressures, but do not include lateral pressures due to surface surcharge loads. Adjacent structures, where present, will increase the at-rest pressures from the values presented in Table 2.5.4-217 per Equation 2.5.4-12.

2.5.4.10.4.2 Dynamic Lateral Active and Passive Forces

The peak lateral forces acting on the active sides of the nuclear islands during seismic loading (F_{active}) were calculated as part of the nuclear island sliding evaluations described in Subsection 2.5.4.10.2.1. The values of F_{active} on each side of the HAR 2 and HAR 3 nuclear islands are presented in Table RAI 02.05.04-8-001. These maximum forces encompass the at-rest plus dynamic earth pressures and the at-rest plus dynamic contributions from adjacent building surcharge loads.

The peak passive forces available to resist sliding during seismic loading (R_{passive}) are presented in Table RAI 02.05.04-8-001 for each side of the HAR 2 and HAR 3 nuclear islands. The total fraction of this available passive resistance that is required to resist sliding with a minimum FS of 1.1 is also presented for each side of the nuclear islands in Table RAI 02.05.04-8-001. As shown, at most only 22 percent of the net available passive force would potentially be required to prevent sliding. As discussed in Subsection 2.5.4.10.2.2, this maximum passive force will be fully transferred from the nuclear island sidewalls to the adjacent sound rock by the concrete fill placed below elevation 69.3 m (227.5 ft).

Hydrostatic forces are not included in the values of F_{active} or R_{passive} presented in Table RAI 02.05.04-8-001. This is because hydrostatic forces balance on opposite sides of the nuclear island and therefore do not contribute a net driving or resisting force to sliding."

5. Add new Subsection 2.5.4 figure (referenced as "Figure RAI 02.05.04-8-001" herein).
6. Add new Subsection 2.5.4 table (referenced as "Table RAI 02.05.04-8-001" herein).
7. Add new COLA Part 10 Table 3.8-3.
8. Add new references as listed below to Subsection 2.5.7.

References

Reference RAI 02.05.04-8-001

Ebasco Services, Inc., "Final Geologic Report on Foundation Conditions: Power Plants, Dams, and Related Structures," Volume 1, 1981.

Reference RAI 02.05.04-8-002

ASCE, "Structural Analysis and Design of Nuclear Plant Facilities," 1980.

Reference RAI 02.05.04-8-003

ASCE, "Seismic Analysis of Safety-Related Nuclear Structures and Commentary," Report ASCE 4-98, 1998.

Reference RAI 02.05.04-8-004

WEC, "Site Specific SSI Analysis of Shearon Harris Site," Calculation HAG-1000-S2C-802, Rev. 0, January 28, 2008.

Attachments/Enclosures:

Technical Memorandum 338884-TMEM-081, Rev. 0

Figure RAI 02.05.04-8-001, Summary of Wedge Configurations and Input Parameters – Sliding Evaluations

Table RAI 02.05.04-8-001, Results of Sliding Stability Evaluations

COLA Part 10 Table 3.8-3, Concrete Fill Inspections, Tests, Analyses, and Acceptance Criteria

NRC Letter No.: HAR-NRC-LTR-020

NRC Letter Date: September 26, 2008

NRC Review of Final Safety Analysis Report

NRC RAI #: 02.05.04-11

Text of NRC RAI:

FSAR 2.5.4.10.4 Lateral Earth Pressures states "Surface surcharge from structures adjacent to the nuclear islands could potentially increase the lateral earth pressures that develop against the nuclear island sidewalls. However, these adjacent structures will likely be founded on sound rock, which is stiffer than the soil backfill adjacent to nuclear islands. Due to this difference in rock and backfill stiffness, it is anticipated that these adjacent structure foundation loads will not be transferred to the soil backfill. Therefore, loads from structures adjacent to nuclear islands (Ps) were considered insignificant in calculation of the at-rest pressure distributions."

Please clarify what structures this paragraph refers to since it appears that the radwaste building and turbine building appear to be founded on engineered backfill. Only the Annex building is founded on concrete on rock.

PGN RAI ID #: H-0443

PGN Response to NRC RAI

PEC response was provided in Reference 2 (PGN-RAI ID # H-0125). Supplemental information is provided in response to NRC RAI #02.05.04-8 (PGN-RAI ID # H-0390) included in this letter.

Associated HAR COL Application Revisions:

See NRC RAI #02.05.04-8 (PGN-RAI ID # H-0390) for proposed COLA revisions.

Attachments/Enclosures:

None.

NRC Letter No.: HAR-NRC-LTR-020

NRC Letter Date: September 26, 2008

NRC Review of Final Safety Analysis Report

NRC RAI #: 02.05.04-12

Text of NRC RAI:

FSAR 2.5.4.10.2, "Resistance to Sliding" states "The nuclear island has been designed such that passive resistance from this backfill is not necessary to prevent sliding." This statement is not in agreement with criteria for sliding presented in AP1000 DCD, Tier 2, Section 2.5.4.6.2 "Properties of Materials Adjacent to Nuclear Island Exterior Walls" where it states "A determination of the static and dynamic engineering properties of the surrounding soil will be made to demonstrate they are competent and provide passive earth pressures greater than or equal to those used in the seismic stability evaluation for sliding of the nuclear island."

Please clarify the statement that backfill is not required for sliding stability of the nuclear island.

PGN RAI ID #: H-0444

PGN Response to NRC RAI

PEC response was provided in Reference 2 (PGN-RAI ID # H-0126). Supplemental information is provided in response to NRC RAI #02.05.04-8 (PGN-RAI ID # H-0390) included in this letter.

Associated HAR COL Application Revisions:

See NRC RAI #02.05.04-8 (PGN-RAI ID # H-0390) for proposed COLA revisions.

Attachments/Enclosures:

None.

NRC Letter No.: HAR-NRC-LTR-020

NRC Letter Date: September 26, 2008

NRC Review of Final Safety Analysis Report

NRC RAI #: 02.05.04-13

Text of NRC RAI:

FSAR Section 2.5.4.10.1.2, "Rock Mass Strength Parameters for Bearing Capacity Analyses" provides the rationale and general procedures used to obtain Mohr-Coulomb strength parameters using the Hoek-Brown criteria for use in determining bearing capacity. However, the rock strength tables do not provide all the Hoek-Brown classification data needed as input to confirm the Mohr-Coulomb strength parameters presented for the various cases analyzed.

Please provide all the assumptions, input data, and a sample calculation showing how those input parameters were derived for the lower bound bearing capacity determination at HAR 3.

PGN RAI ID #: H-0391

PGN Response to NRC RAI

PEC response was provided in Reference 3 (PGN-RAI ID # H-0127). Supplemental information is provided in response to NRC RAI #02.05.04-8 (PGN-RAI ID # H-0390) included in this letter.

Associated HAR COL Application Revisions:

See NRC RAI #02.05.04-8 (PGN-RAI ID # H-0390) for proposed COLA revisions.

Attachments/Enclosures:

None.

NRC Letter No.: HAR-NRC-LTR-020

NRC Letter Date: September 26, 2008

NRC Review of Final Safety Analysis Report

NRC RAI #: 02.05.04-14

Text of NRC RAI:

AP1000 DCD, Tier 2, (Section 2.5.4.6.2 "Properties of Materials Adjacent to Nuclear Island Exterior Walls") states that "A determination of the static and dynamic engineering properties of the surrounding soil will be made to demonstrate they are competent and provide passive earth pressures greater than or equal to those used in the seismic stability evaluation for sliding of the nuclear island."

FSAR Section 2.5.4.5.3, "Properties of Backfill Adjacent to Nuclear Islands" states "Backfill materials will be placed adjacent to the sidewalls of the nuclear islands. The backfill material adjacent to the nuclear island sidewalls is nonsafety-related; the nuclear islands are designed for safe performance independent of the sidewall backfill type." Compare this statement to that found in AP1000 DCD, Tier 2, Section 2.5.4.6.2 "Properties of Materials Adjacent to Nuclear Island Exterior Walls" where it states "A determination of the static and dynamic engineering properties of the surrounding soil will be made to demonstrate they are competent and provide passive earth pressures greater than or equal to those used in the seismic stability evaluation for sliding of the nuclear island." The DCD goes on to state: "If the soil below and adjacent to the exterior walls is made up of clay, sand and clay, or other types of soil other than those classified above as competent, then the Combined License applicant will evaluate the seismic stability against sliding as described in subsection 3.8.5.5.3 using the site-specific soil properties."

Please include engineering data on all the backfill (concrete, cohesionless backfill and cohesive soil backfill) that will be used adjacent to nuclear islands. Also, please supply the borrow area exploration program data, field results on full scale test fills for each type material planned as backfill, including shear wave velocities measured in the test fills, and static and dynamic laboratory test results (including resonant column/torsional shear) for all backfill types intended for use adjacent to the sidewalls of the nuclear island.

PGN RAI ID #: H-0392

PGN Response to NRC RAI

PEC response was provided in Reference 3 (PGN-RAI ID # H-0128). Supplemental information is provided in response to NRC RAI #02.05.04-8 (PGN-RAI ID # H-0390) included in this letter.

Associated HAR COL Application Revisions:

See NRC RAI #02.05.04-8 (PGN-RAI ID # H-0390) for proposed COLA revisions.

Attachments/Enclosures:

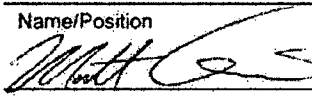
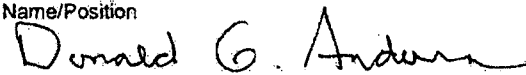
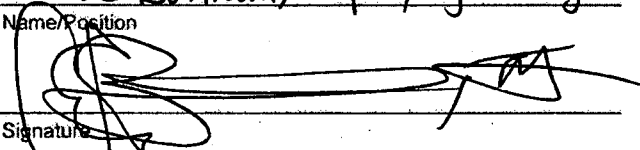
None.

List of Attachments:

1. NRC RAI # 2.05.04-8 (PGN RAI ID #H-0390):
Technical Memorandum 338884-TMEM-081, Rev. 0 (80 pages)
2. NRC RAI # 2.05.04-8 (PGN RAI ID #H-0390):
Figure RAI 02.05.04-8-001, Summary of Wedge Configurations and Input Parameters – Sliding Evaluations (1 page)
3. NRC RAI # 2.05.04-8 (PGN RAI ID #H-0390):
Table RAI 02.05.04-8-001, Results of Sliding Stability Evaluations (1 page)
4. NRC RAI # 2.05.04-8 (PGN RAI ID #H-0390):
COLA Part 10 Table 3.8-3, Concrete Fill Inspections, Tests, Analyses, and Acceptance Criteria (1 page)

ATTACHMENT A
Tech Memo Approval Form

Tech Memo Number: 338884-TMEM-081
 Revision: 0
 Project: PEC COLA
 Review Date: 2/20/2009

Tech Memo Title: Supplemental Evaluations of Sliding Resistance, Bearing Capacity, and Dynamic Passive and Active Lateral Forces Associated with Rock Discontinuities at the HAR Nuclear Islands			
Revision History:			
Revision Number	Description	Approval Date	Affected Pages
A	Owner Acceptance Revision	2/20/2009	All
Document Review and Approval			
Originator:	Matt Gavin / Geotechnical Task Lead	2/20/2009	
	Name/Position	Date	
			
	Signature		
Reviewer	Donald Anderson / Senior Geotechnical Engineer	2/20/09	
	Name/Position	Date	
			
	Signature		
Project Manager:	Claude Buttram / Deputy Project Manager	02/20/09	
	Name/Position	Approval Date	
			
	Signature		

Supplemental Evaluations of Sliding Resistance, Bearing Capacity, and Dynamic Passive and Active Lateral Forces Associated with Rock Discontinuities at the HAR Nuclear Islands

PREPARED FOR: Progress Energy
PREPARED BY: CH2M HILL
DATE: February 20, 2009
PROJECT NUMBER: 338884.N2.01

This memorandum presents supplemental information on the orientations and conditions of discontinuity sets within otherwise sound rock at the proposed Shearon Harris Nuclear Power Plant Units 2 and 3 (HAR 2 and HAR 3), and the influence of these discontinuities on nuclear island (NI) sliding stability and bearing capacity under safe-shutdown earthquake (SSE) seismic loads. The calculated dynamic passive and active lateral forces acting on the NI sidewalls are also presented in this technical memorandum.

This supplemental information is provided in response to the following U.S. Nuclear Regulatory Commission (NRC) requests for additional information (RAIs) on HAR FSAR Subsection 2.5.4:

- RAI 02.05.04-8 requested information on calculation of the dynamic active and passive lateral earth pressures on NI sidewalls.
- RAI 02.05.04-11 requested information regarding surcharge loads from structures adjacent to the NIs, and their influence on the lateral earth pressures on NI sidewalls.
- RAI 02.05.04-14 requested engineering data on NI backfill materials, and demonstration that associated passive pressures from backfill are greater than or equal to those required for seismic sliding stability.

In addition to the above RAIs, the NRC informally requested the following additional information during the HAR FSAR Section 2.5 NRC site visit in October 2008.

- Further consideration of rock intervals with geologic strength index (GSI) less than the "lower bound" values presented in FSAR Subsection 2.5.4.10, and their influence on bearing capacity
- Further consideration of potential modes of bearing capacity failure along oriented rock discontinuity sets, and the associated factor of safety (FS) against failure

The applicant responses to RAIs 02.05.04-8, 11, 13, and 14 committed to providing the above requested additional information. The requested additional information is provided in this memorandum.

Organization of Memorandum

This memorandum presents the following information related to the oriented rock discontinuities and associated stability evaluations:

- Section 1 characterizes the orientations and conditions of four bedding and high-angle discontinuity sets (Sets A through D herein) characterized at HAR 2 and HAR 3. This section also defines appropriately conservative discontinuity interface strength parameters for use in the supplemental stability evaluations.
- Section 2 presents the supplemental stability evaluation methods and results. These evaluations calculate the forces required for equilibrium of a series of rock and soil wedges adjacent to and under the NI under SSE seismic lateral and bearing loads. Sliding and bearing capacity evaluations are described separately, as follows:
 - Section 2.1 presents the sliding evaluation methods, including descriptions of the wedge equilibrium equations and selection of input parameters
 - Section 2.2 describes the bearing capacity evaluation methods.
- Section 3 presents the results of the stability evaluations. These include results of the sliding stability evaluations, minimum compressive strength of the concrete fill around the NI to sufficiently transfer sliding forces, results of bearing capacity evaluations, and evaluation of sensitivity of the evaluation results to variations in key input parameters. This section concludes with a discussion of sources of conservatism in the evaluations.
- Section 4 describes how the specific NRC HAR FSAR Section 2.5 RAIs have been addressed by these supplemental stability evaluations.
- Section 5 describes planned revisions to HAR FSAR Subsections 2.5.4.5 (Excavation and Backfill), 2.5.4.10.1 (Bearing Capacity), 2.5.4.10.2 (Resistance to Sliding), and 2.5.4.10.4 (Lateral Earth Pressures), based on the supplemental stability evaluations and associated RAIs.

Brief overviews of the HAR soil and rock conditions, and overviews of the sliding and bearing capacity evaluations, are presented below.

Overview of HAR Soil and Rock Conditions

The HAR soil and rock conditions, and NI foundation interfaces, are described in detail in HAR FSAR Section 2.5.4. The HAR 2 and HAR 3 NI basemats will be founded at elevation 221.5 ft (NGVD 29), with typical surrounding site grade ground surface at approximate elevation 260 ft. The NI subgrade will be excavated to typical elevation 220 ft, with installation of concrete fill and leveling concrete to elevation 221 ft and installation of a mudmat and waterproofing geomembrane between the subgrade and bottom of the basemat. Top of sound rock is located approximately 7 to 31 ft below the planned site grade ground surface along the sidewalls of the nuclear islands. A commitment has been made to place concrete fill between the NI basemat sidewalls and sound rock below minimum elevation 227.5 ft around the NI perimeters. The sound rock above the subgrade elevation is capable of providing significant passive resistance against sliding of the NIs, as evaluated herein.

Bedding-oriented discontinuities with thin clay seams are present below the top of sound rock. Lateral continuity of some seams has been observed across multiple boreholes at both HAR 2 and HAR 3. These discontinuities are weaker than the surrounding intact rock and are explicitly considered in the stability evaluations herein.

High-angle and vertical joint sets are also present at HAR 2 and HAR 3, as described in HAR FSAR 2.5.4 and in the Shearon Harris Nuclear Power Plant Unit 1 (HNP) foundation conditions report (Ebasco, 1981). These joints are typically rough, undulating, and tight with little to no infilling, as typical for tensional joints. Although these joints will provide significant frictional shearing resistance if loaded in plane, interface strength along these joint sets is less than for intact rock, and these joints are therefore explicitly considered in the stability evaluations herein.

Overview of Stability Evaluations

The stability evaluations herein consider the application of NI sliding and bearing loads, and resistances provided along the rock discontinuities at HAR 2 and HAR 3. The lateral active and passive forces acting on the NI sidewalls during seismic loading are calculated as part of these evaluations. Two types of evaluations were performed; sliding evaluations and bearing resistance evaluations. These are described below.

Sliding Resistance Evaluations

In these evaluations, the FS against sliding was calculated for each of the four NI orthogonal directions at HAR 2 and HAR 3 (for a total of eight two-dimensional profiles). Peak dynamic loads (bearing pressures, inertial sliding force, and active force) and resistances (base shear friction and passive forces) were used to calculate the force equilibrium of a series of five rock and soil wedges adjacent to and below the NI, and to calculate the resulting FS against sliding.

Requirements for NI sliding stability are provided in the AP1000 Design Control Document (DCD) Section 3.8.5.5.3. This requires evaluation of the FS against sliding during the SSE seismic event based on the base shear resistance, the passive resistance (neglecting adjacent building surcharge), the dynamic lateral force (including active earth pressures and adjacent building surcharge), other lateral forces, and buoyancy effects.

The minimum allowable FS against sliding (FS_s) is 1.1. The evaluations herein demonstrate that the HAR site conditions will satisfy the minimum FS_s of 1.1 by significant margin.

Bearing Capacity Evaluations

In these evaluations, the FS against bearing demand was calculated for the Plant West side of the containment (shield) building at HAR 2 and HAR 3, which is the location of peak applied dynamic bearing pressure (design parameter of 35 kips per square foot [ksf]). The driving and resisting forces acting on two wedges (a rock wedge under the NI and a passive wedge outside the NI) were used to calculate the force equilibrium and the resulting FS against peak dynamic bearing demand. A secondary calculation based on the method of Landanyi and Roy, 1971 (as presented in Wyllie, 1999), was also performed as confirmation of the first method.

HAR FSAR Subsection 2.5.4.10 presents the methods and results for bearing capacity evaluations previously performed for HAR 2 and HAR 3. Those previous evaluations were

based primarily on commonly accepted general bearing capacity equations as presented in the U. S. Army Corps of Engineers (USACE) *Rock Foundations Manual* EM 1110-1-2908 (USACE 1994), along with conservative estimates of rock mass strength parameters based on the Hoek-Brown criterion. The rock mass parameters quantify the overall quality of the rock mass, including weathering, fractures, and joint features. However, the bearing capacity evaluations summarized in the HAR FSAR did not explicitly consider the orientations and conditions of specific rock discontinuity sets.

USACE 1994 offers a method to evaluate potential for general shear failure along joints dipping between 20 and 70 degrees (case [f] in Table 6-1 of USACE 1994); however, this method simply neglects the cohesion strength term from the general bearing capacity equation, without consideration of the actual orientations or conditions of the discontinuities. This USACE method is therefore not considered representative of the actual HAR site conditions.

The supplemental evaluations presented herein consider resistance to seismic bearing loads specifically along the actual orientations and conditions of the HAR rock discontinuities. These evaluations are analogous to the dipping joint mode shown as case [f] in Table 6-1 of USACE 1994, but explicitly account for the HAR site conditions. These evaluations also consider the simultaneous application of inertial lateral NI sliding loads and bearing loads resulting from the SSE.

The appropriate minimum FS against dynamic bearing demand (FS_b) is defined in the HAR FSAR as 2.0. This factor of safety is considered highly conservative for the evaluation of stability under the peak dynamic bearing load at the Plant West edge of the NIs; minimum FS_b values against peak seismic loads as low as 1.5 have been used for safety-related structures (Table 7.4 of ASCE 1980). The evaluations herein demonstrate that the HAR site conditions will satisfy the minimum FS_b of 2.0 by a significant margin.

1. Rock Discontinuities at HAR 2 and HAR 3

Four primary sets of oriented rock discontinuities were observed at the HAR 2 and HAR 3 sites during the HAR site investigations and at the HNP during construction. These include the following:

- Bedding planes and associated fractures (discontinuity Set A)
- High-angle dipping joints and fractures (discontinuity Set B)
- Vertical joints (discontinuity Sets C and D)

Detailed discussions of the orientations and conditions of discontinuity Sets A through D are presented below. *Note: the HAR discontinuity Sets A and B described below are assigned as either Sets 1 and 2 or as Sets 2 and 1, respectively, in the sliding stability evaluations described in Section 2 depending on the plant orthogonal direction under consideration.*

1.1 Orientations of Discontinuities

The orientations of bedding planes (denoted Set A in this calculation) are presented in HAR FSAR Table 2.5.4-202. Orientation of high-angle dipping joints and fractures (Set B) encountered in HAR boreholes and acoustic logs are also presented in HAR FSAR

Table 2.5.4-202. Orientations of vertical joints (Sets C and D) were characterized by geologic reconnaissance during construction of the HNP (Ebasco, 1981), as described in HAR FSAR Subsection 2.5.1.

Table 1 lists the average dip angle (from horizontal) and orientations of dip and strike (azimuth relative to state plane north) of the discontinuity sets at HAR 2 and HAR 3 per the above cited inputs. Figure 1 shows a plan view of the strikes of discontinuity Sets A, B, C, and D in relation to the plant orthogonal directions. As shown, the bedding and high-angle dipping discontinuity Sets A and B have roughly parallel strikes (more so at HAR 3 than at HAR 2), but dip in opposite directions from each other.

The designated HAR plant orthogonal directions are as follows:

- Plant North has azimuth of 65 degrees east from state plane north, or N65°E (65 degrees clockwise from north)
- Plant East has azimuth of S25°E (155 degrees clockwise from north)
- Plant South has azimuth of S65°W (245 degrees clockwise from north)
- Plant West has azimuth of N25°W (335 degrees clockwise from north)

As shown on Table 1 and Figure 1, the representative strikes of the bedding and high-angle dipping discontinuity Set A (1 and 23.6 degrees clockwise from state plane north at HAR 2 and HAR 3, respectively) and Set B (38 and 14 degrees clockwise from state plane north at HAR 2 and HAR 3, respectively) are skewed from between 26 and 41 degrees from the plant orthogonal axes. Strike of vertical discontinuity Set C (45 degrees clockwise from state plane north) is skewed approximately 20 degrees from Plant North, and strike of Set D (335 degrees clockwise from state plane north) is oriented approximately parallel to Plant West.

The stability analyses discussed in the subsequent sections of this memorandum are based on an apparent dip along the plant orthogonal directions rather than the true dip of Sets A and B, to account for the skew between the NI orthogonal directions and the direction of true dip, as shown in Figure 1. For movement to occur along the true dip directions, significant shearing of intact rock would be required in part because the strikes of vertical joint sets C and D are not orthogonal to the strikes of sets A and B. Since the strikes of vertical joint sets C and D are more closely aligned with the plant orthogonal axes, shearing along the apparent dip of Sets A and B in the direction of the plant orthogonal direction under evaluation is considered more representative of the true dip conditions. As described in Section 3.5, even the use of the apparent dip angles is considered highly conservative. Nonetheless, influence of the true dip angles for Sets A and B are evaluated as sensitivity checks for each of the eight profiles analyzed at HAR 2 and HAR 3 as described in Section 3.4, but this is considered to represent an unrealistically conservative condition.

Table 2 lists the apparent dips of discontinuity Sets A and B along the plant orthogonal axes. The apparent dip was calculated based on the difference in the azimuth between the plant axis and true dip of the discontinuity. Example calculations of apparent dip for HAR 3 discontinuity Set A along the Plant North and Plant East directions are as follows. *Note: For HAR 3, discontinuity Set A, the upper estimate of the true dip angle associated acoustic televiewer*

logging presented in HAR FSAR Table 2.5.4-202 (23.2 degrees) was conservatively considered in the stability evaluations herein.

Apparent dip of HAR 3 discontinuity Set A in Plant North direction (β_{NS}):

$$\beta_{NS} = \text{Tan}^{-1} \left[\tan(23.2^\circ) \cos(113.6^\circ - 65^\circ) \right] = 15.8^\circ$$

Apparent dip of HAR 3 discontinuity Set A in Plant East direction (β_{EW}):

$$\beta_{EW} = \text{Tan}^{-1} \left[\tan(23.2^\circ) \cos(155^\circ - 113.6^\circ) \right] = 17.8^\circ$$

In Table 2, apparent dips are listed only if the dip is "down" in the corresponding plant orthogonal direction. Apparent dips are not applicable to the approximately vertical discontinuity Sets C and D.

1.2 Conditions of Discontinuities

The four discontinuity sets represent planes of reduced strength relative to the intact rock mass.

- The interface shear strength of clay seams and bedding-oriented fractures associated with discontinuity Set A is controlled by the strength of the clay seams or clay infilling. Under rapid loading, the resistance to shear within the clay seam is determined by the undrained strength of the clay. For loading cases in which excess pore-water pressures fully dissipate during loading, the drained properties of the clay determine resistance to shear.
- The high-angle and vertical joints associated with discontinuity Sets B, C, and D are typically rough and undulating, with little to no infilling, and therefore the interface strength is controlled by the coefficient of friction between the two surfaces. The coefficient of friction can also be defined in terms of a friction angle: $\phi_i = \tan^{-1}(\mu)$, where ϕ_i is the interface friction angle and μ is the coefficient of friction.

Following are summaries of the available field observations and laboratory test data for each discontinuity set, and associated conservative strength properties based on these data.

1.2.1 Bedding and Associated Fractures (Discontinuity Set A)

The majority of bedding features and interfaces observed in the HAR rock cores were intact. Nonetheless, bedding-oriented fractures and clay seams were observed in the rock cores. Information on bedding discontinuities as observed in the rock cores is described below in Subsection 1.2.1.1. Laboratory test data for HAR soil and rock bedding discontinuity samples is then described in Subsection 1.2.1.2, along with the basis for selection of strength parameters for the bedding discontinuity Set A. Subsection 1.2.1.3 provides a summary of the discontinuity Set A strength parameters selected for use in the stability evaluations.

1.2.1.1 Rock Core Log Descriptions

While many of the bedding-oriented fractures were likely mechanical induced from coring, they were not logged by the field geologist or geotechnical engineer as mechanical unless they could be definitively identified as such in the field. Presence of these bedding-oriented

fractures, mechanical induced or not, indicates that bedding planes comprise planes of relative weakness within the rock.

Thin clayey seams and thin intervals with missing recovery (interpreted herein as either washed-out broken rock or clay seams) were also occasionally encountered interbedded within fractured rock and, in some cases, as discrete clay seams several inches thick.

Bedding-oriented fractures are described on the rock core logs as rough to smooth or slickensided, and as tight to loose or infilled, as presented on the borehole logs in HAR FSAR Appendix 2BB. A few discrete bedding-oriented clay seams up to several inches thick were observed in rock cores across multiple boreholes at both HAR 2 and HAR 3. These continuous seams are modeled as potential shearing surfaces in these supplemental stability analyses. The interface strength of discontinuity Set A was represented by the strength of the clayey seams, as described below.

1.2.1.2 Laboratory Test Results

Laboratory soil index tests were performed on 15 clayey seams encountered within sound rock, as presented in HAR FSAR Table 2.5.4-208. Twelve of these samples were tested for Atterberg limits. Most of these samples were classified as low plasticity clays (CL or sandy CL per the Unified Soil Classification System [USCS]). Each of these samples had a moisture content less than the plastic limit (PL), which indicates a stiff condition usually associated with overconsolidated soils. The average PL, plasticity index (PI), and moisture content for these tested samples were 19, 14, and 11 percent, respectively. These results are similar to results from Atterberg limits tests on samples collected using Pitcher tube sampling methods in the soil above sound rock (also reported in HAR FSAR Table 2.5.4-208). The average PL, PI, and moisture content of these soil samples from above the top of rock were 19, 15, and 13, respectively.

Available geotechnical strength test results for the clayey soil-like seams within rock are limited. The soil samples collected from rock cores were partially disturbed by the rock coring process, and therefore use of unconfined compression strength (UCS) tests on these samples was not considered appropriate. Likewise, the quality of the samples was not considered appropriate for direct shear strength tests or triaxial compression tests.

In the absence of strength test information on clay seams within sound rock, multiple approaches were used to estimate the undrained (total stress) and drained (effective stress) shear strength properties of clay seams within rock. These include the following:

- Estimation of strength parameters from correlation with laboratory index properties
- Estimation of strength parameters from comparison with laboratory strength tests on soil samples collected via Pitcher tubes near the ground surface with similar index properties
- Estimation of strength parameters from literature-based values

Brief summaries of shear strength properties from each approach are presented below.

Correlation with Index Properties

Empirical correlations between strength parameters and soil classification properties were used to estimate the effective stress and total stress strengths. For the clayey seams within sound rock, the effective stress parameters would be appropriate for drained, long-term loading, whereas the total stress parameters would be appropriate for undrained loading. The undrained loading condition is most common in clayey soils during a seismic event; however, checks on drained strength parameters are normally performed to confirm that critical conditions do not occur in this state of drainage.

Undrained (Total Stress) Conditions

The undrained shear strength (S_u) of a cohesive soil can be correlated with the vertical effective overburden pressure (σ'_v) and the overconsolidation ratio (OCR). The normal form of this relationship is as follows:

$$S_u / \sigma'_v = a (\text{OCR})^m$$

where a and m are parameters determined from laboratory testing programs. The S_u / σ'_v ratio was estimated for HAR clay soils using the following correlation (Coduto 1994):

$$S_u / \sigma'_v = 0.23 (\text{OCR})^{0.8}$$

The OCR can be correlated with the liquidity index (LI). For moisture content less than the liquid limit, the LI is negative, and the soil is considered highly overconsolidated with OCR significantly greater than 4.

For an OCR of 4, the above correlation gives:

$$S_u / \sigma'_v = 0.23 (4)^{0.8} = 0.70$$

The effective overburden stress, σ'_v , near the NI subgrade elevation (approximate elevation of 221 ft) was determined as the product of the buoyant soil and rock unit weights (γ) and the depth below the ground surface. The typical γ for native soil and rock at HAR 2 and HAR 3 are 140 pounds per cubic foot (pcf) and 160 pcf, respectively. The water table is assumed to occur at the ground surface. For these conditions the σ'_v at subgrade ranges as follows:

$$\sigma'_v = [31 \text{ ft} (140 - 62.4) \text{ pcf} + 8 \text{ ft} (160 - 62.4) \text{ pcf}] = 3200 \text{ psf}$$

$$\sigma'_v = [7 \text{ ft} \times (140 - 62.4) \text{ pcf} + 32 \text{ ft} \times (160 - 62.4) \text{ pcf}] = 3700 \text{ psf}$$

depending on the depth of soil. The static bearing pressure of the NI (8900 pounds per square foot [psf]) will be more than twice these values; after consolidation under static NI bearing loads, the corresponding effective stress under the NI footprints will therefore be greater than the above values. The increase in strength from the NI weight was neglected for conservatism.

Based on the S_u / σ'_v correlation above, clayey seams within discontinuity Set A at the nuclear island subgrade elevation have estimated S_u as follows:

$$S_u = 0.7 (3200) = 2200 \text{ psf}$$

Under NI bearing loads, resistance will be mobilized along discontinuity Set A clay seams at depths significantly deeper than the NI subgrade elevation. As a representative example, discontinuity Set A clay seams located approximately 50 ft below the NI subgrade elevation have estimated σ'_v as follows:

$$\sigma'_v = 3200 \text{ psf} + [50 \text{ ft} (160 - 62.4) \text{ pcf}] = 8080 \text{ psf}$$

The associated estimated S_u at depth of 50 ft below the NI subgrade elevation is:

$$S_u = 0.7 (8080) = 5650 \text{ psf}$$

An average S_u of 1500 psf (with no friction angle) is considered appropriate and conservative to represent discontinuity Set A clay seams located above the NI subgrade elevation (for both the sliding and bearing capacity evaluations).

An average S_u of between 2200 and 5650 psf (with no friction angle) is appropriate to represent discontinuity Set A within rock below and within 50 ft of the NI subgrade elevation. Therefore, an average S_u of 2200 psf is conservatively assigned to discontinuity Set A clay seams located below the NI subgrade elevation for the bearing capacity evaluations.

Under rapid dynamic loading, the undrained shear strength will control the stability. The influence of use of the drained friction angle on stability is evaluated as a sensitivity check in the event that drainage occurs during shear, which is unlikely in these materials.

Drained (Effective Stress) Conditions

Mitchell (1992) presents a correlation between effective stress friction angle (ϕ') of normally consolidated cohesive soil at critical void ratio and the plasticity index, as follows:

$$\sin(\phi') = 0.8 - 0.094 \ln(\text{PI})$$

For PI of 14 percent, the corresponding estimated effective stress friction angle at critical void ratio is

$$\phi' = \sin^{-1} [0.8 - 0.094 \ln(14)] = 33 \text{ degrees}$$

The void ratio of a clay with a water content below the PL, as encountered at HAR, would be lower than the critical void ratio of a normally consolidated clay as represented by the above equation. The corresponding apparent effective stress friction angle would be higher from dilation during shear. Therefore, use of a drained friction angle of 30 degrees (with no cohesion) is considered a conservative representation of the effective (drained) stress conditions.

Comparison with Results of Strength Tests on Soil Pitcher Tube Samples

Unconfined compression (UC) and unconsolidated-undrained (UU) triaxial tests were performed on Pitcher tube samples of clayey soils collected above rock near HAR 2 and HAR 3. Three sets of consolidated-undrained (CU) tests were also performed. These results are presented in a calculation in HAR FSAR Table 2.5.4-209.

The UU tests were performed at various total stress confining pressures (σ_3), nine of which were set to approximate the in-situ effective vertical overburden stress (σ'_v) at the depth of the specific sample. The average σ_3 (and approximate σ'_v) from these nine tests was

1000 psf. The corresponding σ'_v for these nine samples is therefore less than the average σ'_v along clay seams within rock near the NI subgrade elevation. Since the index properties are similar, the undrained strength from tests on samples obtained above the top of rock provide a conservative estimate of strengths below the top of rock because of the greater effective stress. As summarized previously, the classification properties are very similar suggesting that the strengths from the UU tests can be used to define the strength in the clay seams.

The average S_u from these nine UU tests is approximately 3500 psf. This average strength is significantly greater than the values used for the stability analyses. The average value of S_u/σ'_v of these nine UU tests is approximately 3.5, which is significantly greater than the ratio of S_u/σ'_v of 0.7 calculated above based on correlations with OCR of 4. This indicates that use of the ratio of S_u/σ'_v of 0.7 to estimate S_u , as presented above, is conservative.

The three sets of CU tests performed on clayey soil samples resulted in effective stress friction angles of between 34 and 51 degrees, which are each greater than the value of 33 degrees estimated based on correlation with PI as presented above.

Comparison with Literature Values

A wide range of literature values have been published for peak shear strength of clay-filled discontinuities. These strengths depend on the type and condition of the infilling material. For overconsolidated clay infilling, representative strength parameters can range from approximately 12 degrees with little cohesion to 20 degrees with approximately 4000 psf cohesion (Wyllie, 1999).

The wide range in strength values given in the literature indicates that published data should not be used and correlations of site-specific index and strength data should be used for design. The site-specific strength results presented above are bounded by the range of literature values. An undrained shear strength of 1500 psf has been conservatively assigned to represent discontinuity Set A in the stability evaluations. Influences of other strength values have been evaluated as sensitivity checks in Section 3.4.

1.2.1.3 Discontinuity Set A Strength Parameters Used in Analyses

An average S_u of 1500 psf (with no friction angle) was conservatively assigned to represent discontinuity Set A clayey seams located above the NI subgrade elevation. This strength is applied to discontinuity Set A at all depths in the sliding stability evaluations, because sliding resistance will be provided predominantly by clay seams located near and above the NI subgrade elevation. A higher strength could have been assigned to clay seams located under the NI subgrade elevation, such as below the basemat, but this was conservatively not considered.

For the bearing capacity evaluations, an S_u of 2200 psf (with no friction angle) was conservatively assigned to represent deeper discontinuity Set A clayey seams below the NI subgrade elevation, because deeper clay seams will significantly contribute to the bearing resistance.

The influence of use of an effective stress friction angle of 30 degrees for discontinuity Set A clayey seams was evaluated as a sensitivity check.

1.2.2 High-Angle Dipping Joints and Fractures (Discontinuity Set B)

High-angle fractures encountered in the HAR rock core logs (HAR FSAR Appendix 2BB) with dip greater than 50 degrees were predominantly described as rough and undulating with little to no infilling. Where aperture could be determined, the discontinuities were predominantly described as tight. A few observations of loose or slickensided conditions were reported on the logs. The predominantly rough and undulating conditions are typical for tensional joints.

The conditions of high-angle and vertical joints were documented as part of foundation excavation mapping for HNP (Ebasco, 1981). Page 30 of the Ebasco foundation report provides the following description of these joints:

Joints are most prominent in the sandstones and siltstones, they are barely visible and rarely mappable in the shaley siltstone unit. Three joint sets are present. Two dominant sets are approximately vertical, one striking N40° - 50°E and the other N20° - 30°W. A third set strikes north-northwest and dips 55° to 70° to the southwest. Most of the joints are tight and do not extend vertically for more than a few feet. Some joints which were observed during the inspection and mapping, mostly at the power plant excavation, extended vertically as much as 10 - 15 ft and were opened up due to blasting. Joint surfaces were generally clean with a few having a very thin grayish-green clay infilling.

Maps of excavations in the HNP plant area (Ebasco, 1981) are consistent with this description. High-angle and nearly vertical joints are typically spaced a few to tens of feet apart. Section maps typically show high-angle joints originating and terminating at the interfaces of bedding units, with vertical extents of several to tens of feet. As noted above, Ebasco stated that the longer lengths were opened due to construction-related blasting, suggesting that the vertical extent of most vertical joints is limited to several feet. Joint traces shown on the excavation maps commonly undulate several feet from planar over the mapping extent.

Observations in the HAR rock cores are consistent with this description. A commitment is made to perform excavation mapping of the HAR foundations prior to construction, similar to the mapping performed for HNP. The conditions at the HAR sites are expected to be similar to HNP.

For clean discontinuities in rock, such as for the high-angle and vertical joints, shear strength has been defined by the coefficient of friction between the two rock surfaces, represented by a friction angle (without cohesion). Surface undulations and irregularities (asperities) will produce additional interlock which will contribute significantly to the interface shear strength. The peak shear strength of the rock interface has contributions from the base friction for a planar rock surface (denoted as ϕ_b herein) plus a friction contribution due to asperities. The friction contribution from asperities is determined by the joint roughness coefficient (JRC), the compressive strength of the rock on the joint surface (JCS), and the applied normal stress on this surface (σ'). The resulting discontinuity interface shear strength (τ) can be estimated as follows (Wyllie, 1999):

$$\tau = \sigma' \tan \left(\phi_b + JRC \log_{10} \frac{JCS}{\sigma'} \right)$$

The peak interface strength friction angle (denoted as ϕ_r herein) can be estimated as the expression within parenthesis in the above equation. The following parameters were used when estimating discontinuity interface strength for the high-angle joint Set B:

- The base friction angle for planar rock ϕ_b typically ranges between 27 and 34 degrees for medium strength sandstone and siltstone, such as the rock found at the HNP sites.
- JRC of 20 is applicable to rough, undulating surfaces such as tension joints (Wyllie, 1999); the field-scale undulations observed during foundation mapping of HNP further confirm that JRC of 20 is appropriate for the high-angle discontinuities.
- The average UCS of intact rock below elevation 220 ft is greater than 6000 pounds per square inch (psi) at both HAR 2 and HAR 3, as presented in HAR Table 2.5.4-206. Since the high-angle joints cut across bedding planes and through various rock types and strengths, use of approximately half of this average UCS (3000 psi) to represent the typical JCS is considered conservative.
- The applied normal stress along the high-angle discontinuities, σ' , is approximately half of the effective vertical overburden pressure (based on K_h of 0.5 for a vertical feature, and considering that Set B is somewhat inclined from vertical); therefore within a typical representative depth of 50 ft below the NI subgrade elevation, the average σ' based on soil and rock overburden is on the order of

$$\sigma' = [20 \text{ ft } (140-62.4) \text{ pcf} + (19 + 50/2) \text{ ft } (160-62.4) \text{ pcf}] * 0.5 = 3000 \text{ psf.}$$

In the above equation, the depth of soil is approximated as 20 ft, and the depth of rock to the foundation subgrade elevation is 19 ft. The unit weights of soil and rock are 140 pcf and 160 pcf, respectively, and the groundwater table occurs at the ground surface.

The static bearing pressure of the NI (8900 psf) will be more than twice this value. After consolidation under static NI bearing loads (conservatively assumed to be equal to 8900 psf at the depth under consideration, without reduction due to stress distribution), the corresponding average effective stress within a representative depth of 50 ft below the NI subgrade elevation may be represented as

$$\sigma' = [8900 \text{ psf} + (50/2) \text{ ft } (160-62.4) \text{ pcf}] * 0.5 = 6420 \text{ psf.}$$

Based on the above values, the peak interface strength friction angle ϕ_r could be greater than

$$\phi_r = [27 + 20 * \log_{10} (3000 * 144 \text{ psf} / 6420 \text{ psf})] = 63 \text{ degrees.}$$

For the sliding and bearing stability evaluations, the ϕ_r of the high-angle dipping joints and fracture was selected as 45 degrees. Use of ϕ_r of 45 degrees is considered conservative to represent discontinuity Set B below the top of sound rock, for both drained (effective) and undrained (total) stress conditions. For the portion of discontinuities in weathered rock and soil above sound rock, a friction angle of $\phi = 30$ degrees was used. This friction angle is considered appropriate, as it is similar to both the effective friction angle for clay seams and to the base (residual) siltstone interface friction angle, without asperities, as described

above. The influences of variations in these friction angles on stability are evaluated as a sensitivity check.

1.2.3 Vertical Joints (Discontinuity Sets C and D)

Based on the HNP foundation excavation mapping report (Ebasco, 1981), conditions of the vertical joints (discontinuity Sets C and D) are similar to the high-angle joints and fractures (discontinuity Set B). Therefore, ϕ_r of 45 and 30 degrees below and above top of sound rock, respectively, are considered appropriate for these joints.

2. Stability Evaluation Methods

The stability evaluations herein incorporate the application of NI sliding loads, bearing loads, and resistances provided along the rock discontinuities at HAR 2 and HAR 3. The active and passive forces acting on the NI sidewalls under seismic loading were calculated as part of these evaluations. Two types of evaluations were performed:

- The FS against sliding was calculated for each of the four NI orthogonal directions at HAR 2 and HAR 3, for a total of eight different two-dimensional profiles. Peak dynamic loads (bearing pressures, inertial NI sliding forces, and active force) and resistive forces (base shear friction and passive force) were used to calculate the force equilibrium of a series of five rock and soil wedges adjacent to and under the NI, and to calculate the resulting FS against sliding.
- The FS against bearing demand was calculated for the Plant West side of the containment (shield) building at HAR 2 and HAR 3. The Plant West direction was evaluated because it is the location of peak applied dynamic bearing pressure (generic design parameter of 35 ksf as specified in the AP1000 DCD). The driving and resisting forces over two wedges (a rock wedge under the NI and a passive wedge outside the NI) were used to calculate the force equilibrium and the resulting FS against peak dynamic bearing demand. A secondary calculation based on the method of Landanyi and Roy, 1971 (as presented in Wyllie, 1999), was also performed as confirmation for each case.

The methodologies used to evaluate FS against sliding and bearing demand are presented in Subsections 2.1 and 2.2 below, respectively:

2.1 Sliding Stability Evaluation

The following subsections describe the methodology (Section 2.1.1) and the selection of input parameters for the sliding stability evaluations (Section 2.1.2)

2.1.1 Sliding Stability Evaluation Methodology

The sliding stability methodology is presented in three subsections: a general description, followed by detailed descriptions of the five rock wedges evaluated in the model, and finally a description of the calculation of FS against sliding.

2.1.1.1 General Description

The sliding stability evaluations were based on the force equilibrium of five wedges representing the rock below and on the active and passive sides of the NI. Figure 2 shows

the configuration of the NI and associated rock and soil wedges considered in the sliding stability evaluations. Conservative assumptions were applied to convert the three-dimensional NI and subsurface configuration to an equivalent limited-width two-dimensional model, as described in Section 3.5. Two-dimensional profiles associated with each of the four orthogonal directions at HAR 2 and HAR 3 (total of eight profiles) were evaluated. The FS against sliding in each direction were then compared to minimum required value of 1.1.

Discontinuity resistances were based on the orientations and conditions of rock mass discontinuities as described in Section 1. Driving forces included the inertial lateral and vertical forces of the nuclear island due to the SSE and the external lateral forces acting on the active side of the NI. Dynamic forces were represented by equivalent static loads. These loads represented instantaneous peak forces computed on the basis of spectral accelerations from the NI foundation interface response spectrum (FIRS) and ground motion response spectrum (GMRS) for the HAR 2 and HAR 3 sites. In Figure 2, SSE seismic forces are directed to the left, with concentration of bearing load near the left side of the NI. Vertical forces associated with SSE loading were assumed to occur in the direction that causes the lowest FS against sliding.

Two sets of dipping discontinuities (based on apparent dip) were considered in the model, denoted as Set 1 (apparent dip down in the direction of SSE loading) and Set 2 (apparent dip in opposite direction). The dip angles from horizontal (β_1 and β_2) and strength properties in rock (ϕ_{1r} , ϕ_{2r} and c_{1r} , c_{2r}) were assigned based on the NI orthogonal direction under consideration; Set 1 was assigned properties consistent with the discontinuity Set (A or B) that dips down in the modeled direction of SSE loading. Set 2 was assigned properties of either discontinuity Set B or A that were not assigned to Set 1. Depth to sound rock was modeled separately on either side of the NI (D_{s1} and D_{s2}).

The length of the nuclear island perpendicular to the direction of sliding (denoted X) was assigned as the NI length of 255 ft in the Plant North-South dimension, and as the equivalent rectangle width of 124 ft in the Plant East-West dimension.

2.1.1.2 Rock Wedge Descriptions

Five rock and soil wedges are considered in the model. Three of the wedges contribute net driving forces (Wedges 1, 4, and 5) that must be resisted for stability, and two provide net resisting forces (Wedges 2 and 3). For each wedge, driving and/or resisting forces are contributed by the wedge self weight and lateral inertial force; whether these act as a driving or resisting force depends on the dip direction of the base of the wedge. Resisting forces are provided by friction and cohesion along the base and the sidewalls of each wedge. Groundwater table is conservatively modeled at site grade for all calculations. Figures 3a through 3e present summary diagrams of the forces acting on Wedges 1 through 5, respectively. An example MathCAD template that shows the details of the sliding stability evaluation for HAR 2 Plant West is presented as Attachment A.

The five wedges are described as follows:

- **Wedge 1** represents rock below the NI between the passive edge of the NI and a trial discontinuity that daylight at the NI subgrade a distance B_1 back from the edge of the NI. The concentrated fraction (P_1) of the NI weight (W_s) acting over Wedge 1 is applied

as a vertical driving force. B_L is the distance over which a net compressive load is applied to the NI subgrade during dynamic loading, based on WEC Report APP-GW-GLR-044 Rev. 0, and as described in Section 2.1.2.3. The trial distance B_1 is varied to find the lowest FS. Wedge 1 will tend to move downward relative to Wedge 3 prior to movement under dynamic loading, and shear resistance will develop along the vertical interface between Wedges 1 and 3. Wedge 1 imposes a lateral driving force (F_{lat1}) against the side of Wedge 3. Additional details of the Wedge 1 forces are presented in Figure 3a and in the MathCAD template in Attachment A.

- **Wedge 2** represents rock below the NI under distance B_2 (the difference between distance B_1 and B_L) behind the passive edge of the NI. The remaining fraction ($P_2 = 1 - P_1$) of the NI weight (W_s) acts over width B_2 . This wedge contributes an available resistance to sliding (denoted R_{lat2}). The available sliding resistance contributed by Wedge 2 is reduced by driving force F_{lat4} from Wedge 4 (see below), and is also limited by the available resistance to NI basemat sliding along the most critical interface near the NI subgrade over Wedge 2 (the waterproofing membrane, with design interface friction angle of 28.8 degrees, corresponding to coefficient of friction of 0.55). As described in Section 2.1.2.3, the net vertical structure load is reduced for buoyant and dynamic inertial forces to calculate the minimum available sliding resistance.

The net base shear resistance (R_{base}) is assigned as the lesser of the following:

- $R_{lat2} - F_{lat4}$, or
- Shear resistance along the most critical basemat interface over width B_2 (along the waterproofing membrane)

Additional details of the Wedge 2 forces are presented in Figure 3b and in the MathCAD template in Attachment A.

- **Wedge 3** represents rock and soil that provides passive resistance to sliding (denoted R_{lat3}) at the passive endwall of the NI. Wedge 3 is adjacent to the passive NI endwall and extends to the base of Wedge 1 (to depth D_1 below the NI subgrade). Concrete fill is required between the NI basemat sidewalls and sound rock (up to minimum elevation 227.5 ft) to allow transfer of lateral load from the bottom 6 ft of the NI to the adjacent rock. If trial B_1 is set to zero, D_1 is also zero, which represents passive resistance adjacent to the NI endwall only. Wedge 3 will tend to move upward relative to Wedge 1 prior to movement under dynamic loading, and shear resistance will develop along this interface. Shear resistance between Wedge 3 and the NI sidewalls above the foundation elevation is conservatively not considered in this evaluation. Likewise, passive resistance contribution from adjacent building surcharge over Wedge 3 is not considered.

The net passive resistance ($R_{passive}$) is calculated as R_{lat3} less F_{lat1} . If B_1 is set to zero, F_{lat1} and depth D_1 are both zero, and therefore $R_{passive}$ is the same as R_{lat3} (this represents passive resistance provided adjacent to the NI endwall only).

Additional details of the Wedge 3 forces are presented in Figure 3c and in the MathCAD template in Attachment A.

- **Wedge 4** represents rock that provides an active driving force (denoted F_{lat4}) to the back side of Wedge 2. This reduces the net sliding resistance provided by Wedge 2. Additional details of the Wedge 4 forces are presented in Figure 3d and in the MathCAD template in Attachment A.
- **Wedge 5** represents rock and soil that applies a driving force against the active endwall of the NI. If a building is present adjacent to the active side of the NI, the corresponding building surface surcharge (S_s) is incorporated in the calculation of these forces. A hydrostatic force also acts on the endwall; however, this hydrostatic force is balanced against the hydrostatic force on the opposite side of the NI.

Two separate methods are used to calculate the driving force on the active side of the NI. The first method is based on wedge equilibrium (resulting force is $F_{lat5.wedge}$). The second is based on the elastic force from compacted backfill, based on the elastic method presented in ASCE 4-98 (resulting force is $F_{lat5.backfill}$). This second method conservatively considers that the granular backfill is present from site grade to the NI subgrade elevation.

The net lateral active force on the NI endwall (F_{active}) is assigned as the greater of the following:

- $F_{lat5.wedge}$, or
- $F_{lat5.backfill}$

Additional details of the Wedge 5 forces are presented in Figure 3e and in the MathCAD template in Attachment A.

2.1.1.3 Evaluation of FS Against Sliding

Based on the input parameters, the stability of each wedge was calculated sequentially starting with Wedge 1. For Wedges 1, 4, and 5, the separate external lateral forces required for wedge stability (denoted F_{lat1} , F_{lat4} , and F_{lat5} , respectively) were calculated, which act as driving forces in the overall NI stability calculation. For Wedges 2 and 3, the additional external lateral forces that can be resisted while maintaining stability (denoted R_{lat2} and R_{lat3} , respectively) were calculated, which act as resisting forces in the overall NI stability calculation.

The inertial driving force from the NI during seismic loading ($F_{lat.struct}$) was calculated as presented in Section 2.1.2.4. The FS against sliding (FS_{slide}) was calculated directly as the ratio of the sum of lateral resisting forces to the sum of lateral driving forces, as follows:

$$FS_{slide} = (R_{passive} + R_{base}) / (F_{active} + F_{lat.struct})$$

The resulting FS_{slide} was then compared to the minimum allowable sliding FS ($FS_s = 1.1$) for evaluation of acceptable stability.

2.1.2 Selection of Input Parameters

The basis for selection of key input parameters to the sliding evaluation are presented below.

2.1.2.1 Discontinuity Orientation and Strength Parameters

The dip angles of discontinuity Sets 1 and 2 (β_1 and β_2) were assigned as the apparent dips of discontinuity Sets A and B (or Sets B and A) along the NI orthogonal axis depending on the direction under consideration, as summarized in Table 2. The apparent dip angles provide the best estimate of the average dip in the direction of movement. As noted previously, for movement to occur along the true dip directions, significant shearing of intact rock would be required. Therefore, use of the apparent dip angles is considered appropriate. Use of the true dip angles was evaluated as a sensitivity check (without the shearing of intact rock), as described in Section 3.4, but this is considered to represent an unrealistically conservative condition. The rock discontinuity strength parameters (ϕ_{1r} , ϕ_{2r} and c_{1r} , c_{2r}) were assigned based on the strength parameters for discontinuity Sets A and B presented in Section 1.2.

The vertical discontinuity Sets C and D were oriented approximately parallel to the NI orthogonal axes. Strength parameters for vertical discontinuity Sets C and D in soil and rock (ϕ_{vs} , ϕ_{vr} and c_{vs} , c_{vr}) were the same as those assigned for Set B. The wedge sidewalls were conservatively modeled parallel to the direction of seismic motion, so use of the at-rest lateral earth pressure coefficient is considered appropriate and conservative as described in Section 3.5.

Lateral at-rest earth pressure coefficients for soil and rock acting normal to vertical discontinuities along wedge sidewalls (K_{hr} and K_{hs}) were assigned as 0.5. The actual values of K_{hr} and K_{hs} are difficult to quantify along rock discontinuities. For granular materials, a lower value is common (such as $1 - \sin[35 \text{ deg}] = 0.42$) (Das, 1994), but the tight nature of the rock discontinuities and presence of asperities, as described in section 2.1.2.2, indicate that significantly higher normal forces will develop along the vertical discontinuities, especially upon application of shearing forces. Overconsolidation will also tend to increase the at-rest lateral earth pressure coefficients. Due to these uncertainties, the sensitivity of the evaluation results to variations in K_{hr} and K_{hs} was evaluated as described in Section 3.4.

2.1.2.2 Dynamic Rock and Soil Accelerations

The design peak accelerations for soil and rock adjacent to the NI were based on the GMRS at very small period (0.01 sec), which is the peak ground acceleration (PGA) at the top of the competent outcrop. The PGAs in the horizontal and vertical directions from the GMRS are presented in HAR FSAR Figure 2.5.2-307. Based on this, the design horizontal rock acceleration (a_{rh}) is 0.14g, and the vertical rock acceleration (a_{rv}) is 0.11g, at the top of sound rock.

For soil and weathered rock above sound rock, design accelerations (a_{rhs} and a_{rvs}) were increased by a factor F of 1.2 to incorporate potential effects of additional site amplification between sound rock and ground surface. Soil depths range from a few to 31 ft below site grade, and therefore only limited amplification is expected. Note that the GMRS spectral accelerations incorporate site amplification effects between hard rock and the GMRS elevation. This factor F is based on Site Class C (IBC, 2006), and is considered conservative to represent the entire soil profile between site grade and sound rock. Nonetheless, the influence of variations in F on the evaluation results is evaluated as a sensitivity check in Section 3.4.

2.1.2.3 Nuclear Island Vertical Load Distribution

The total dead weight of the nuclear island (W_s) is 286,387 kips, and the buoyant force acting on the nuclear island (W_b) is 76,003 kips. During seismic loading, the subgrade bearing pressures will be concentrated near the outer edge (passive edge) of the NI. The peak vertical foundation pressure distributions across the NI footprint during seismic loading in the Plant East and Plant West directions, based on 2D SASSI analyses, are presented in WEC Report APP-GW-GLR-044, R0, also known as Technical Report TR-85 (Figure 2.4-2 of that report) (WEC, 2006). The bearing pressure distribution in the Plant West direction is more concentrated near the passive edge than in the Plant East direction, due to affects of the curved edge of the containment building on the Plant West side of the NI.

These foundation pressure distributions in Figure 2.4-2 of the WEC report were used to estimate relationships between the trial distance B_1 from the NI passive edge and the corresponding fraction of the NI structure weight (P_1) acting over this distance B_1 for motions in the Plant East and Plant West directions. These relationships were developed as follows:

1. The foundation pressures at representative distances B_1 from the NI passive edge were scaled from Figure 2.4-2 of WEC report TR-85.
2. The average pressure acting over representative width intervals was calculated (ksf), as was the load acting over each interval (kip/ft, or kips per unit length of NI into the section).
3. The total load was calculated as the sum of the interval loads. The fraction of the total load applied over each interval was then calculated.
4. The cumulative load with increasing distance B_1 was calculated by sequentially adding the fractions over adjacent intervals.

Figure 4 presents the load profile from Figure 2.4-2 of WEC report TR-85, and the corresponding relationship between B_1 and P_1 for the Plant West direction. Relationships between B_1 and P_1 in the Plant North and Plant South directions were estimated based on the foundation pressure distribution in the Plant West direction, with distances increased by the ratio of NI widths in the Plant North-South to the Plant East-West directions (255 ft / 160 ft = 1.59). This ratio stretches the bearing pressure profile to match the longer Plant North-South dimension. Table 3 lists the resulting relationships between B_1 and P_1 for seismic motion in the Plant North, South, East, and West directions.

The total vertical NI structure load acting over Wedge 1 (over distance B_1) was calculated as the product of W_s , P_1 , and an additional factor, C_{bp} . The factor C_{bp} was used to scale up the applied load so that the peak foundation pressure near the Plant West side of the NI is 35 ksf (the DCD site parameter for dynamic bearing demand). The peak pressure of 26.5 ksf is indicated at 6 ft from the Plant West side of the NI on WEC Report TR-85, Figure 2.4-2. The value of C_{bp} was therefore calculated as $35 / 26.5 = 1.32$. Use of this factor C_{bp} is conservative because the HAR FIRS is enveloped by the AP1000 design response spectrum, and therefore the peak HAR NI bearing load is less than 35 ksf. The value of C_{bp} was nonetheless used to allow direct comparison of the sliding stability evaluation results with consideration of the DCD site parameter for dynamic bearing pressure of 35 ksf.

The fraction of the NI dead weight acting over Wedge 2 (over distance B_2) was calculated as $P_2 = (1 - P_1)$. However, not all of this NI dead weight was considered to contribute to Wedge 2 sliding resistance. Rather, the smaller buoyant dead weight was used. A further reduction in the dead weight was made to account for the effective vertical acceleration of the NI mass. The vertical force reduction due to acceleration was calculated as $C_{asv}(a_{sv})(W_s)(P_2)$, where C_{asv} is a coefficient equal to 0.4, as described in Section 2.1.2.4. The combination of buoyant and effective vertical inertial forces provides a conservative value of the normal force available for base sliding resistance. Calculation of a_{sv} is described in Section 2.1.2.4.

2.1.2.4 Nuclear Island Inertial Forces

The HAR-specific peak NI inertial forces under seismic loading in the Plant North-South (X), Plant East-West (Y), and vertical (Z) directions were calculated based on guidance from WEC. WEC has performed a HAR-specific SSI analysis as presented in their calculation HAG-1000-S2C-802. In that calculation, WEC presented the in-structure response spectra for HAR conditions compared with the 0.3g SSE design spectra at six key locations within the NI. Those WEC results were used to calculate the HAR-specific peak NI inertial forces as follows:

1. The ratio of the peak structure response between HAR and the 0.3g case (at 100 Hz) was calculated for each of these six locations, in three orthogonal directions (Plant North-South, Plant East-West, and vertical).
2. The average of these ratios from the three locations nearest site grade was calculated for each of the three orthogonal directions. These averages are considered representative of the ratio of peak inertial forces between HAR and the WEC 0.3g SSE design conditions.
3. The absolute peak seismic reactions (due to peak NI inertial forces) at the bottom of the basemat for the 0.3g SSE design case were obtained from WEC for each of the three orthogonal directions. The values envelop the highest reactions among the various soil conditions evaluated by WEC.
4. The HAR-specific peak NI inertial forces under seismic loading in each of the three orthogonal directions (denoted F_x , F_y , and F_z) were calculated as the product of items 2 and 3 above.

The peak lateral NI inertial force used for the sliding evaluation ($F_{lat,struct}$) was assigned as $F_x = 50,248$ kips for the Plant North-South sliding analyses, and as $F_y = 60,634$ kips for the Plant East-West sliding analyses.

The peak vertical NI inertial force was assigned as $F_z = 51,307$ kips. The equivalent vertical NI structure acceleration, a_{sv} , was calculated as:

$$a_{sv} = F_z / W_s = 0.179g$$

Section 3.8.5.4.1 of the DCD states, "The safe shutdown earthquake loads are applied as equivalent static loads using the assumption that while maximum response from one direction occurs, the responses from the other two directions are 40 percent of the maximum. Combinations of the three directions of the safe shutdown earthquake are considered." Based on this, a_{sv} was multiplied by the factor $C_{asv} = 0.4$ in the force

equilibrium equations for Wedge 2. Lateral forces perpendicular to the NI axis direction under evaluation were not considered to have any net affect on the sliding stability evaluation, since these forces are orthogonal to the modeled loading direction.

The above values of $F_{lat.struct}$ and a_{sv} represent the inertial structure loads for the sliding stability evaluations.

2.1.2.5 Adjacent Structure Surcharge Loads (S_s)

Structures will be constructed adjacent to the Plant North, East, and South sides of the NI. These structures will add surface surcharge (S_s) contributions to the lateral force on the active sides of the NIs. Following the requirements in the DCD, increases in lateral forces on the passive sides of the NIs due to surcharge effects are not included in the stability analyses.

The adjacent structure surcharge loads were provided by WEC as follows:

- Turbine Building (Plant North of NI): $S_s = 1700$ psf
- Annex Building (Plant East of NI): $S_s = 1700$ psf
- Radwaste Building (Plant South of NI): $S_s = 520$ psf

The above surcharge values were included in the Wedge 5 equilibrium equations as shown on Figure 3e.

2.2 Bearing Capacity Evaluation Methodology

Supplemental evaluations of bearing capacity along oriented rock discontinuities were performed as described in this section. The evaluations correspond to the Plant West side of the circular shield buildings at HAR 2 and HAR 3, which are the locations of peak dynamic foundation bearing pressures (design parameter of 35 ksf). The force equilibrium of two rock and soil wedges, similar to Wedges 1 and 3 in the sliding evaluation discussed in Section 2.1.1.2, were evaluated to calculate the resulting FS against peak dynamic bearing demand. Secondary bearing capacity calculations based on the method of Landanyi and Roy, 1971 (as presented in Wyllie, 1999), were also performed as an order-of-magnitude confirmation of the first method. Section 2.2.1 describes the wedge force equilibrium method (Method 1). Section 2.2.2 describes the secondary method based on Landanyi and Roy, 1971 (Method 2).

2.2.1 Bearing Capacity Evaluation Method 1 – Wedge Force Equilibrium

Figure 5 shows the configuration of the NI and two associated rock and soil wedges considered in the bearing capacity evaluations. Orientations of discontinuity Sets 1 and 2 were defined the same as for the sliding evaluations described in Section 2.1.1.1. Only Wedges 1 and 3 were considered in the bearing capacity evaluations. The weighted average S_u along the base of Wedge 3 in rock (bedding assigned as discontinuity Set 2 for these evaluations) was calculated based on the relative depths of Set 2 above the NI subgrade elevation ($D_{emb} - D_{s2}$) with S_u of 1500 psf and below the subgrade elevation (D_1) with S_u of 2200 psf, which is a function of distance B_1 . The dimension of Wedges 1 and 3 perpendicular to the direction of seismic loading (denoted X_b) is the width of the circular shield building corresponding to distance B_1 , as shown on Figure 5.

An example MathCAD template that shows the details of bearing capacity evaluation Method 1 for HAR 2 Plant West is presented as Attachment B. The force equilibrium equations for Wedges 1 and 3 were very similar to those used for the sliding stability evaluation, with three exceptions:

- First, the total vertical NI structure load acting over Wedge 1 was calculated as the product of the peak bearing pressure at any point under the NI (σ_{peak} , which is assigned as a trial value), the subscribed area of the circular shield building within trial distance B_1 (denoted A_{load}), and the ratio P_{1b} that relates the average bearing pressure applied within distance B_1 to σ_{peak} . The basis for the B_1 to P_{1b} relationship is described below.
- Second, an additional lateral driving force due to the seismic inertia of the NI was applied horizontally to Wedge 1 ($F_{\text{lat1,traction}}$). This lateral force is proportional to the fraction of the total NI vertical weight applied over Wedge 1.
- Finally, the distance X_b was defined differently than the distance X used in the sliding evaluations, as shown on Figure 5.

The relationship between distance B_1 and the corresponding peak pressure ratio P_{1b} is derived based on the shape of the foundation bearing pressure distribution presented in WEC Report TR-85, Figure 2.4-2. The bearing pressure distribution is the same as used to derive the B_1 to P_1 relationship for the sliding evaluations, as shown on Figure 4. The values of P_{1b} corresponding to various distances B_1 were calculated by the following steps:

- First, the representative foundation pressure at various distances B_1 were determined as shown in Figure 4. Additional distances B_1 were added between points shown on Figure 4; for example, at B_1 of 3 ft, the pressure was calculated as 25.15 psf (the average of 23.8 and 26.5 psf for adjacent distances B_1 of 0 and 6 ft).
- Second, the fractions of the peak foundation pressure at various distances B_1 were calculated, based on a peak foundation pressure (26.5 psf) at B_1 of 6 ft. For example, at B_1 of 3 ft, the fraction is 25.15 psf / 26.5 psf = 0.95.
- Third, the average fraction of peak foundation pressure (P_i) was calculated for each representative interval of B_1 . For example, for the interval from 3 to 6 ft, the fraction P_i is 0.975 (the average of 0.95 and 1.0 at adjacent distances B_1 of 3 and 6 ft).
- Fourth, the areas under the curved NI shield building (A_i) within each representative interval of B_1 were calculated. Equations used to calculate the total area under the curved side of the shield building corresponding to distance B_1 are the same as presented in the MathCAD template in Attachment B for calculation of A_{load} . For example, for B_1 of 3 ft, the corresponding distance X_b is 41.3 ft and interval area A_i under the shield building between B_1 of 0 to 3 ft is 83 square feet (sf). For B_1 of 6 ft, the total area is 233 sf, so the interval area A_i between B_1 of 3 to 6 ft is (233 sf - 83 sf) = 150 sf.
- Fifth, the weighted average fraction of peak foundation pressure corresponding to distance B_1 was calculated based on the sum of the products of A_i and P_i for each interval within distance B_1 , divided by the total area within distance B_1 . This is defined as P_{1b} . For example, for distance B_1 of 6 ft, P_{1b} is calculated based on the intervals within distance B_1 of 6 ft (from 0 to 3 ft and from 3 to 6 ft in this case), as follows:

$$P_{1b} \text{ (at } B_1 \text{ of 6 ft)} = (83 \text{ sf} \times 0.924 + 150 \text{ sf} \times 0.975) / (83 \text{ sf} + 150 \text{ sf}) = 0.96$$

Values of P_{1b} were calculated for various distances of B_1 to encompass the radius of the shield building. The resulting B_1 to P_{1b} relationship is presented in the MathCAD template in Attachment B.

For the corresponding trial values of σ_{peak} and B_1 , the external lateral force required for Wedge 1 stability (F_{lat1}) was calculated. Likewise, the lateral resistance provided by Wedge 3 (R_{lat3}) was calculated. The trial value of σ_{peak} was iterated until force equilibrium between Wedges 1 and 3 was obtained ($F_{\text{lat1}} = R_{\text{lat3}}$). The corresponding value of σ_{peak} at equilibrium is defined as σ_{ult} for the trial distance B_1 . The FS against bearing demand (FS_b) for the trial distance B_1 was calculated as the ratio of σ_{ult} to the peak dynamic bearing demand (σ_{demand}) of 35 ksf. This process was repeated for various distances B_1 to find the critical low value of FS_b .

This method modeled bearing loads near the circular edge of the shield building. As stated in Attachment B, the model is only considered valid for distances B_1 of approximately 55 ft or less, which bounds the most critical portion of the foundation loading profile. Since the Plant West building edge is circular, loads may be applied in various directions from Plant Southwest to Plant West with similar modeled structure geometry. Therefore, both the Plant West apparent dips and the true dips of discontinuity Sets A and B were input into the evaluation (as Sets 2 and 1, respectively) as separate cases. The sources of conservatism inherent in the sliding stability evaluations, as described in Section 3.5, are also applicable to bearing capacity evaluation Method 1.

2.2.2 Bearing Capacity Evaluation Method 2 – Landanyi and Roy, 1971

The method of Landanyi and Roy, 1971 (as presented in Wyllie, 1999), was used as an order-of-magnitude confirmation of the FS against bearing demand. In this method, the ultimate bearing capacity provided by a foundation rock wedge (Wedge A) was calculated based on the available lateral passive resistance provided by the rock wedge adjacent to the foundation (Wedge B). The geometry and interface strength parameters for Wedges A and B are shown in Figure 6.

In this method, the highest bearing pressure that can be supported over the rectangular upper surface of Wedge A under wedge force equilibrium ($\sigma_{\text{peak_average}}$) was first calculated based on the orientations and interface strength parameters for discontinuity Sets 1 and 2, and the trial distance B_1 . The corresponding highest bearing pressure within the subscribed area of the circular shield building within trial distance B_1 ($\sigma_{\text{peak_struct}}$) was then calculated. The corresponding absolute peak bearing pressure that can be applied at any point under the NI, defined as the ultimate bearing capacity (σ_{ult}) was then calculated based on the ratio P_{1b} that relates the average bearing pressure applied within distance B_1 to σ_{peak} . The basis for the B_1 to P_{1b} relationship is presented in Subsection 2.2.1.

The FS against bearing demand (FS_b) for the trial distance B_1 was calculated as the ratio of σ_{ult} to the peak dynamic bearing demand (σ_{demand}) of 35 ksf. This process was repeated for various distances B_1 to find the critical low value of FS_b .

This bearing capacity evaluation Method 2 incorporates several approximations and limitations that are less representative of the HAR subsurface conditions than Method 1.

- First, only rock and discontinuities at and below the foundation elevation are explicitly modeled, though rock and soil above the foundation elevation over Wedge B are incorporated as an equivalent vertical surcharge pressure. This conservative approximation neglects the significant contribution from shear resistance above the foundation elevation.
- Second, Method 2 models the foundation as an infinitely long strip, such that wedge side resistances are not considered. Neglecting the side friction is a conservative approximation for the finite length wedge configurations near the curved Plant West sides of the NIs.
- Finally, the method does not account for lateral loads. This is an unconservative limitation of this method for calculation of dynamic bearing capacity. However, considering the relatively small ratio of lateral NI loads to peak dynamic bearing loads incorporated in the bearing capacity evaluation, the effect of this limitation on the resulting FS_b are likely offset by the other conservative model limitations described above.

The other sources of conservatism inherent in the sliding stability evaluations, as described in Section 3.5, are also applicable to bearing capacity evaluation Method 2. Due to the above additional limitations, the results from Method 2 are considered approximate and used only as an order-of-magnitude confirmation of the results from Method 1.

3. Stability Evaluation Results

Results of the stability evaluation cases are summarized below. This summary includes results of the sliding stability evaluations, minimum compressive strength of the concrete fill around the NI to sufficiently transfer sliding forces, results of bearing capacity evaluations, and evaluation of sensitivity of the evaluation results to variations in key input parameters. This section concludes with a discussion of sources of conservatism in the evaluations.

3.1 Sliding Stability Evaluation Results

Table 4 presents the key input parameters used in the sliding stability evaluations, the net driving (lateral) forces $F_{lat.struct}$ and F_{active} , the net resisting forces R_{base} and $R_{passive}$, and the resulting FS against sliding (FS_{slide}) for each of the NI orthogonal directions at HAR 2 and HAR 3.

For each NI orthogonal direction, multiple iterations were performed to identify the critical value of B_1 that results in the lowest FS_{slide} . Two results are presented for each NI orthogonal direction. The first result corresponds to the distance B_1 that resulted in the lowest FS_{slide} . The second result corresponds to B_1 of zero, such that bearing pressures did not contribute to the lateral sliding forces. This second result represents a typical sliding evaluation decoupled from the bearing capacity evaluation.

As shown in Table 4, FS_{slide} is 1.75 or greater for each case evaluated; therefore, each of these results satisfies the minimum FS of 1.1 required against sliding. The lowest FS_{slide} corresponds to seismic loading in the Plant West direction at HAR 3, coincident with B_1 of

15 ft. The critical FS in the Plant South direction at HAR 3 also corresponds to B_1 of 15 ft. For the other six profiles considered (HAR 2 North, East, South and West, and HAR 3 North and East), the lowest FS_{slide} corresponds to B_1 of zero, indicating that the simultaneous application of NI bearing pressures does not reduce FS_{slide} .

The resulting FS_{slide} for each of the Plant North and Plant East profiles at HAR 2 and HAR 3 were very high, with FS_{slide} greater than 12 for each case. This is due in part to the steep dip angle and high friction angle of discontinuity Set B, which is oriented to resist sliding in the Plant North and Plant East directions.

Table 4 also lists the passive force required to provide a minimum FS_{slide} of 1.1 for each profile. As shown, for six of the eight profiles, no passive force is required. For the Plant West profiles at HAR 2 and HAR 3, only 17 and 22 percent of the available net passive resistances are needed to provide the minimum FS_{slide} of 1.1, respectively.

3.2 Compressive Strength of Concrete Fill to Resist Sliding Forces

As shown in Table 4, the largest net passive resistance required to provide a minimum FS of 1.1 is 3.02×10^4 kips along the Plant West side of HAR 2. This net passive resistance will be transferred to the rock mass through the concrete fill adjacent to the NI basemat sidewalls below elevation 227.5 ft. The NI dimensions are 255 ft in the Plant North-South direction and the vertical thickness of concrete fill between sound rock and the NI sidewalls will be at least 6 ft.

The corresponding minimum compressive strength of the concrete (f'_c) required to transfer the above maximum net passive force to the rock mass in the HAR 2 Plant West direction is calculated based on a conservative load factor of 1.3 and resistance factor of 0.7 as follows:

$$f'_c = (3.02 \times 10^4 \text{ kip}) \times 1000 \times 1.3 / (0.7 \times 6 \text{ ft} \times 255 \text{ ft}) = 3.67 \times 10^4 \text{ psf} = 255 \text{ psi}$$

The concrete fill will have a minimum unconfined compressive strength of 2500 psi, which is significantly greater than the strength required to transfer the required passive force to the adjacent rock mass.

3.3 Bearing Capacity Evaluation Results

Table 5 presents the resulting FS against dynamic bearing demand (FS_b) for each case evaluated using Method 1. As shown in Table 5, the dynamic FS_b is greater than 2.0 for each of the four cases analyzed. The lowest FS_b of 2.6 corresponds to the Plant West side of HAR 3 based on the true dip values. The resulting FS_b based on the apparent dip values are higher. For the reasons discussed in Section 3.5, use of the true dip angles in the stability evaluations is considered excessively conservative.

FS_b values resulting from bearing capacity evaluation Method 2 (based on Landanyi and Roy, 1971) are also each greater than 2.0. The lowest FS_b values correspond to very small distance B_1 (5 to 7 ft); at B_1 of 20 ft, the FS_b values are 2.5 or greater for each case. As discussed in Section 2.2.2, various limitations of Method 2 make it less representative of the HAR subsurface conditions than Method 1. In view of these limitations, the results of Method 2 provide an order of magnitude confirmation of the results of Method 1.

3.4 Sensitivity of Sliding Stability to Variations in Input Parameters

Sensitivity of FS_{slide} to variations in several key input parameters was evaluated as presented below. Descriptions of parameter variations and results of the corresponding sensitivity cases are summarized in Table 6. The Plant West profile at HAR 3 was used as the benchmark case for most of the sensitivity checks, because it corresponds to the lowest FS_{slide} as summarized in Table 4.

Following are key observations from these sensitivity checks:

- **Effect of Dip Angle:** As shown in Table 6, use of the true dip values instead of the apparent dip values for discontinuity Sets 1 and 2 resulted in a small to a negligible reduction (less than 5 percent) of the calculated FS_{slide} for three of the four cases evaluated. In one case (HAR2-W-Sens1), the reduction was greater but still resulted in a high FS_{slide} . In this case, the original result (HAR2-W1 in Table 4) was based on a very flat apparent dip angle for Set 2, which resulted in a relatively higher passive resistance and FS_{slide} than the other cases in the Plant West or South directions. These sensitivity analyses did not consider the beneficial effects of shearing through rock, which would need to occur to allow mobilization in the true dip directions, as discussed previously. If shearing through rock were accounted for, the resistance to sliding would have been significantly higher.
- **Effect of Strength Parameter Variations:** As shown in Table 6, variations in the strength parameters along discontinuity Sets 1 and 2 (ϕ_1 , ϕ_2 , c_2) influence the resulting FS_{slide} . However, even when using excessively conservative values of these parameters, the resulting FS_{slide} values are still greater than 1.44 and are therefore acceptable.
- **Effects of Sidewall Resistance:** Variations in the parameters affecting the sidewall resistance (ϕ_{vr} , ϕ_{vs} , K_{hr} , and K_{hs}) had little influence on the resulting FS_{slide} (less than 2 percent reductions). Most of the resistance to sliding is provided by the dipping discontinuities, not the wedge sidewalls, since the normal forces along the sidewalls are limited to the at-rest conditions. Therefore, while the true values of K_{hr} and K_{hs} in the sidewall shear computation are difficult to quantify for the jointed rock mass, these parameters have relatively little influence on the overall sliding stability results.
- **Effects of Peak Ground Acceleration in Soil:** Variation of the peak ground accelerations of soil between site grade and sound rock (a_{rth} and a_{rvs}) from the estimated value of $1.2 \times (a_{rh}$ and $a_{rv})$ to $1.5 \times (a_{rh}$ and $a_{rv})$ has a small affect on FS_{slide} (approximately 8 percent reduction). However, since this parameter represents the average affects on soil in the layer above rock (not just at site grade), use of $1.2 \times (a_{rh}$ and $a_{rv})$ is considered conservative. Even if $1.5 \times (a_{rh}$ and $a_{rv})$ is used, the FS results are still greater than 1.6 and are therefore acceptable. The affect of this change is greatest at HAR 3 Plant West compared to the other sections, due to the relatively large depth of soil on the Plant West side of HAR 3.
- **Effects of direction of vertical rock and soil accelerations:** The full peak vertical rock and soil accelerations (a_{rv} and a_{rvs}) are modeled upward (as uplift) for each of the cases in Table 4. Application of 40 percent of these peak vertical accelerations in the downward direction results in a slight increase in the FS_{slide} (about 5 percent). The

upward orientations for vertical rock and soil accelerations used in the standard cases are therefore conservative.

3.5 Sources of Conservatism

Following are primary sources of conservatism in the sliding and bearing capacity stability evaluations:

- **Two Dimensional Model:** Use of a two-dimensional model to represent the complex three-dimensional NI interface with the underlying dipping bedding and high-angle discontinuities required conservative simplifications. The strike of the bedding features (discontinuity Set A) and high-angle joints (discontinuity Set B) are actually oriented at a skew of approximately 20 to 40 degrees from the NI orthogonal axes and to the vertical joint Sets C and D. Based on this true configuration, as load is applied down- or up-dip along these dipping discontinuities, a high normal force will develop along at least one vertical joint interface (Set C or D) that forms a "sidewall" of the loaded wedge. Due to the very tight nature of Sets C and D and high interface friction angle, a corresponding high frictional resistance will develop along this discontinuity. In the two-dimensional model, no such normal force increase is considered to develop on the vertical sidewalls – they are modeled as parallel to the direction of motion (perpendicular to strike Sets 1 and 2), and only at-rest normal forces are considered for the friction force along the vertical wedge sidewalls.
- **Friction Angle of Discontinuity Sets B, C, and D:** The value of ϕ_{vr} and ϕ_{lr} of 45 degrees, while a high friction angle, likely under-represents the true resistance provided by the high-angle and vertical joints (Sets B, C, and D). In this evaluation, these joints are modeled as continuous planes. As described in Section 1.2.2, these vertical joints were observed at HNP to frequently initiate and terminate vertically at interfaces with bedding planes, and often indicate deviations from planar of several feet over the mapped extent. These deviations from plane would require significant shearing of intact rock prior to failure, resulting in a very high equivalent friction value.
- **Distance Between Discontinuities:** The model conservatively assumes that for a given dimension B_1 , parallel discontinuity planes are present at the locations of the bottoms of Wedge 2 and 3. Such discontinuities are not necessarily present at these modeled locations.
- **NI Sidewall Shear Resistance:** Interface shear resistances between backfill materials and the vertical sides of the NI walls were not included in the stability evaluations. These interfaces will actually provide additional resistance to sliding, and excluding them is conservative.
- **Peak Dynamic Bearing Pressure:** The AP1000 design parameter for dynamic bearing pressure is 35 ksf, corresponding to the 0.3g SSE design event. As discussed in the WEC response to RAI-TR85-SEB1-03 (WEC, 2009), this peak dynamic bearing pressure corresponds to hard rock conditions with no side soil. For a firm rock site (such as HAR), WEC indicates that the peak dynamic bearing pressure is 27.9 ksf for the 0.3g SSE event. The HAR-specific peak dynamic bearing pressure will be significantly less than even this value because the HAR GMRS and FIRS are bounded by the 0.3g SSE design

spectra at all structural frequencies. For these reasons, use of 35 ksf as the peak bearing pressure in these HAR-specific sliding stability and bearing capacity evaluations is considered very conservative.

- **Minimum FS_b of 2.0 against Dynamic Loads:** A minimum FS_b against the peak dynamic bearing pressure at the extreme Plant West side of the NIs less than 2.0 is considered justified. A minimum FS_b of 1.5 against peak seismic loads for safety-related structures has been suggested in the past, as presented in Table 7.4 of ASCE 1980. Use of such a lower, justifiable minimum FS_b would provide larger margins of safety than considered herein. These and other sources of conservatism in the analyses provide assurance that the results in Tables 4 through 6 envelop the actual conditions at HAR 2 and HAR 3.

4. Supplemental Responses to NRC RAIs

This memorandum provides the additional information requested by NRC in RAIs 02.05.04-8, 11, and 14, and by informal requests during the HAR FSAR Section 2.5 NRC site visit in October 2008, as follows:

- The dynamic active forces acting on the NI sidewalls, and the available net dynamic passive forces available at the NI sidewalls, are presented in Table 4. The methodology applied to determine these forces is described in Section 2.1 of this memorandum. This information was requested in RAI 02.05.04-8.
- The influence of adjacent structure surcharge loads on the NI active forces was incorporated in the evaluations as described in Section 2.1. This information was requested in RAI 02.05.04-11.
- Supplemental engineering data on NI backfill materials are presented in this memorandum. Concrete fill will be placed between the NI sidewalls and rock excavation below minimum elevation of 227.5 ft about the perimeter of each NI. The required passive force will be fully transferred from the NI to the surrounding rock by this concrete fill, such that compacted backfill above elevation 227.5 ft. is not required to prevent sliding. An inspections, test, analyses, and acceptance criteria (ITAAC) specifying the concrete fill minimum elevation of 227.5 ft and minimum UCS of 2500 psi will be added to Rev. 1 of the HAR FSAR. This information was requested in RAI 02.05.04-14.

Regarding additional information informally requested during the HAR FSAR Section 2.5 NRC site visit in October 2008:

- The sliding and bearing capacity evaluations presented in this memorandum specifically incorporate planes of weakness relative to the typical rock mass. Discontinuity Set A models the properties of bedding-plane oriented clay seams within rock, with a low S_u of 1500 psf to 2200 psf. Intermittent rock core intervals with GSI values less than the "lower bound" values of 54 (HAR 2) and 48 (HAR 3) are present at HAR 2 and HAR 3, as addressed in the applicant response to RAI 02.05.04-13. Such intervals are conservatively modeled as discontinuity Set A in these stability evaluations; therefore,

the effects of GSI values less than the "lower bound values" are explicitly considered in the sliding and bearing capacity evaluations presented in this memorandum.

- The bearing capacity evaluations explicitly consider the orientations and conditions of the HAR rock discontinuity sets. The corresponding FS values under peak dynamic bearing loads, as presented in Table 5, are acceptable.

5. Description of Planned Revisions to HAR FSAR 2.5.4

This section describes planned HAR FSAR Subsection 2.5.4 revisions based on the supplemental information presented in this memorandum.

- Subsection "2.5.4.5.3 - Properties of Backfill Adjacent to Nuclear Islands" will be amended to add the commitment to use concrete fill between sound rock and the NI basemat to minimum elevation 227.5 ft.
- New Subsection "2.5.4.10.1.1.4 - Oriented Rock Discontinuity Model" will be added to the bearing capacity methodology descriptions. This subsection will include a brief summary of the information presented in Section 2.2 of this memorandum.
- Subsection 2.5.4.10.1.2 will be renamed "Rock Mass and Discontinuity Strength Parameters for Bearing Capacity Analyses." Current contents of Subsection 2.5.4.10.1.2 will be lowered one level and renamed "Subsection 2.5.4.10.1.2.1 - Rock Mass Strength Parameters."
- New Subsection "2.5.4.10.1.2.2 - Rock Discontinuity Strength Parameters" will be added, which will include a brief summary of strength properties of discontinuity Sets A, B, C, and D as presented in Section 1.2 of this memorandum.
- Subsection 2.5.4.10.1.3 will be subdivided into lower-level subsections. Current contents of Subsection 2.5.4.10.1.3 will be subdivided into Subsection "2.5.4.10.1.3.1 - General Bearing Capacity Method Results," Subsection "2.5.4.10.1.3.2 - Empirical Method Results," and Subsection "2.5.4.10.1.3.3 - Two-dimensional Finite Element Modeling Results."
- New Subsection "2.5.4.10.1.3.4 - Oriented Rock Discontinuity Model Results" will be added, presenting a summary of Section 3.3 of this memorandum, specifically the values of FS_b against dynamic bearing loads from Methods 1 and 2.
- Subsection "2.5.4.10.2 - Resistance to Sliding" will be rewritten to include a brief summary of the sliding evaluation methodology and results in Sections 2.1 and 3.1 of this memorandum. Memorandum Figure 2 and Table 4 will be added to the FSAR.
- Subsection "2.5.4.10.4 - At-Rest Lateral Earth Pressures" will be significantly modified to incorporate the results of this memorandum. The subsection will be subdivided into two lower-level subsections. Current contents of Subsection 2.5.4.10.4 will be moved to lower-level Subsection "2.5.4.10.4.1 - Static Lateral Earth Pressures."
- New Subsection "2.5.4.10.4.2 - Dynamic Lateral Active and Passive Forces" will be added. Cross-references to memorandum Table 4 (to be called out in new FSAR Subsection 2.5.4.10.2), listing the active and passive dynamic forces on each side of each

NI, will be added. This will include the maximum required passive forces required to resist sliding with an FS_{slide} of 1.1 on each side of each NI, and the corresponding fraction of the available passive forces that may be required.

- A new ITAAC specifying the concrete fill below elevation 227.5 ft will be added to COLA Part 10 as Table 3.8-3.

6. References

- ASCE. 1998. *Seismic Analysis of Safety-Related Nuclear Structures and Commentary*. Report ASCE 4-98.
- ASCE. 1980. *Structural Analysis and Design of Nuclear Plant Facilities*.
- Coduto, Donald P. 1994. *Foundation Design – Principles and Practice*. Prentice Hall.
- Das, Braja M. 1994. *Principles of Geotechnical Engineering*. PWS Publishing.
- Ebasco Services Incorporated. 1981. *Final Geologic Report on Foundation Conditions, Power Plant, Dams and Related Structures – Shearon Harris Nuclear Power Plant*.
- FHWA. 1997. *Geotechnical Engineering Circular No. 3. Design Guidance: Geotechnical Earthquake Engineering for Highways. Volume I – Design Principles*. Publication No. FHWA-SA-97-076. May.
- International Code Council. 2006. *International Building Code (IBC)*.
- Landanyi, B. and A. Roy. 1971. "Some Aspects of Bearing Capacity of Rock Mass." Proceedings of the 7th Canadian Symposium on Rock Mechanics, Edmundton.
- Mitchell, James K. 1992. *Fundamentals of Soil Behavior*. Second Edition. Wylie Interscience.
- USACE 1994. *Rock Foundations*. EM 1110-1-2908.
- WEC. 2009. Response from WEC to CH2M HILL Request for Information (RFI) No. 361. January 22.
- WEC. 2009. Response from WEC response to NRC RAI-TR85-SEB1-03, Rev. 1. January 9.
- WEC. 2008. Calculation HAG-1000-S2C-802, Rev. 0. "Site Specific SSI Analysis of Shearon Harris Site." January 28.
- WEC. 2006. Report APP-GW-GLR-044 Rev. 0. *AP1000 Standard Combined License Technical Report – Nuclear Island Basemat and Foundation*. TR-85. Westinghouse Electric Company LLC, Pittsburgh, PA.
- Wyllie, D. 1999. Second Edition. *Foundations on Rock*. Chapman & Hall, London.

Tables

Table 1
Summary of Discontinuity Set Orientations

Discontinuity Set	Description	Dip Angle	Dip Azimuth	Strike Azimuth	Source of Data
		(Deg. from horizontal)	(Deg. clockwise from State Plane North)	(Deg. clockwise from State Plane North)	
HAR 2					
Set A	Bedding & Associated Fractures	6 to 8.9 (8.9)	75.5 to 96 (91)	(1)	Marker beds, shear-wave velocity profiles, and acoustic televiewer features (FSAR Table 2.5.4-201)
Set B	High Angle Dipping Joints	66	308	38	Acoustic televiewer features (FSAR Figure 2.5.4-216A)
Set C	Vertical Joints	Vertical	N. A.	40-50 (45)	Geologic reconnaissance (FSAR Section 2.5.1.4.2)
Set D	Vertical Joints	Vertical	N. A.	330-340 (335)	Geologic reconnaissance (FSAR Section 2.5.1.4.2)
HAR 3					
Set A	Bedding & Associated Fractures	19.9 to 23.2 (23.2)	109 to 114 (113.6)	(23.6)	Marker beds, shear-wave velocity profiles, and acoustic televiewer features (FSAR Table 2.5.4-201)
Set B	High Angle Dipping Joints	61	284	14	Acoustic televiewer features (FSAR Figure 2.5.4-216B)
Set C	Vertical Joints	Vertical	N. A.	40-50 (45)	Geologic reconnaissance (FSAR Section 2.5.1.4.2)
Set D	Vertical Joints	Vertical	N. A.	330-340 (335)	Geologic reconnaissance (FSAR Section 2.5.1.4.2)

Notes:

Where range of dip and direction are listed, the conservative representative value considered for analysis is shown in parentheses.
N. A. indicates that dip direction of vertical discontinuities is not applicable.

Table 2
 Apparent Dips of Discontinuity Sets A and B Along Plant Orthogonal Axes

Discontinuity Set	Description	True Dip Angle (Deg. from horizontal)	True Dip Azimuth (Deg. clockwise from State Plane North)	Apparent Dip Along Plant Orthogonal Axis (Deg. from Horizontal)			
				Plant North	Plant East	Plant South	Plant West
			Orthogonal Axis Azimuth:	65	155	245	335
HAR 2							
Set A	Bedding & Associated Fractures	8.9	91	8.0	3.9	---	---
Set B	High Angle Dipping Joints	66	308	---	---	45.6	63.4
HAR 3							
Set A	Bedding & Associated Fractures	23.2	113.6	15.8	17.8	---	---
Set B	High Angle Dipping Joints	61	284	---	---	54.5	48.6

Notes:

Apparent dip is down from horizontal in the plant orthogonal direction listed

Apparent dips are not applicable to vertical discontinuity Sets C and D

--- indicates that apparent dip is not down in the corresponding orthogonal direction

Table 3Relationship Between Distance B_1 and Load Fraction P_1 Along NI Orthogonal Axes

Plant North		Plant East		Plant South		Plant West	
B_1	P_1	B_1	P_1	B_1	P_1	B_1	P_1
(ft)		(ft)		(ft)		(ft)	
0.0		0	0	0.0		0	0
9.6	0.11	4	0.06	9.6	0.11	6	0.11
15.9	0.18	10	0.15	15.9	0.18	10	0.18
31.9	0.33	20	0.26	31.9	0.33	20	0.33
47.8	0.45	30	0.36	47.8	0.45	30	0.45
63.8	0.55	40	0.46	63.8	0.55	40	0.55
79.7	0.64	50	0.54	79.7	0.64	50	0.64
95.6	0.71	60	0.62	95.6	0.71	60	0.72
127.5	0.84	80	0.76	127.5	0.84	80	0.85
159.4	0.93	100	0.87	159.4	0.93	100	0.94
191.3	0.98	120	0.95	191.3	0.98	120	0.99
208.8	1.00	140	0.99	208.8	1.00	131	1.00
--	--	149	1.00	--	--	--	--

Table 4
Results of Sliding Stability Evaluations

Case ID	Plant Direction of Seismic Loading	Discontinuity Set 1 Strength Parameters			Discontinuity Set 2 Strength Parameters			Depth to Sound Rock (below site grade)		Adjacent Building Surcharge S_a	Critical B_1	Net Passive Resistance $R_{passive}$	Net Base Sliding Resistance R_{base}	Inertial Sliding Force $F_{lat,struct}$	Net Active Force F_{active}	Resulting FS_{slide}	Net Passive Force Required for $FS_{slide} = 1.1$	
		β_1	ϕ_{1r}	c_{1r}	β_2	ϕ_{2r}	c_{2r}	Active Side D_{s1}	Passive Side D_{s2}								Required Passive Force	Percent of $R_{passive}$
		(deg)	(deg)	(psf)	(deg)	(deg)	(psf)	(ft)	(ft)								(kips x 10^3)	(%)
HAR 2																		
HAR2-N1	North	8	0	1500	45.6	45	0	8	11	520	0	946.0	104.4	50.3	8.3	17.9	0.0	0%
HAR2-N2	North	8	0	1500	45.6	45	0	8	11	520	0	946.0	104.4	50.3	8.3	17.9	0.0	0%
HAR2-E1	East	3.9	0	1500	63.4	45	0	15	6	0	0	1073.0	104.4	60.6	14.0	15.8	0.0	0%
HAR2-E2	East	3.9	0	1500	63.4	45	0	15	6	0	0	1073.0	104.4	60.6	14.0	15.8	0.0	0%
HAR2-S1	South	45.6	45	0	8	0	1500	11	8	1700	0	49.4	76.0	50.3	11.7	2.03	0.0	0%
HAR2-S2	South	45.6	45	0	8	0	1500	11	8	1700	0	49.4	76.0	50.3	11.7	2.03	0.0	0%
HAR2-W1	West	63.4	45	0	3.9	0	1500	6	15	1700	0	175.6	62.8	60.6	24.0	2.82	30.2	17%
HAR2-W2	West	63.4	45	0	3.9	0	1500	6	15	1700	0	175.6	62.8	60.6	24.0	2.82	30.2	17%
HAR 3																		
HAR3-N1	North	15.8	0	1500	54.5	45	0	27	17	520	0	652.5	104.4	50.3	8.3	12.9	0.0	0%
HAR3-N2	North	15.8	0	1500	54.5	45	0	27	17	520	0	652.5	104.4	50.3	8.3	12.9	0.0	0%
HAR3-E1	East	17.8	0	1500	48.6	45	0	31	7	0	0	1811.0	104.4	60.6	14.0	25.7	0.0	0%
HAR3-E2	East	17.8	0	1500	48.6	45	0	31	7	0	0	1811.0	104.4	60.6	14.0	25.7	0.0	0%
HAR3-S1	South	54.5	45	0	15.8	0	1500	17	27	1700	15	40.5	86.6	50.3	11.7	2.05	0.0	0%
HAR3-S2	South	54.5	45	0	15.8	0	1500	17	27	1700	0	27.2	104.4	50.3	11.7	2.13	0.0	0%
HAR3-W1	West	48.6	45	0	17.8	0	1500	7	31	1700	15	70.6	77.8	60.6	24.0	1.75	15.3	22%
HAR3-W2	West	48.6	45	0	17.8	0	1500	7	31	1700	0	49.6	104.4	60.6	24.0	1.82	0.0	0%

Table 5
Results of Dynamic Bearing Capacity Evaluations

Case ID	Bearing Capacity Case Description	Discontinuity Set 1 Strength Parameters			Discontinuity Set 2 Strength Parameters			Depth to Sound Rock (below site grade) (ft)	Method 1 Results		Method 2 Results		
		β_1	ϕ_{1r}	c_{1r}	β_2	ϕ_{2r}	c_{2r}		Critical B_1	Dynamic FS_b	Critical B_1	Dynamic FS_b	FS_b at $B_1 = 20$ ft
		(deg)	(deg)	(psf)	(deg)	(deg)	(psf)		(ft)	(-)	(ft)	(-)	(-)
HAR 2													
HAR2-BC-W1	Dynamic - Apparent Dips	63.4	45	0	3.9	0	1500	15	20	10.6	5	2.19	2.8
HAR2-BC-W2	Dynamic - True Dips	66	45	0	8.9	0	1500	15	20	5.4	5	2.2	2.9
HAR3-BC-W1	Dynamic - Apparent Dips	48.6	45	0	17.8	0	1500	31	30	3.7	7	2.04	2.5
HAR3-BC-W2	Dynamic - True Dips	61	45	0	23.2	0	1500	31	20	2.6	5	2.09	2.7

Table 6
Sensitivity of Sliding Evaluation Results to Variations in Key Input Parameters

Case ID	Variations from Parameters Used in Original Analyses			Original Results		Modified Results	
	Parameter ID	Original Value	Modified Value(s)	FS _{slide}	Critical B ₁	FS _{slide}	Critical B ₁
					(ft)		(ft)
HAR2-S-Sens1	Dip - Set 1 and 2	Apparent Dips	True Dips	2.03	0	2.03	0
HAR2-W-Sens1	Dip - Set 1 and 2	Apparent Dips	True Dips	2.82	0	1.99	0
HAR3-S-Sens1	Dip - Set 1 and 2	Apparent Dips	True Dips	2.05	15	1.99	11
HAR3-W-Sens1	Dip - Set 1 and 2	Apparent Dips	True Dips	1.75	15	1.71	8
HAR3-W-Sens2	ϕ_{2r} and c_{2r} (Set 2)	$\phi_{2r} = 0, c_{2r} = 1500$ psf	$\phi_{2r} = 30$ deg, $c_{2r} = 0$	1.75	15	1.55	0
HAR3-W-Sens3	c_{2r}, c_{2s}	1500 psf	1000 psf	1.75	15	1.44	21
HAR3-W-Sens4	c_{2r}, c_{2s}	1500 psf	2000 psf	1.75	15	2.02	0
HAR3-W-Sens7	ϕ_{1r}, ϕ_{1s} (Set 1)	45 deg, 30 deg	40 deg, 27 deg	1.75	15	1.68	20
HAR3-W-Sens8	ϕ_{vr}, ϕ_{vs} (Sides)	45 deg, 30 deg	40 deg, 27 deg	1.75	15	1.74	18
HAR3-W-Sens5	K_{hr}, K_{hs}	0.5, 0.5	0.3, 0.3	1.75	15	1.72	20
HAR3-W-Sens6	a_{rhs}, a_{rvs}	1.2 x a_{rh}, a_{rv}	1.5 x a_{rh}, a_{rv}	1.75	15	1.61	20
HAR3-W-Sens9	a_{rv}, a_{rvs}	a_{rv}, a_{rvs}	-0.4 x a_{rv}, a_{rvs}	1.75	15	1.85	10

Figures

Figure 1: Plan View of Discontinuity Orientations (Strikes) and NI Orthogonal Axes

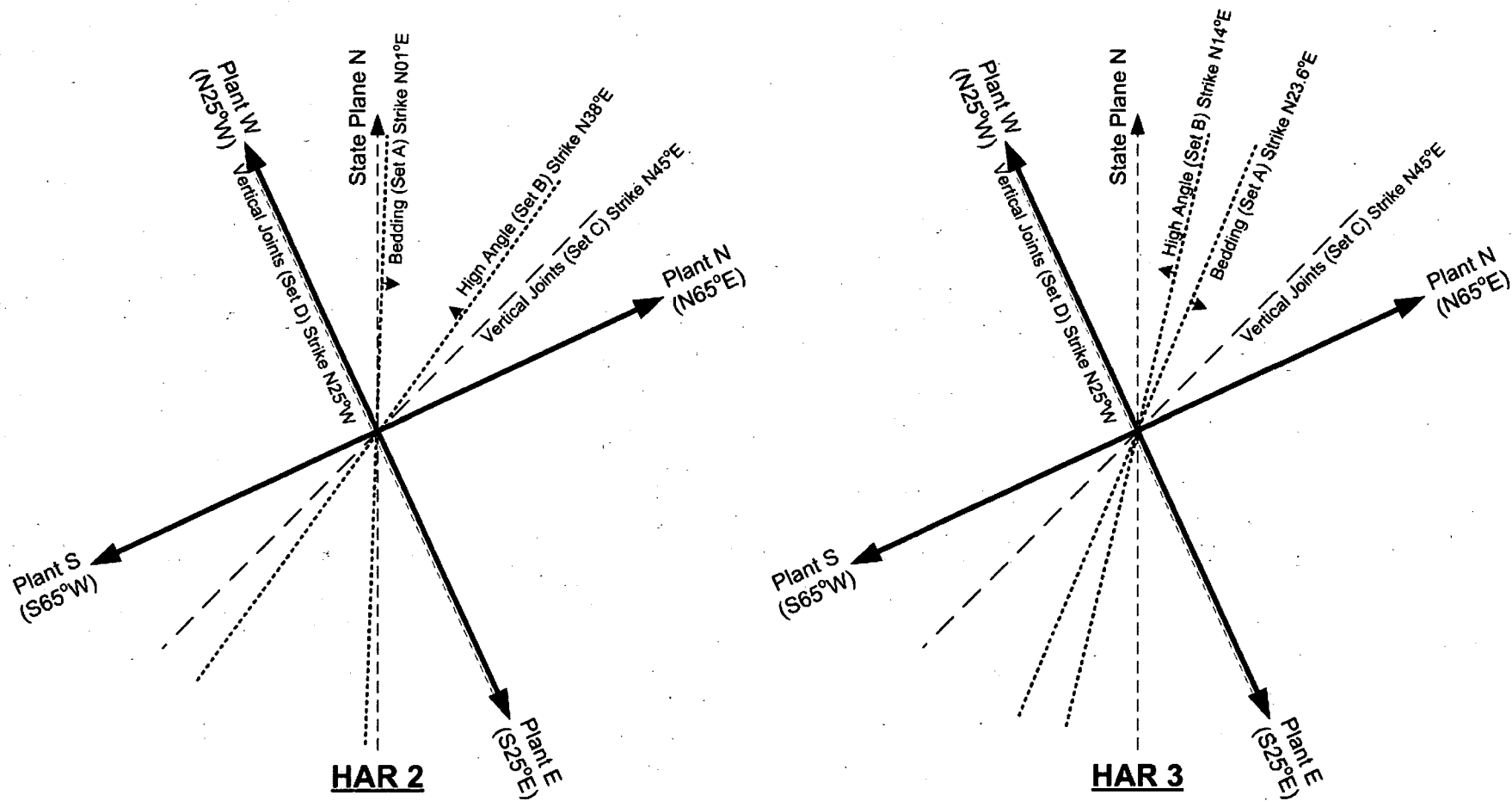


FIGURE 2: Summary of Wedge Configurations and Input Parameters – Sliding Evaluations

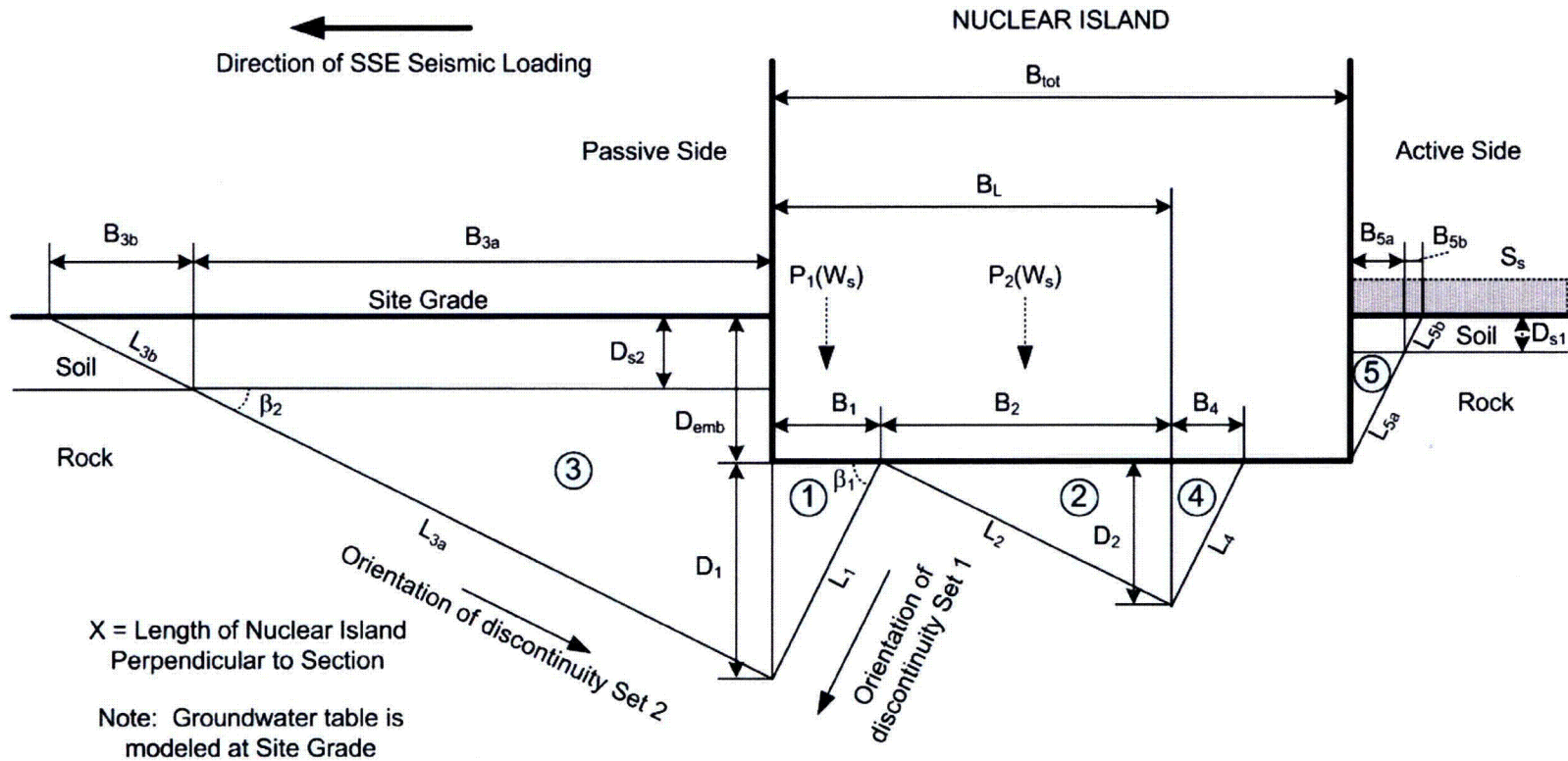
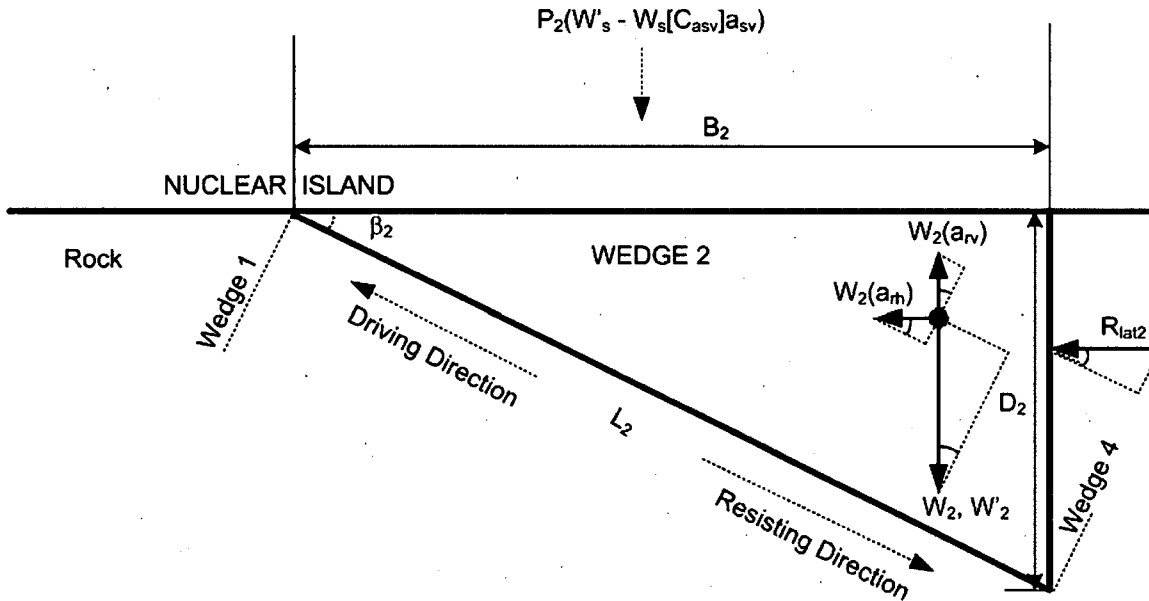


Figure 3b: Summary of Wedge 2 Forces



Summary of Driving Forces (Up Slope) – Sum is F_{d2} :

Horiz. Wedge Accel. = $(W_2 a_{rh}) \cos(\beta_2)$

Summary of Resisting Forces (Down Slope) – Sum is F_{r2} :

- Net Wedge Weight = $(W'_2 - W_2 a_{rv}) \sin(\beta_2)$
- Friction (Net Wedge Weight) = $(W'_2 - W_2 a_{rv}) \cos(\beta_2) \tan(\phi_{2r})$
- Horiz. Wedge Accel. Friction = $(W_2 a_{rh}) \sin(\beta_2) \tan(\phi_{2r})$
- Cohesion Base of Wedge = $A_2 C_{2r}$
- Sides of Wedge = $2 A_{s2} [c_{vr} + \sigma_{s2} \tan(\phi_{vr})]$
- Structure Load = $P_2 (W'_s - W_s C_{asv} a_{sv}) \sin(\beta_2)$
- Structure Load Friction = $P_2 (W'_s - W_s C_{asv} a_{sv}) \cos(\beta_2) \tan(\phi_{2r})$

A total external lateral force R_{lat2} can be resisted by Wedge 2 while satisfying wedge force equilibrium. This R_{lat2} includes the external force F_{lat4} from Wedge 4. The components of these forces in the driving direction (F_{d2add}) are as follows:

$$F_{d2add} = R_{lat2} [\cos(\beta_2) - \sin(\beta_2) \tan(\phi_{2r})]$$

For wedge force equilibrium, the driving and resisting forces must balance:

$$F_{d2} + F_{d2add} = F_{r2}$$

Solving for R_{lat2} :

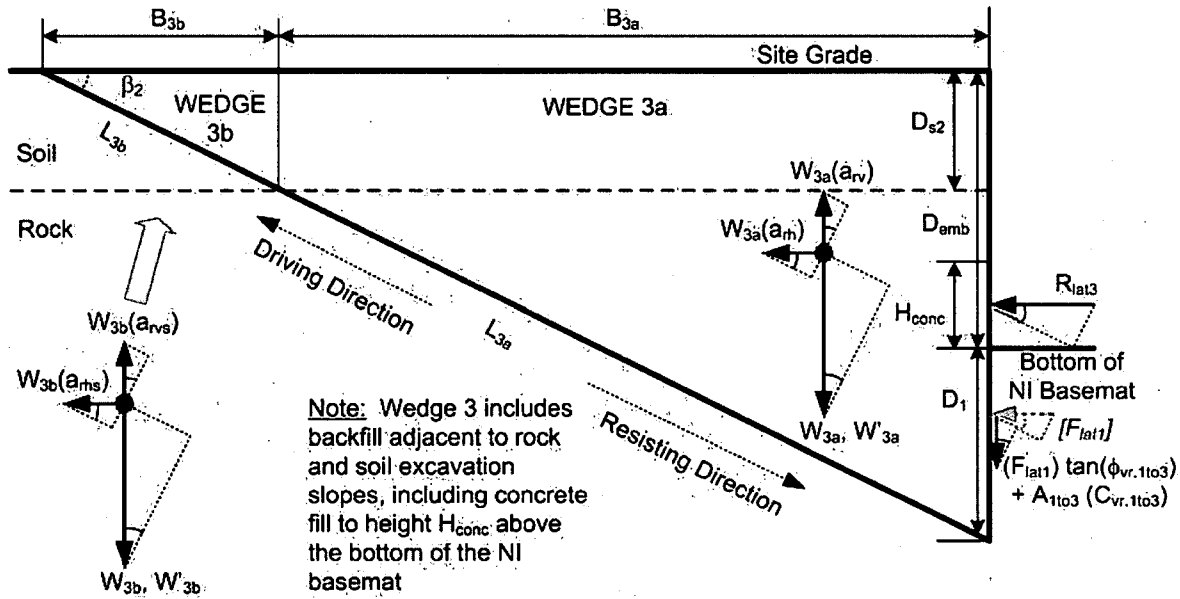
$$R_{lat2} = (F_{r2} - F_{d2}) / [\cos(\beta_2) - \sin(\beta_2) \tan(\phi_{2r})]$$

This additional external force R_{lat2} can be supported while maintaining equilibrium, and therefore is considered a resisting force in the overall stability of the Nuclear Island. The net resistance is reduced by the lateral force from Wedge 4. Also, the total resistance to sliding over Wedge 2 will be limited by the friction along the most critical interface of the basemat or waterproofing geomembrane. The net base shear sliding resistance provided by/over Wedge 2 is therefore calculated as follows:

$R_{base} = \text{Minimum of:}$
 $(R_{lat2} - F_{lat4})$ OR;
 $P_2 (W'_s - W_s C_{asv} a_{sv}) \tan(\phi_{geomemb})$ [the sliding resistance along the most critical basemat subgrade or geomembrane interface]

See MathCAD template for additional definitions of parameters.

Figure 3c: Summary of Wedge 3 Forces



Summary of Driving Forces (Up Slope) – Sum is F_{d3} :

Horiz. Wedge Accel. = $(W_3 a_{rh}) \cos(\beta_2)$

Summary of Resisting Forces (Down Slope) – Sum is F_{r3} :

Net Wedge Weight	= $(W'_{3ar} - W_{3ar} a_{rv}) \sin(\beta_2)$	(Plus similar for Wedge 3a Soil and Wedge 3b)
Friction (Net Wedge Weight)	= $(W'_{3ar} - W_{3ar} a_{rv}) \cos(\beta_2) \tan(\phi_{2r})$	(" ")
Horiz. Wedge Accel. Friction	= $(W_{3ar} a_{rh}) \sin(\beta_2) \tan(\phi_{2r})$	(" ")
Cohesion Base of Wedge	= $A_{3a} C_{2r}$	(Plus similar for Wedge 3b)
Sides of Wedge	= $2 A_{s3ar} [C_{vr} + \sigma_{s3a4} \tan(\phi_{vr})]$	(Plus similar for Wedge 3a Soil and Wedge 3b)
Friction (Wedge 1 to 3 Interface)	= $F_{lat1} \tan(\phi_{vr.1to3}) [\sin(\beta_2) + \cos(\beta_2) \tan(\phi_{2r})]$	
Cohesion (Wedge 1 to 3 Interface)	= $A_{1to3} (C_{vr.1to3}) [\sin(\beta_2) - \cos(\beta_2) \tan(\phi_{2r})]$	

A total external lateral force R_{lat3} can be resisted by Wedge 3 while satisfying wedge force equilibrium. In this calculation, the external force from Wedge 1 (F_{lat1}) is considered as part of R_{lat3} . The components of these forces in the driving direction (F_{d3add}) are as follows:

$$F_{d3add} = R_{lat3} [\cos(\beta_2) - \sin(\beta_2) \tan(\phi_{2r})]$$

For wedge force equilibrium, the driving and resisting forces must balance:

$$F_{d3} + F_{d3add} = F_{r3}$$

Solving for R_{lat3} :

$$R_{lat3} = (F_{r3} - F_{d3}) / [\cos(\beta_2) - \sin(\beta_2) \tan(\phi_{2r})]$$

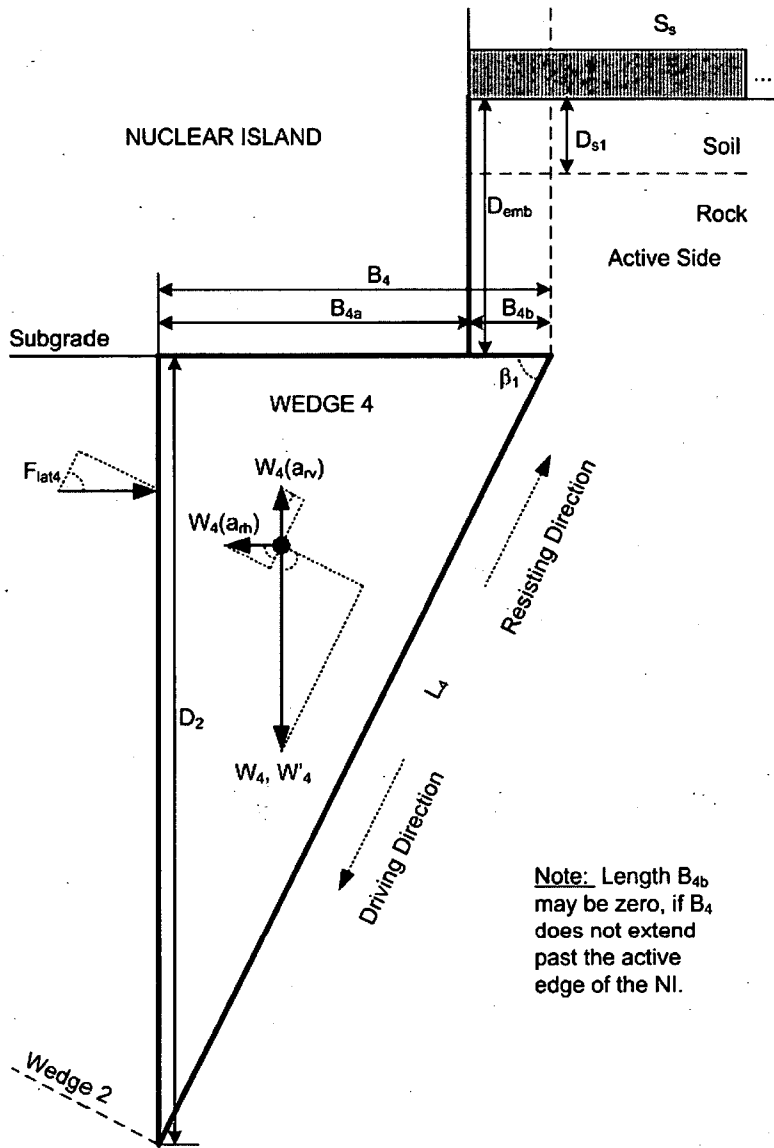
This additional external force R_{lat3} can be supported while maintaining equilibrium, and therefore is considered a resisting force in the overall stability of the Nuclear Island.

The net NI passive resistance provided by Wedge 3 to resist NI sliding is calculated as follows:

$$R_{passive} = R_{lat3} - F_{lat1}$$

See MathCAD template for additional definitions of parameters.

Figure 3d: Summary of Wedge 4 Forces



Note: Length B_{4b} may be zero, if B_4 does not extend past the active edge of the NI.

Summary of Driving Forces (Down Slope) – Sum is F_{d4} :

Net Wedge Weight	= $(W'_4 - W_4 a_{rv}) \sin(\beta_1)$
Horiz. Wedge Accel.	= $(W_4 a_{rh}) \cos(\beta_1)$
Load over Width B_{4b}	= $(B_{4b} X) [D_{s1} \gamma_s + (D_{emb} - D_{s1}) \gamma_r + S_s] \sin(\beta_1)$

Summary of Resisting Forces (Up Slope) – Sum is F_{r4} :

Friction (Net Wedge Weight)	= $(W'_4 - W_4 a_{rv}) \cos(\beta_1) \tan(\phi_{1r})$
Horiz. Wedge Accel. Friction Reduction	= $(-1) (W_4 a_{rh}) \sin(\beta_1) \tan(\phi_{1r})$
Cohesion Base of Wedge	= $A_4 c_{1r}$
Sides of Wedge	= $2 A_{s4} [c_{vr} + \sigma_{s4} \tan(\phi_{vr})]$
Friction from Load over Width B_{4b}	= $(B_{4b} X) [D_{si} \gamma_s + (D_{emb} - D_{si}) \gamma_r + S_s] \cos(\beta_1) \tan(\phi_{1r})$

Additional resisting force F_{lat4} is required for wedge force equilibrium, acting normal to the Wedge 2 interface. Friction along the Wedge 2 to Wedge 4 interface is conservatively not considered, since the NI does not impose a downward load over Wedge 4. The components of these forces in the resisting direction (F_{r4add}) are as follows:

$$F_{r4add} = F_{lat4} [\cos(\beta_1) + \sin(\beta_1) \tan(\phi_{1r})]$$

For wedge force equilibrium, the driving and resisting forces must balance:

$$F_{d4} = F_{r4} + F_{r4add}$$

Solving for F_{lat4} :

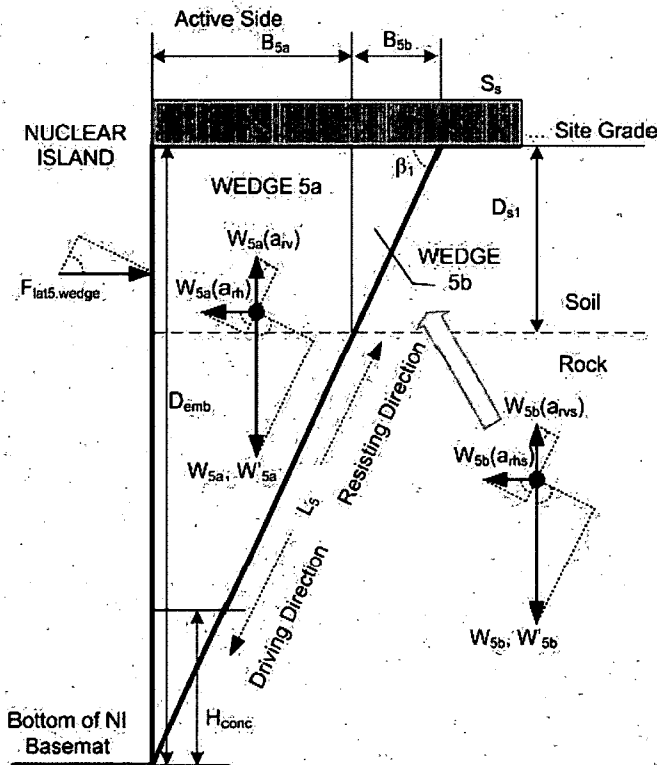
$$F_{lat4} = (F_{d4} - F_{r4}) / [\cos(\beta_1) + \sin(\beta_1) \tan(\phi_{1r})]$$

This external resisting force F_{lat4} is required for wedge stability, and therefore is considered a driving force in the overall stability of the Nuclear Island. It will act to reduce the net resistance to base sliding provided by Wedge 2.

See MathCAD template for additional definitions of parameters.

Figure 3e: Summary of Wedge 5 Forces

Force Diagram for Calculation of $F_{lat5,wedge}$:



Wedge 5 represents soil and rock adjacent to the active endwall of the NI. The total lateral force acting on the active endwall (F_{active}) is conservatively assigned as the GREATER of:

- Force $F_{lat5,wedge}$: This is the external lateral force (from the NI endwall) needed to support a rock and soil wedge with bottom defined along discontinuity Set 1, based on wedge force equilibrium.
- Force $F_{lat5,backfill}$: This represents the lateral forces associated with compacted granular backfill adjacent to the NI endwall, which conservatively assumes that backfill extends from ground surface to the bottom of the basemat. At-rest and dynamic forces from the backfill and adjacent structure surcharge load S_s are included in this force.

A) CALCULATION OF FORCE $F_{lat5,wedge}$:

Summary of Driving Forces (Down Slope) – Sum is F_{d5} :

Net Wedge Weight	= $(W'_{5ar} - W_{5ar} a_{rv}) \sin(\beta_1)$	(plus similar for Wedge 3a Soil and Wedge 3b)
Horiz. Wedge Accel.	= $(W_{5ar} a_{rh}) \cos(\beta_1)$	(" "
Surcharge	= $X (S_s) (B_{5a} + B_{5b}) \sin(\beta_1)$	(" "

Summary of Resisting Forces (Up Slope) – Sum is F_{r5} :

Friction (Net Wedge Weight)	= $(W'_{5ar} - W_{5ar} a_{rv}) \cos(\beta_1) \tan(\phi_{1r})$	(" "
Horiz. Wedge Accel. Friction Reduction	= $(-1) (W_{5ar} a_{rh}) \sin(\beta_1) \tan(\phi_{1r})$	(" "
Cohesion Base of Wedge	= $A_{5a} c_{1r}$	(plus similar for Wedge 3b)
Sides of Wedge	= $2 A_{5sar} [c_{vr} + \sigma_{s5ar} \tan(\phi_{vr})]$	(plus similar for Wedge 3a Soil and Wedge 3b)
Surcharge Friction	= $X (S_s) (B_{5a}) \cos(\beta_1) \tan(\phi_{1r})$	(plus similar for Wedge 3b)

Additional resisting force $F_{lat5,wedge}$ is required for wedge force equilibrium, acting normal to the NI active endwall. Friction along the NI endwall is conservatively not considered. $F_{lat5,wedge}$ has a force component upslope [$F_{lat5,wedge} \cos(\beta_1)$], and a frictional component along the wedge base, distributed above and below top of sound rock based on the ratio of D_{s1} to D_{emb} . The components of these forces in the resisting direction (F_{r5add}) are as follows:

$$F_{r5add} = F_{lat5,wedge} \left[\cos(\beta_1) + \frac{D_{s1}}{D_{emb}} [\sin(\beta_1) \tan(\phi_{1s})] + \frac{(D_{emb} - D_{s1})}{D_{emb}} [\sin(\beta_1) \tan(\phi_{1r})] \right]$$

For wedge force equilibrium, the driving and resisting forces must balance:

$$F_{d5} = F_{r5} + F_{r5add}$$

Solving for $F_{lat5,wedge}$:

$$F_{lat5,wedge} = (F_{d5} - F_{r5}) / \left[\cos(\beta_1) + \frac{D_{s1}}{D_{emb}} [\sin(\beta_1) \tan(\phi_{1s})] + \frac{(D_{emb} - D_{s1})}{D_{emb}} [\sin(\beta_1) \tan(\phi_{1r})] \right]$$

B) CALCULATION OF FORCE $F_{lat5,backfill}$:

Total lateral forces from backfill (assumed to extend to full depth D_{emb} along the NI active endwall) are based on at-rest condition ($K_0 = 1 - \sin(\phi_{backfill})$) plus an additional dynamic force based on the elastic method in ASCE 4-98. Lateral loads associated with static and dynamic effects of adjacent building surcharge S_s are also included.

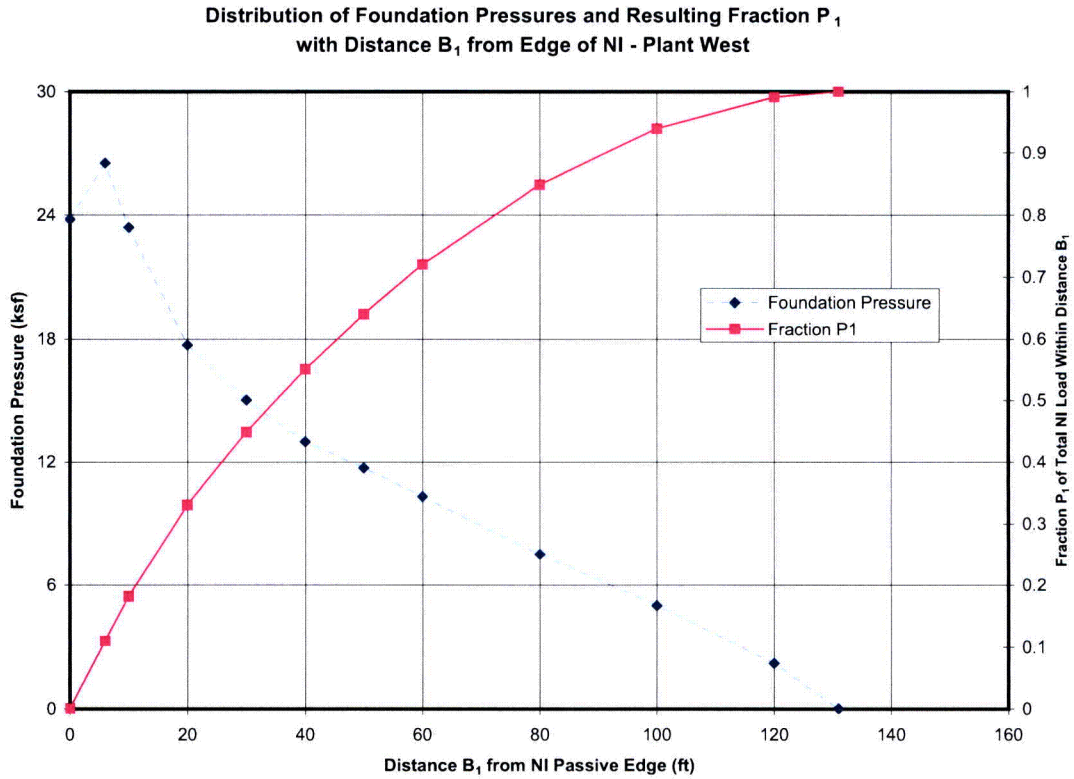
C) CALCULATION OF FORCE F_{active} :

The driving lateral force acting on the NI active endwall for the stability evaluations (F_{active}) is calculated as follows:

$$F_{active} = \text{GREATER OF } F_{lat5,wedge} \text{ OR } F_{lat5,backfill}$$

See the MathCAD template for additional definitions of parameters and equations for $F_{lat5,backfill}$.

Figure 4
Distribution of Foundation Pressures and Resulting Fraction P_1 with Distance B_1 from Edge of NI - Plant West



Notes:
 Foundation bearing pressures are as shown for case "SM-Min" in WEC Report APP-GW-GLR-044, R0 (Figure 2.4-2)
 Fraction P_1 is calculated from the foundation bearing pressure distribution as follows (example for Plant West side of NI):

Distance from Plant West Edge (B_1) (ft)	Foundation Pressure (ksf)	Interval ID	Width (ft)	Avg. Pressure (ksf)	Width * Avg. Pressure (kip/ft)	Fraction of Total Load within Interval:	Cumulative Fraction of Load within B_1 (P_1)
0	23.8						0
6	26.5	1	6	25.15	150.9	0.109	0.11
10	23.4	2	4	24.95	99.8	0.072	0.18
20	17.7	3	10	20.55	205.5	0.149	0.33
30	15	4	10	16.35	163.5	0.118	0.45
40	13	5	10	14	140	0.101	0.55
50	11.7	6	10	12.35	123.5	0.089	0.64
60	10.3	7	10	11	110	0.080	0.72
80	7.5	8	20	8.9	178	0.129	0.85
100	5	9	20	6.25	125	0.091	0.94
120	2.2	10	20	3.6	72	0.052	0.99

Figure 5: Summary of Wedge Configurations Bearing Capacity Evaluation Method 1

Based on Wedge Force Equilibrium

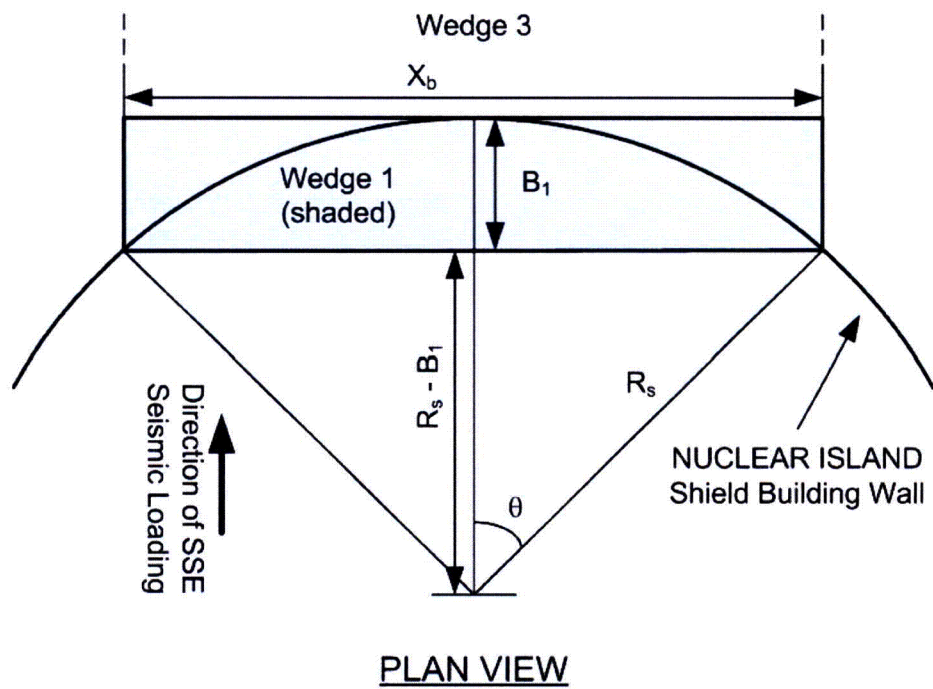
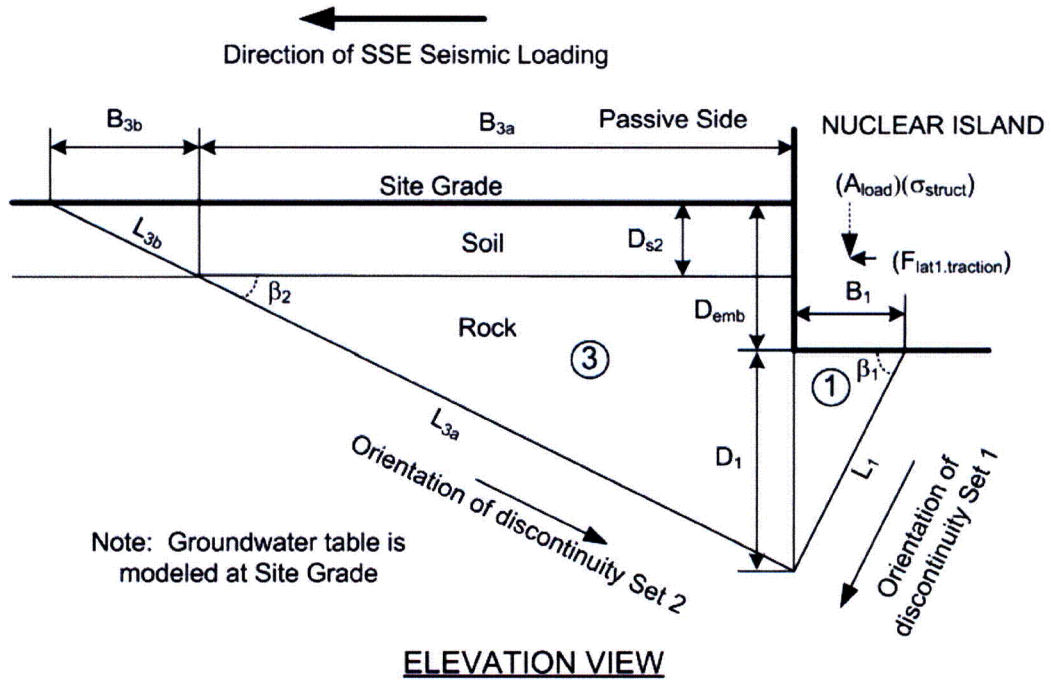
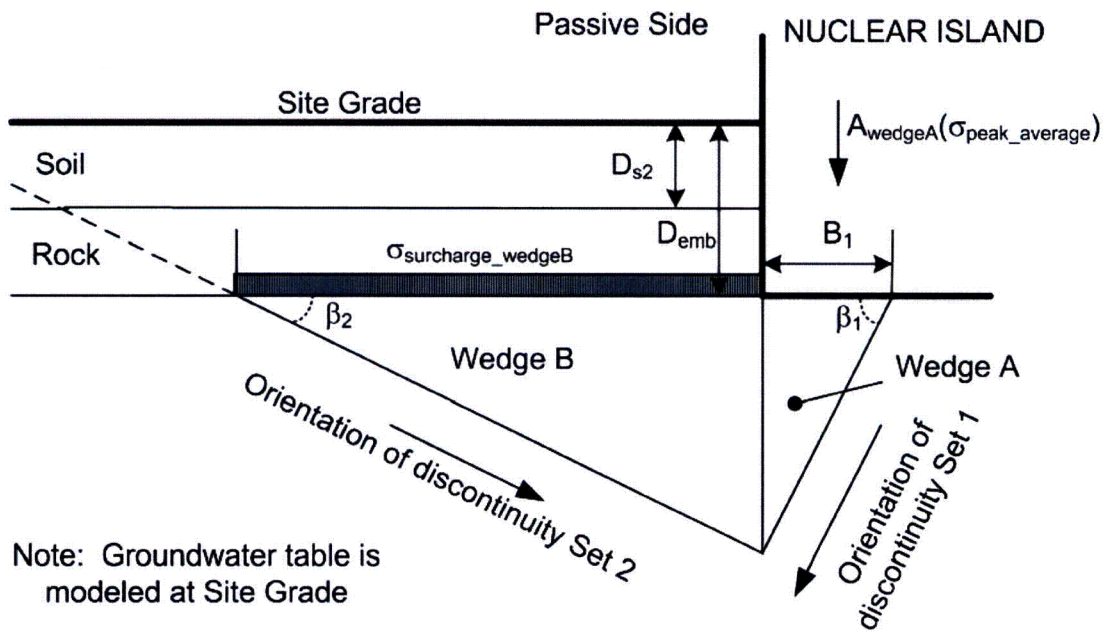


Figure 6: Summary of Wedge Configurations Bearing Capacity Evaluation Method 2

Based on Landanyi and Roy, 1971 (in Wyllie, 1999)



Attachments

ATTACHMENT A

Progress Energy HAR COLA

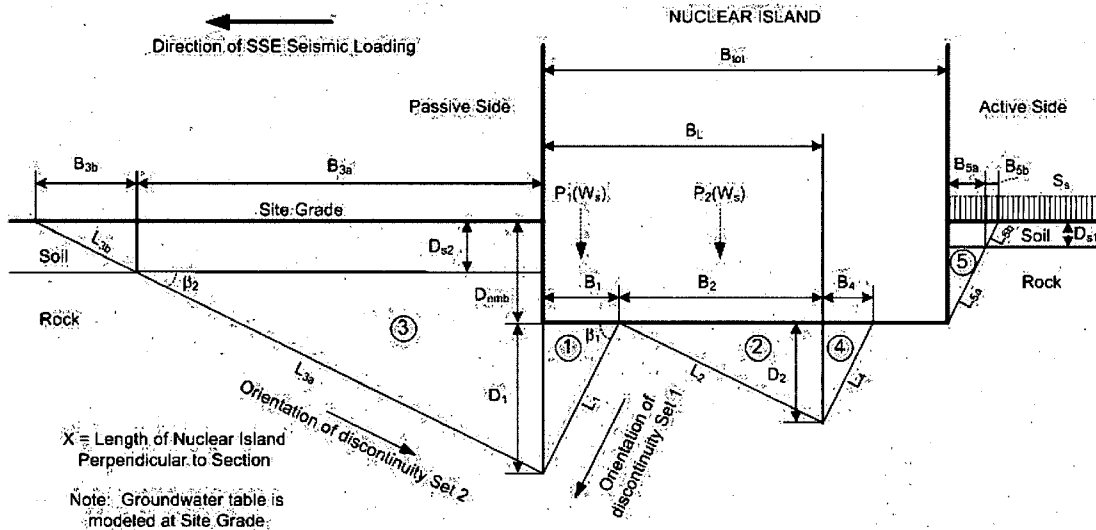
NI Sliding Resistance Along Oriented Discontinuities
Case HAR3-W1

Engineer: MDG

1. Purpose and Scope:

Stability of the HAR 2 and 3 Nuclear Islands (NI) along oriented rock discontinuities under SSE seismic sliding and bearing loads is evaluated in this calculation. The limit equilibrium of five wedges that represent rock and soil adjacent to and under the NI is calculated. Inputs include the orientations and strength parameters of rock discontinuity sets, NI structure loads, and design accelerations for the structure and for soil and rock. The resulting FS against sliding (FS_{slide}) is calculated.

The configurations of the NI, the five wedges, and definitions of select input parameters are shown in the following diagram:



File: Case_HAR3_W1.xmcd
Date: 2/5/2009
Page: 1

2. Input Parameters:

General Geometry Parameters

$$B_{\text{tot}} := 160\text{ft}$$

Width of Nuclear Island (NI)

$$B_L := 131\text{ft}$$

Width of NI under compression during SSE seismic loading

$$B_1 := 15\text{ft}$$

ENTER Width of trial wedge under NI

$$B_2 := B_L - B_1$$

Width of area under compression behind trial wedge

$$B_2 = 116\text{ft}$$

$$X := 255\text{ft}$$

Length of NI (perpendicular to section)

$$\text{Elev}_{\text{site}} := 260\text{ft}$$

Site Grade Elevation (ft NGVD 29)

$$\text{Elev}_{\text{basemat}} := 221.5\text{ft}$$

Bottom of NI Basemat Elevation (ft NGVD 29)

$$D_{\text{emb}} := \text{Elev}_{\text{site}} - \text{Elev}_{\text{basemat}}$$

Depth of NI embedment

$$D_{\text{emb}} = 38.5\text{ft}$$

$$H_{\text{conc}} := 6\text{ft}$$

Height of concrete sidewall fill above the bottom of basemat (in contact with rock)

$$D_{s1} := 7\text{ft}$$

Depth to sound rock below site grade on Active wedge side

$$D_{s2} := 31\text{ft}$$

Depth to sound rock below site grade on Passive wedge side

* NOTE: depth to GW is conservatively assigned as zero (at site grade) for all calculations

Discontinuity Set #1 Parameters

$$\beta_1 := 48.6\text{deg}$$

Dip of discontinuity set #1 from horizontal

$$\phi_{1r} := 45\text{deg}$$

Friction angle of discont. set #1 in rock

$$c_{1r} := 0\text{psf}$$

Cohesion of discont. set #1 in rock

$$\phi_{1s} := 30\text{deg}$$

Friction angle of discont. set #1 in soil

$$c_{1s} := 0\text{psf}$$

Cohesion of discont. set #1 in soil

File: Case_HAR3_W1.xmcd
Date: 2/5/2009
Page: 2

Discontinuity Set #2 Parameters

$$\beta_2 := 17.8\text{deg}$$

Dip of discontinuity set #2 from horizontal

$$\phi_{2r} := 0\text{deg}$$

Friction angle of discont. set #2 in rock

$$c_{2r} := 1500\text{psf}$$

Cohesion of discont. set #2 in rock

$$\phi_{2s} := 0\text{deg}$$

Friction angle of discont. set #2 in soil

$$c_{2s} := 1500\text{psf}$$

Cohesion of discont. set #2 in soil

Vertical Discontinuity Parameters

$$\phi_{vr} := 45\text{deg}$$

Friction angle of vertical discont. in rock

$$c_{vr} := 0\text{psf}$$

Cohesion of vertical discont. in rock

$$\phi_{vs} := 30\text{deg}$$

Friction angle of vertical discont. in soil

$$c_{vs} := 0\text{psf}$$

Cohesion of vertical discont. in soil

$$\phi_{vr.1to3} := 45\text{deg}$$

Friction angle of vertical joint between
Wedges 1 and 3

$$c_{vr.1to3} := 0\text{psf}$$

Cohesion of vertical joint between
Wedges 1 and 3

$$K_{hs} := 0.5$$

Lateral earth pressure coefficients in soil
and rock along vertical discontinuities in
direction perpendicular to section

$$K_{hr} := 0.5$$

Other Parameters

$$\phi_{geomemb} := 28.8\text{deg}$$

Lowest (design) interface friction angle at
the basemat subgrade

$$\phi_{backfill} := 35\text{deg}$$

Internal friction angle of granular backfill
adjacent to the NI sidewalls, above
concrete fill

$$\gamma_{backfill} := 130\text{pcf}$$

Saturated unit weight of granular backfill

$$B_{\text{north}} := \begin{pmatrix} 0.0 \\ 9.6 \\ 15.9 \\ 31.9 \\ 47.8 \\ 63.8 \\ 79.7 \\ 95.6 \\ 127.5 \\ 159.4 \\ 191.3 \\ 208.8 \end{pmatrix} \text{ ft} \quad P_{\text{north}} := \begin{pmatrix} 0 \\ 0.11 \\ 0.18 \\ 0.33 \\ 0.45 \\ 0.55 \\ 0.64 \\ 0.72 \\ 0.85 \\ 0.94 \\ 0.99 \\ 1.00 \end{pmatrix}$$

$$B_{\text{south}} := \begin{pmatrix} 0.0 \\ 9.6 \\ 15.9 \\ 31.9 \\ 47.8 \\ 63.8 \\ 79.7 \\ 95.6 \\ 127.5 \\ 159.4 \\ 191.3 \\ 208.8 \end{pmatrix} \text{ ft} \quad P_{\text{south}} := \begin{pmatrix} 0 \\ 0.11 \\ 0.18 \\ 0.33 \\ 0.45 \\ 0.55 \\ 0.64 \\ 0.72 \\ 0.85 \\ 0.94 \\ 0.99 \\ 1.00 \end{pmatrix}$$

$$P_1 := \text{interp}(B_{\text{west}}, P_{\text{west}}, B_1) \quad P_1 = 0.255$$

P_1 is the fraction of NI vertical load acting over width B_1 , based on the above relationship between B_{xxx} and P_{xxx} .

$$C_{\text{bp}} := 1.32$$

Coefficient applied to structure load fraction P_1 to scale peak load over Wedge 1 to 35 ksf.

$$P_2 := 1 - P_1 \quad P_2 = 0.745$$

Fraction of NI weight acting over width B_2

$$C_{\text{asv}} := 0.4$$

Coefficient applied to vertical NI structure acceleration (a_{sv}) for load over width B_2

Other Load and Weight Parameters

$$\gamma_s := 140 \text{ pcf}$$

Unit weight of soil (total)

$$\gamma_r := 160 \text{ pcf}$$

Unit weight of rock (total)

$$\gamma_w := 62.4 \text{ pcf}$$

Unit weight of water

$$S_s := 1700 \text{ psf}$$

Surface surcharge due to adjacent building on active side of NI

$$F_{\text{lat.struct}} := 60634 \text{ kip}$$

Lateral seismic inertial force of the NI (driving force to sliding calculation)

Required Sliding Factor of Safety (FS)

$$FS_s := 1.1$$

Required FS against sliding

Accelerations due to Seismic Loading (fraction of g)

Note: Positive direction is driving (horizontal) or up (vertical)

$a_{sv} := 0.179$	Structure acceleration - vertical (reduces sliding resistance over Wedge 2 - positive is uplift)
$a_{rh} := 0.14$	Rock mass acceleration below top of sound rock - horizontal
$a_{rv} := 0.11$	Rock mass acceleration below top of sound rock - vertical (positive is up)
$a_{rhs} := 1.2 \cdot a_{rh} = 0.168$	Soil and weathered rock mass acceleration between site grade and top of sound rock - Horizontal
$a_{rvs} := 1.2 \cdot a_{rv} = 0.132$	Soil and weathered rock mass acceleration between site grade and top of sound rock - vertical (positive is up)

3. Wedge Calculations:

3.1 Wedge 1 - Below NI Width B_1

Wedge 1 represents rock below the NI between the passive edge of the NI and a trial discontinuity that daylight at the NI subgrade a distance B_1 from the edge. The external force F_{lat1} required to act on the passive side of the wedge, for force equilibrium, is calculated.

Wedge 1 Dimensions and Weights

$L_1 := \frac{B_1}{\cos(\beta_1)}$	$L_1 = 22.682 \cdot \text{ft}$	Length of Wedge 1 along discontinuity set #1
$D_1 := B_1 \cdot \tan(\beta_1)$	$D_1 = 17.014 \cdot \text{ft}$	Depth of Wedge 1 below NI
$A_1 := L_1 \cdot X$	$A_1 = 5.784 \times 10^3 \cdot \text{ft}^2$	Area of Wedge 1 along discontinuity Set #1
$A_{s1} := \frac{B_1 \cdot D_1}{2}$	$A_{s1} = 127.606 \cdot \text{ft}^2$	Side Area of Wedge 1 (parallel to section)
$A_{1to3} := D_1 \cdot X$	$A_{1to3} = 4.339 \times 10^3 \cdot \text{ft}^2$	Area of interface between Wedge 1 and 3
$W_1 := A_{s1} \cdot X \cdot \gamma_r$	$W_1 = 5.206 \times 10^3 \cdot \text{kip}$	Total Weight of Wedge 1 Rock

File: Case_HAR3_W1.xmcd
Date: 2/5/2009
Page: 6

$$W'_1 := A_{s1} \cdot X \cdot (\gamma_r - \gamma_w)$$

$$W'_1 = 3.176 \times 10^3 \cdot \text{kip}$$

Effective Weight of Wedge 1 Rock

$$\sigma_{s1} := K_{hr} \left[D_{s2} \cdot (\gamma_s - \gamma_w) + \left(D_{emb} + \frac{D_1}{3} - D_{s2} \right) \cdot (\gamma_r - \gamma_w) \right]$$

$$\sigma_{s1} = 1.846 \times 10^3 \cdot \text{psf}$$

Average lateral pressure on side of Wedge 1
(at centroid of side area)

Driving Forces - Wedge 1:

$$F_{d1} := (W'_1 - W_1 \cdot a_{rv}) \cdot \sin(\beta_1) + W_1 \cdot a_{rh} \cdot \cos(\beta_1) + P_1 \cdot W_s \cdot (C_{bp}) \cdot \sin(\beta_1)$$

$$F_{d1} = 7.474 \times 10^4 \cdot \text{kip}$$

Driving forces acting down-dip along
discontinuity set #1.

Resisting Forces - Wedge 1:

$$F_{r1} := \left[(W'_1 - W_1 \cdot a_{rv}) \cos(\beta_1) - W_1 \cdot a_{rh} \cdot \sin(\beta_1) \right] \cdot \tan(\phi_{1r}) + A_1 \cdot c_{1r} \dots$$

$$+ A_{s1} \cdot 2 \cdot (c_{vr} + \sigma_{s1} \cdot \tan(\phi_{vr})) + P_1 \cdot W_s \cdot (C_{bp}) \cos(\beta_1) \cdot \tan(\phi_{1r}) \dots$$

$$+ A_{1to3} \cdot c_{vr.1to3} \cdot (\sin(\beta_1) - \cos(\beta_1) \cdot \tan(\phi_{1r}))$$

$$F_{r1} = 6.539 \times 10^4 \cdot \text{kip}$$

Resisting forces acting up-dip along
discontinuity set #1

Calculate F_{lat1} , the lateral force required at the passive side of Wedge 1 for force equilibrium:

$$F_{lat1_trial} := \frac{F_{d1} - F_{r1}}{(\cos(\beta_1) + \sin(\beta_1) \cdot \tan(\phi_{1r})) + \tan(\phi_{vr.1to3}) \cdot \sin(\beta_1) - \tan(\phi_{vr.1to3}) \cos(\beta_1) \tan(\phi_{1r})}$$

$$F_{lat1_trial} = 6.232 \times 10^3 \cdot \text{kip}$$

F_{lat1} acts as a driving force in overall stability
calculations presented later

$$F_{lat1} := \max(F_{lat1_trial}, 0)$$

If F_{lat1_trial} is negative, no lateral force required for
stability - assigns value of 0 to F_{lat1}

$$F_{lat1} = 6.232 \times 10^3 \cdot \text{kip}$$

F_{lat1} acts as a driving force in overall stability
calculations presented later

File: Case_HAR3_W1.xmcd

Date: 2/5/2009

Page: 7

3.2 Wedge 2 - Below NI Width B₂

Wedge 2 represents rock within width B₂ below the NI between the trial distance B₁ and the back side of the compression load of the NI during seismic loading. The base of this wedge is oriented along discontinuity Set 2. The resistance to sliding of this wedge in the direction of seismic loading is calculated as R_{lat2}.

This force R_{lat2} is available to resist sliding due to frictional forces provided by the NI bearing load over B₂. The net lateral resistance to sliding (R_{lat2} less driving force from Wedge 4) is limited to the sliding resistance provided by basemat friction along the most critical subgrade interface, as calculated later.

Wedge 2 Dimensions and Weights

$L_2 := \frac{B_2}{\cos(\beta_2)}$	$L_2 = 121.832 \cdot \text{ft}$	See Sketch
$D_2 := B_2 \cdot \tan(\beta_2)$	$D_2 = 37.244 \cdot \text{ft}$	
$A_2 := L_2 \cdot X$	$A_2 = 3.107 \times 10^4 \cdot \text{ft}^2$	Area of Wedge 2 along discontinuity set #2
$A_{s2} := \frac{B_2 \cdot D_2}{2}$	$A_{s2} = 2.16 \times 10^3 \cdot \text{ft}^2$	Side area of Wedge 2
$W_2 := A_{s2} \cdot X \cdot \gamma_r$	$W_2 = 8.813 \times 10^4 \cdot \text{kip}$	Total weight of Wedge 2

$W'_2 := A_{s2} \cdot X \cdot (\gamma_r - \gamma_w)$	Effective weight of Wedge 2
------------------------------------------------------	-----------------------------

$$W'_2 = 5.376 \times 10^4 \cdot \text{kip}$$

$$\sigma_{s2} := K_{hr} \cdot \left[(\gamma_s - \gamma_w) \cdot \frac{D_{s2} + D_{s1}}{2} + \left(D_{emb} - \frac{D_{s2} + D_{s1}}{2} + \frac{D_2}{3} \right) \cdot (\gamma_r - \gamma_w) \right]$$

$$\sigma_{s2} = 2.295 \times 10^3 \cdot \text{psf}$$

Average lateral pressure on side of Wedge 2 (at centroid of side area)

Driving Forces - Wedge 2:

$$F_{d2} := W_2 \cdot a_{rh} \cdot \cos(\beta_2)$$

$$F_{d2} = 1.175 \times 10^4 \cdot \text{kip}$$

Driving forces acting up-dip along discontinuity set #2

Resisting Forces - Wedge 2:

$$F_{r2} := (W'_2 - W_2 \cdot a_{rv}) \cdot \cos(\beta_2) \cdot \tan(\phi_{2r}) + W_2 \cdot a_{rh} \cdot \sin(\beta_2) \cdot \tan(\phi_{2r}) + (W'_2 - W_2 \cdot a_{rv}) \cdot \sin(\beta_2) \dots$$

$$+ A_2 \cdot c_{2r} + 2 \cdot A_{s2} \cdot (c_{vr} + \sigma_{s2} \cdot \tan(\phi_{vr})) + (W'_s - W_s \cdot C_{asv} \cdot a_{sv}) \cdot P_2 \cdot \cos(\beta_2) \cdot \tan(\phi_{2r}) \dots$$

$$+ (W'_s - W_s \cdot C_{asv} \cdot a_{sv}) \cdot P_2 \cdot \sin(\beta_2)$$

$$F_{r2} = 1.132 \times 10^5 \cdot \text{kip}$$

Resisting forces acting down-dip along discontinuity set #2

Calculate R_{lat2} , the lateral force that can be resisted by Wedge 2 under static equilibrium:

$$\text{Alpha} := (\cos(\beta_2) - \sin(\beta_2) \cdot \tan(\phi_{2r}))$$

$$\text{Alpha} = 0.952$$

$$\text{Alpha}_{eff} := \text{if}(\text{Alpha} > 0.01, \text{Alpha}, 0.01)$$

$$R_{lat2} := \frac{F_{r2} - F_{d2}}{(\text{Alpha}_{eff})}$$

$$R_{lat2} = 1.066 \times 10^5 \cdot \text{kip}$$

"Alpha" and "Alpha_{eff}" are used to limit the denominator of the R_{lat2} equation to a minimum of 0.01. This will prevent a negative number if total net resistance is very high - i.e., if β_2 is steep enough and/or ϕ_{2r} is large enough that effectively any magnitude of lateral load R_{lat2} could be supported in the direction of seismic loading. Such a condition could result in negative denominator in the R_{lat2} equation, and hence a negative R_{lat2} (which is inaccurate), if Alpha_{eff} were not limited to a minimum small positive value.

R_{lat2} acts as a resisting force in overall stability calculations presented later.

3.3 Wedge 3 - Passive Wedge

Wedge 3 represents soil and rock on the passive side of the NI to a depth of D_1 below the NI. The base of this wedge is oriented along discontinuity set # 2, passing through depth D_1 on the passive side of the NI. Note that if B_1 is set to zero, D_1 is also zero, and Wedge 3 represents the passive wedge adjacent to the subsurface passive NI endwall only.

The total lateral resistance that can be provided by this wedge is calculated as R_{lat3} . This force is available to resist F_{lat1} and to provide additional passive resistance to NI sliding forces.

Wedge #3 Dimensions and Weights

$$B_{3a} := \frac{(D_{cemb} + D_1 - D_{s2})}{\tan(\beta_2)} \quad B_{3a} = 76.353 \cdot \text{ft} \quad \text{See Sketch}$$

$$L_{3a} := \frac{B_{3a}}{\cos(\beta_2)} \quad L_{3a} = 80.191 \cdot \text{ft}$$

File: Case_HAR3_W1.xmcd
Date: 2/5/2009
Page: 9

$$B_{3b} := \frac{D_{s2}}{\tan(\beta_2)} \quad B_{3b} = 96.554 \cdot \text{ft}$$

$$L_{3b} := \frac{B_{3b}}{\cos(\beta_2)} \quad L_{3b} = 101.408 \cdot \text{ft}$$

$$A_{3a} := L_{3a} \cdot X \quad A_{3a} = 2.045 \times 10^4 \cdot \text{ft}^2$$

Area of Wedge 3a along discontinuity set #2

$$A_{s3ar} := \frac{[B_{3a} \cdot (D_{\text{emb}} + D_1 - D_{s2})]}{2}$$

Side area of Wedge 3a in rock

$$A_{s3ar} = 935.861 \cdot \text{ft}^2$$

$$A_{s3as} := B_{3a} \cdot D_{s2} \quad A_{s3as} = 2.367 \times 10^3 \cdot \text{ft}^2$$

Side area of Wedge 3a in soil

$$A_{3b} := L_{3b} \cdot X \quad A_{3b} = 2.586 \times 10^4 \cdot \text{ft}^2$$

Area of Wedge 3b along discontinuity set #2

$$A_{s3bs} := \frac{B_{3b} \cdot D_{s2}}{2} \quad A_{s3bs} = 1.497 \times 10^3 \cdot \text{ft}^2$$

Side area of Wedge 3b in soil

$$W_{3ar} := A_{s3ar} \cdot X \cdot \gamma_r \quad W_{3ar} = 3.818 \times 10^4 \cdot \text{kip}$$

Total weight of Wedge 3a, rock

$$W_{3as} := A_{s3as} \cdot X \cdot \gamma_s \quad W_{3as} = 8.45 \times 10^4 \cdot \text{kip}$$

Total weight of Wedge 3a, soil

$$W'_{3ar} := A_{s3ar} \cdot X \cdot (\gamma_r - \gamma_w) \quad W'_{3ar} = 2.329 \times 10^4 \cdot \text{kip}$$

Effective weight of Wedge 3a, rock

$$W'_{3as} := A_{s3as} \cdot X \cdot (\gamma_s - \gamma_w) \quad W'_{3as} = 4.684 \times 10^4 \cdot \text{kip}$$

Effective weight of Wedge 3a, soil

$$W_{3b} := A_{s3bs} \cdot X \cdot \gamma_s \quad W_{3b} = 5.343 \times 10^4 \cdot \text{kip}$$

Total weight of Wedge 3b

$$W'_{3b} := A_{s3bs} \cdot X \cdot (\gamma_s - \gamma_w) \quad W'_{3b} = 2.961 \times 10^4 \cdot \text{kip}$$

Effective weight of Wedge 3b

$$\sigma_{s3ar} := K_{hr} \left[D_{s2} \cdot (\gamma_s - \gamma_w) + \frac{(D_{\text{emb}} + D_1 - D_{s2}) \cdot (\gamma_r - \gamma_w)}{3} \right]$$

$$\sigma_{s3ar} = 1.602 \times 10^3 \cdot \text{psf}$$

Average lateral pressure on side of Wedge 3a, rock portion (at centroid of rock side area)

$$\sigma_{s3as} := K_{hs} \cdot \left[\frac{D_{s2} \cdot (\gamma_s - \gamma_w)}{2} \right]$$

$$\sigma_{s3as} = 601.4 \cdot \text{psf}$$

Average lateral pressure on side of Wedge 3a,
soil portion (at centroid of soil side area)

$$\sigma_{s3bs} := K_{hs} \cdot \left[\frac{D_{s2} \cdot (\gamma_s - \gamma_w)}{3} \right]$$

$$\sigma_{s3bs} = 400.933 \cdot \text{psf}$$

Average lateral pressure on side of Wedge 3b,
soil portion (at centroid of soil side area)

Driving Forces - Wedge 3:

$$F_{d3} := [W_{3ar} \cdot a_{rh} + (W_{3as} + W_{3b}) \cdot a_{rhs}] \cdot \cos(\beta_2) \quad \text{Driving forces acting up-dip along discontinuity set \#2}$$

$$F_{d3} = 2.715 \times 10^4 \cdot \text{kip}$$

Resisting Forces - Wedge 3:

$$\begin{aligned} F_{r3} := & (W'_{3ar} - W_{3ar} \cdot a_{rv} + W'_{3as} - W_{3as} \cdot a_{rvs}) \cdot \cos(\beta_2) \cdot \tan(\phi_{2r}) \dots \\ & + (W_{3ar} \cdot a_{rh} + W_{3as} \cdot a_{rhs}) \cdot \sin(\beta_2) \cdot \tan(\phi_{2r}) \dots \\ & + (W'_{3b} - W_{3b} \cdot a_{rvs}) \cdot \cos(\beta_2) \cdot \tan(\phi_{2s}) + W_{3b} \cdot a_{rhs} \cdot \sin(\beta_2) \cdot \tan(\phi_{2s}) \dots \\ & + (W'_{3ar} - W_{3ar} \cdot a_{rv} + W'_{3as} - W_{3as} \cdot a_{rvs}) \cdot \sin(\beta_2) + (W'_{3b} - W_{3b} \cdot a_{rvs}) \cdot \sin(\beta_2) \dots \\ & + A_{3a} \cdot c_{2r} + A_{3b} \cdot c_{2s} \dots \\ & + 2 \cdot \left[A_{s3ar} \cdot (c_{vr} + \sigma_{s3ar} \cdot \tan(\phi_{vr})) + A_{s3as} \cdot (c_{vs} + \sigma_{s3as} \cdot \tan(\phi_{vs})) \dots \right] \dots \\ & \quad \left[+ A_{s3bs} \cdot (c_{vs} + \sigma_{s3bs} \cdot \tan(\phi_{vs})) \right] \dots \\ & + F_{lat1} \cdot \tan(\phi_{vr.1to3}) \cdot (\sin(\beta_2) + \cos(\beta_2) \tan(\phi_{2r})) \dots \\ & + A_{1to3} \cdot c_{vr.1to3} \cdot (\sin(\beta_2) + \cos(\beta_2) \tan(\phi_{2r})) \end{aligned}$$

$$F_{r3} = 1.003 \times 10^5 \cdot \text{kip}$$

Resisting forces acting down-dip along
discontinuity set #2

Calculate R_{lat3} , the external lateral force along the NI side of Wedge 3 that can be resisted under force equilibrium:

$$\text{Beta} := (\cos(\beta_2) - \sin(\beta_2) \cdot \tan(\phi_{2r}))$$

$$\text{Beta} = 0.952$$

$$\text{Beta}_{eff} := \text{if}(\text{Beta} > 0.01, \text{Beta}, 0.01)$$

$$\text{Beta}_{eff} = 0.952$$

$$R_{lat3} := \frac{F_{r3} - F_{d3}}{(\text{Beta}_{eff})}$$

$$R_{lat3} = 7.687 \times 10^4 \cdot \text{kip}$$

"Beta" and "Beta_{eff}" are used to limit the denominator of the R_{lat3} equation to a minimum of 0.01. This will prevent a negative number if total net resistance is very high - i.e., if β_2 is steep enough and/or ϕ_{2r} is large enough that effectively any magnitude of lateral load R_{lat3} could be supported in the direction of seismic loading. Such a condition could result in negative denominator in the R_{lat3} equation, and hence a negative R_{lat3} (which is inaccurate), if Beta_{eff} were not limited to a minimum small positive value.

R_{lat3} acts as a resisting force in overall stability calculations presented later.

3.4 Wedge 4 - Active Wedge below NI, behind Wedge 2

Wedge 4 represents soil and rock on the active side of Wedge 2, under the NI. The base of this wedge is oriented along discontinuity set #1, passing through depth D_2 on the side of Wedge 2. The lateral force from Wedge 4 acting on Wedge 2 is calculated as F_{lat4} .

This force F_{lat4} will act to reduce the available base sliding resistance provided by Wedge 2.

Wedge 4 Dimensions and Weights

$$B_4 := \frac{D_2}{\tan(\beta_1)} \quad B_4 = 32.835 \cdot \text{ft}$$

See Sketch

$$B_{4a} := \min(B_4, B_{tot} - B_L) \quad B_{4a} = 29 \cdot \text{ft}$$

Widths B_{4a} and B_{4b} represent the portions of width B_4 that are under the NI and outside of the NI active endwall, respectively

$$B_{4b} := \max(0, B_4 - B_{4a}) \quad B_{4b} = 3.835 \cdot \text{ft}$$

$$L_4 := \frac{B_4}{\cos(\beta_1)} \quad L_4 = 49.651 \cdot \text{ft}$$

$$A_4 := L_4 \cdot X \quad A_4 = 1.266 \times 10^4 \cdot \text{ft}^2$$

Area of Wedge 4 along discontinuity set #1

$$A_{s4} := \frac{B_4 \cdot D_2}{2} \quad A_{s4} = 611.438 \cdot \text{ft}^2$$

Side area of Wedge 4

$$W_4 := A_{s4} \cdot X \cdot \gamma_r \quad W_4 = 2.495 \times 10^4 \cdot \text{kip}$$

Total weight of Wedge 4

$$W'_4 := A_{s4} \cdot X \cdot (\gamma_r - \gamma_w)$$

Effective weight of Wedge 4

$$W'_4 = 1.522 \times 10^4 \cdot \text{kip}$$

$$N_{4b} := B_{4b} \cdot X \cdot [D_{s1} \cdot \gamma_s + (D_{emb} - D_{s1}) \cdot \gamma_r + S_s]$$

Additional vertical force from rock, soil and building surcharge on active side of NI, acting over width B_{4b}

$$N_{4b} = 7.549 \times 10^3 \cdot \text{kip}$$

$$\sigma_{s4} := \sigma_{s2} = 2.295 \times 10^3 \cdot \text{psf}$$

Average lateral pressure on side of Wedge 4 (at centroid of rock side area)

Driving Forces - Wedge 4:

$$F_{d4} := (W'_4 - W_4 \cdot a_{rv}) \cdot \sin(\beta_1) + W_4 \cdot a_{rh} \cdot \cos(\beta_1) + N_{4b} \cdot \sin(\beta_1)$$

$$F_{d4} = 1.733 \times 10^4 \cdot \text{kip}$$

Driving forces acting down-dip along discontinuity set #1

Resisting Forces - Wedge 4:

$$F_{r4} := \left[(W'_4 - W_4 \cdot a_{rv}) \cos(\beta_1) - W_4 \cdot a_{rh} \cdot \sin(\beta_1) \right] \cdot \tan(\phi_{1r}) + A_4 \cdot c_{1r} \dots$$

$$+ A_{s4} \cdot 2 \cdot (c_{vr} + \sigma_{s4} \cdot \tan(\phi_{vr})) + N_{4b} \cdot \cos(\beta_1) \cdot \tan(\phi_{1r})$$

$$F_{r4} = 1.343 \times 10^4 \cdot \text{kip}$$

Resisting forces acting up-dip along discontinuity set #1

Calculate F_{lat4} , the lateral force required at the Wedge 2 to Wedge 4 interface for Wedge 4 force equilibrium:

$$F_{lat4_trial} := \frac{F_{d4} - F_{r4}}{(\cos(\beta_1) + \sin(\beta_1) \cdot \tan(\phi_{1r}))}$$

$$F_{lat4_trial} = 2.764 \times 10^3 \cdot \text{kip}$$

$$F_{lat4} := \max(F_{lat4_trial}, 0)$$

If F_{lat4_trial} is negative, no lateral force required for stability - assigns value of 0 to F_{lat4}

$$F_{lat4} = 2.764 \times 10^3 \cdot \text{kip}$$

F_{lat4} acts as a driving force in overall stability calculations presented later

3.5 Wedge 5 - Active Wedge on the Back Side of the NI

Wedge 5 represents soil and rock on the active side of the NI. The total lateral force acting on the active side of the NI (F_{active}) is conservatively assigned as the GREATER of:

- A) Force $F_{lat5.wedge}$: This represents a rock and soil wedge with the bottom defined along discontinuity Set 1, with bottom at the NI subgrade elevation. Surface surcharge load from adjacent structures is included.
- B) Force $F_{lat5.backfill}$: This represents the forces associated with compacted granular backfill adjacent to the nuclear island. Force $F_{lat5.backfill}$ is the sum of forces from static at-rest backfill ($F_{BF.atrest}$), static surcharge load ($F_{surch.atrest}$), dynamic earth pressure ($F_{BF.dynamic}$), and dynamic surcharge load ($F_{surch.dynamic}$). Static forces conservatively assume at-rest soil conditions, corresponding to insignificant displacement of the NI sidewall relative to the backfill. Backfill is conservatively modeled to extend from ground surface to the subgrade elevation, without reduction due to the concrete fill within 6 feet above subgrade.

Force F_{active} will act to as a driving force in calculation of FS_{slide} .

3.5.1 Calculation of force $F_{lat5.wedge}$

Wedge #5 Dimensions and Weights

$B_{5a} := \frac{(D_{emb} - D_{s1})}{\tan(\beta_1)}$	$B_{5a} = 27.771 \cdot ft$	See Sketch
$L_{5a} := \frac{B_{5a}}{\cos(\beta_1)}$	$L_{5a} = 41.994 \cdot ft$	
$B_{5b} := \frac{D_{s1}}{\tan(\beta_1)}$	$B_{5b} = 6.171 \cdot ft$	
$L_{5b} := \frac{B_{5b}}{\cos(\beta_1)}$	$L_{5b} = 9.332 \cdot ft$	
$A_{5a} := L_{5a} \cdot X$	$A_{5a} = 1.071 \times 10^4 \cdot ft^2$	Area of Wedge 5a along discontinuity set #1
$A_{s5ar} := \frac{B_{5a} \cdot (D_{emb} - D_{s1})}{2}$	$A_{s5ar} = 437.393 \cdot ft^2$	Side area of Wedge 5a in rock
$A_{s5as} := B_{5a} \cdot D_{s1}$	$A_{s5as} = 194.397 \cdot ft^2$	Side area of Wedge 5a in soil
$A_{5b} := L_{5b} \cdot X$	$A_{5b} = 2.38 \times 10^3 \cdot ft^2$	Area of Wedge 5b along discontinuity set #1
$A_{s5bs} := \frac{B_{5b} \cdot D_{s1}}{2}$	$A_{s5bs} = 21.6 \cdot ft^2$	Side area of Wedge 5b in soil

File: Case_HAR3_W1.xmcd
Date: 2/5/2009
Page: 14

$$W_{5ar} := A_{s5ar} \cdot X \cdot \gamma_r \quad W_{5ar} = 1.785 \times 10^4 \cdot \text{kip} \quad \text{Total weight of Wedge 5a, rock}$$

$$W_{5as} := A_{s5as} \cdot X \cdot \gamma_s \quad W_{5as} = 6.94 \times 10^3 \cdot \text{kip} \quad \text{Total weight of Wedge 5a, soil}$$

$$W'_{5ar} := A_{s5ar} \cdot X \cdot (\gamma_r - \gamma_w) \quad W'_{5ar} = 1.089 \times 10^4 \cdot \text{kip} \quad \text{Effective weight of Wedge 5a, rock}$$

$$W'_{5as} := A_{s5as} \cdot X \cdot (\gamma_s - \gamma_w) \quad W'_{5as} = 3.847 \times 10^3 \cdot \text{kip} \quad \text{Effective weight of Wedge 5a, soil}$$

$$W_{5b} := A_{s5bs} \cdot X \cdot \gamma_r \quad W_{5b} = 881.266 \cdot \text{kip} \quad \text{Total weight of Wedge 5b}$$

$$W'_{5b} := A_{s5bs} \cdot X \cdot (\gamma_s - \gamma_w) \quad W'_{5b} = 427.414 \cdot \text{kip} \quad \text{Effective weight of Wedge 5b}$$

$$\sigma_{s5ar} := K_{hr} \left[D_{s1} \cdot (\gamma_s - \gamma_w) + \frac{(D_{emb} - D_{s1}) \cdot (\gamma_r - \gamma_w)}{3} \right]$$

$$\sigma_{s5ar} = 784 \cdot \text{psf}$$

Average lateral pressure on side of Wedge 5a, rock portion (at centroid of rock side area)

$$\sigma_{s5as} := K_{hs} \left[\frac{D_{s1}}{2} \cdot (\gamma_s - \gamma_w) \right]$$

$$\sigma_{s5as} = 135.8 \cdot \text{psf}$$

Average lateral pressure on side of Wedge 5a, soil portion (at centroid of soil side area)

$$\sigma_{s5bs} := K_{hs} \left[\frac{D_{s1}}{3} \cdot (\gamma_s - \gamma_w) \right]$$

$$\sigma_{s5bs} = 90.533 \cdot \text{psf}$$

Average lateral pressure on side of Wedge 5b, soil portion (at centroid of soil side area)

Driving Forces - Wedge 5:

$$F_{d5} := \left[(W'_{5ar} + W'_{5as} + W'_{5b}) - a_{rv} \cdot W_{5ar} - a_{rvs} \cdot (W_{5as} + W_{5b}) \right] \cdot \sin(\beta_1) \dots \\ + \left[W_{5ar} \cdot a_{rh} + (W_{5as} + W_{5b}) \cdot a_{rhs} \right] \cdot \cos(\beta_1) \dots \\ + S_s \cdot X \cdot (B_{5a} + B_{5b}) \cdot \sin(\beta_1)$$

$$F_{d5} = 2.268 \times 10^4 \cdot \text{kip}$$

Driving forces acting down-dip along discontinuity set #1.

Resisting Forces - Wedge 5:

$$F_{r5} := \left[\begin{aligned} & (W'_{5ar} - W_{5ar} \cdot a_{rv}) + (W'_{5as} - W_{5as} \cdot a_{rvs}) \cdot \cos(\beta_1) \cdot \tan(\phi_{1r}) \dots \\ & + (-1)(W_{5ar} \cdot a_{rh} + W_{5as} \cdot a_{rhs}) \cdot \sin(\beta_1) \cdot \tan(\phi_{1r}) \dots \\ & + (W'_{5b} - W_{5b} \cdot a_{rvs}) \cdot \cos(\beta_1) \cdot \tan(\phi_{1s}) - W_{5b} \cdot a_{rhs} \cdot \sin(\beta_1) \cdot \tan(\phi_{1s}) \dots \\ & + S_s \cdot X \cdot B_{5a} \cdot \cos(\beta_1) \cdot \tan(\phi_{1r}) + S_s \cdot X \cdot B_{5b} \cdot \cos(\beta_1) \cdot \tan(\phi_{1s}) \dots \\ & + A_{5a} \cdot c_{1r} + A_{5b} \cdot c_{1s} \dots \\ & + 2 \left[\begin{aligned} & A_{s5ar} \cdot (c_{vr} + \sigma_{s5ar} \cdot \tan(\phi_{vr})) + A_{s5as} \cdot (c_{vs} + \sigma_{s5as} \cdot \tan(\phi_{vs})) \dots \\ & + A_{s5bs} \cdot (c_{vs} + \sigma_{s5bs} \cdot \tan(\phi_{vs})) \end{aligned} \right] \end{aligned} \right]$$

$$F_{r5} = 1.485 \times 10^4 \text{ kip}$$

Resisting forces acting up-dip along discontinuity set #1

Calculate F_{lat5} , the lateral force required from the NI sidewall acting on Wedge #5 for static stability:

$$F_{lat5_trial} := \frac{F_{d5} - F_{r5}}{\left[\cos(\beta_1) + \left(\frac{D_{s1}}{D_{emb}} \right) \cdot \sin(\beta_1) \cdot \tan(\phi_{1s}) + \left[\frac{(D_{emb} - D_{s1})}{D_{emb}} \right] \cdot \sin(\beta_1) \cdot \tan(\phi_{1r}) \right]}$$

$$F_{lat5_trial} = 5.789 \times 10^3 \text{ kip}$$

$$F_{lat5.wedge} := \max(F_{lat5_trial}, 0)$$

If F_{lat5_trial} is negative, no lateral force required for stability - assigns value of 0 to F_{lat5}

$$F_{lat5.wedge} = 5.789 \times 10^3 \text{ kip}$$

F_{lat5} acts as a driving force in overall stability calculations presented later

3.5.2 Calculation of force $F_{lat5.backfill}$

$$K_o := 1 - \sin(\phi_{backfill})$$

$$K_o = 0.426$$

At-rest earth pressure coefficient for compacted backfill

$$F_{BF.atrest} := \frac{1}{2} K_o \cdot D_{emb}^2 \cdot (\gamma_{backfill} - \gamma_w) \cdot X$$

$$F_{BF.atrest} = 5.448 \times 10^3 \text{ kip}$$

$$F_{\text{surch.atrest}} := K_o \cdot S_s \cdot D_{\text{emb}} \cdot X$$

$$F_{\text{surch.atrest}} = 7.117 \times 10^3 \cdot \text{kip}$$

$$F_{\text{BF.dynamic}} := a_{\text{rhs}} \cdot (1.04) \cdot \gamma_{\text{backfill}} \cdot D_{\text{emb}}^2 \cdot X$$

$$F_{\text{BF.dynamic}} = 8.585 \times 10^3 \cdot \text{kip}$$

$$F_{\text{surch.dynamic}} := a_{\text{rhs}} \cdot S_s \cdot D_{\text{emb}} \cdot X$$

$$F_{\text{surch.dynamic}} = 2.804 \times 10^3 \cdot \text{kip}$$

$$F_{\text{lat5.backfill}} := F_{\text{BF.atrest}} + F_{\text{surch.atrest}} + F_{\text{BF.dynamic}} + F_{\text{surch.dynamic}}$$

$$F_{\text{lat5.backfill}} = 2.395 \times 10^4 \cdot \text{kip}$$

3.5.3 Calculation of force F_{active}

$$F_{\text{active}} := \max(F_{\text{lat5.wedge}}, F_{\text{lat5.backfill}})$$

$$F_{\text{active}} = 2.395 \times 10^4 \cdot \text{kip}$$

4. Overall Stability Against Sliding

4.1 Wedge Lateral Force Summary:

Driving Forces:

$$F_{\text{lat1}} = 6.232 \times 10^3 \cdot \text{kip}$$

$$F_{\text{lat4}} = 2.764 \times 10^3 \cdot \text{kip}$$

$$F_{\text{active}} = 2.395 \times 10^4 \cdot \text{kip}$$

$$F_{\text{lat.struct}} = 6.063 \times 10^4 \cdot \text{kip}$$

Resisting Forces:

$$R_{\text{lat2}} = 1.066 \times 10^5 \cdot \text{kip}$$

$$R_{\text{lat3}} = 7.687 \times 10^4 \cdot \text{kip}$$

4.2 Net Passive Resistance (R_{passive})

The difference between R_{lat3} and F_{lat1} is the remaining passive force available to resist sliding, R_{passive} .

$$R_{\text{passive}} := R_{\text{lat3}} - F_{\text{lat1}} \quad R_{\text{passive}} = 7.064 \times 10^4 \cdot \text{kip}$$

4.3 Net Base Shear Resistance (R_{base})

The base shear resistance force (denoted R_{base}) is the lesser of the net difference between R_{lat2} and F_{lat4} (denoted R_{lat2net}), or the available sliding along the most critical horizontal interface of the NI basemat subgrade based on ϕ_{geomemb} (denoted R_{geomemb}). This resistance at the NI basemat subgrade is based on the net buoyant structure load acting over the Wedge 2 area, reduced for vertical structure acceleration a_{sv} , and scaled by factor P_2 .

$$R_{\text{geomemb}} := P_2 \cdot (W'_s - C_{\text{asv}} \cdot a_{\text{sv}} \cdot W_s) \tan(\phi_{\text{geomemb}}) \quad R_{\text{geomemb}} = 7.777 \times 10^4 \cdot \text{kip}$$

$$R_{\text{lat2net}} := R_{\text{lat2}} - F_{\text{lat4}} \quad R_{\text{lat2net}} = 1.038 \times 10^5 \cdot \text{kip}$$

$$R_{\text{base}} := \min(R_{\text{lat2net}}, R_{\text{geomemb}}) \quad R_{\text{base}} = 7.777 \times 10^4 \cdot \text{kip}$$

4.4 Factor of Safety Against Sliding (FS_{slide})

The **FS against sliding** (FS_{slide}) is calculated as the ratio of available sliding resistance to lateral driving forces.

$$FS_{\text{slide}} := \frac{R_{\text{passive}} + R_{\text{base}}}{F_{\text{lat.struct}} + F_{\text{active}}} \quad FS_{\text{slide}} = 1.754$$

4.5 Check of potential traction force over width B₁

A traction force ($F_{lat1.traction}$) may develop over width B_1 under seismic loading, caused by the lateral inertial structure load and the basemat interface friction. This force is calculated here, and checked as an additional force to be resisted by R_{lat3} . The value of $F_{lat1.traction}$ is calculated as the fraction P_1 of the total lateral NI inertial load ($F_{lat.struct}$), limited by the available frictional resistance along the critical basemat subgrade interface.

$$F_{lat1.traction} := \min(P_1 \cdot F_{lat.struct}, P_1 \cdot W_s \cdot \tan(\phi_{geomemb}))$$

$$F_{lat1.traction} = 1.546 \times 10^4 \cdot \text{kip}$$

$$R_{lat3.check} := R_{lat3} - F_{lat1} - F_{lat1.traction}$$

$$R_{lat3.check} = 5.518 \times 10^4 \cdot \text{kip}$$

This force will not affect overall sliding resistance FS_{slide} . However, if $R_{lat3.check}$ is less than zero, the bearing capacity should be further evaluated.

4.6 Comparison of actual FS and and required FS_b and FS_s

$$\text{Slide_FS_Text} := \text{if}(FS_s < FS_{slide}, \text{"Acceptable Sliding FS"}, \text{"Sliding FS is not sufficient"})$$

$$\text{Slide_FS_Text} = \text{"Acceptable Sliding FS"}$$

4.7 Summary of Results

$$\text{Results} := \begin{pmatrix} \frac{B_1}{\text{ft}} \\ \frac{R_{\text{passive}}}{\text{kip}} \\ \frac{R_{\text{base}}}{\text{kip}} \\ \frac{F_{\text{lat.struct}}}{\text{kip}} \\ \frac{F_{\text{active}}}{\text{kip}} \\ FS_{\text{slide}} \\ \frac{R_{\text{lat3.check}}}{\text{kip}} \end{pmatrix}$$

$$\text{Results} = \begin{pmatrix} 15 \\ 7.064 \times 10^4 \\ 7.777 \times 10^4 \\ 6.063 \times 10^4 \\ 2.395 \times 10^4 \\ 1.754 \\ 5.518 \times 10^4 \end{pmatrix}$$

Parameter Values:

- B_1 (ft)
- R_{passive} (kip)
- R_{base} (kip)
- $F_{\text{lat.struct}}$ (kip)
- F_{active} (kip)
- FS_{slide} (--)
- $R_{\text{lat3.check}}$ (kip)

ATTACHMENT B

Progress Energy HAR COLA

Bearing Resistance Along Oriented Discontinuities Case HAR3-BC-W1

Engineer: MDG
Project: PEC COLA

1. Purpose and Scope:

The ultimate bearing capacity (σ_{ult}) under the Plant West side of the nuclear island is calculated based on the force equilibrium of two rock and soil wedges; Wedge 1 under the NI and Wedge 3 on the passive side of the NI. A trial peak dynamic load (σ_{peak}) is first assigned. The corresponding total vertical structure load acting over Wedge 1 is calculated based on σ_{peak} , the arc segment area of the NI (circular shield building) within distance B_1 , and the ratio P_{1b} of σ_{peak} to the overall bearing pressure over Wedge 1 as a function of distance B_1 .

The trial σ_{peak} is varied until wedge force equilibrium is satisfied between Wedge 1 and Wedge 3 for the trial distance B_1 . The corresponding σ_{peak} at equilibrium is defined as σ_{ult} . The force equilibrium equations for Wedge 1 and 3 are similar to those used for the sliding stability evaluations, except that an additional lateral driving force due to the seismic inertia of the NI is applied directly to Wedge 1. NI sliding stability is not directly evaluated in this calculation.

The FS_b against bearing load is calculated as the ratio of σ_{ult} to the peak dynamic bearing demand (σ_{demand}) of 35 ksf.

2. Input Parameters:

General Geometry and Input Parameters

$$R_s := 72.6\text{ft}$$

Radius of shield building

$$B_1 := 30\text{ft}$$

Width of trial wedge. Valid for $B_1 \sim < 55$ ft

$$\sigma_{peak} := 131\text{ksf}$$

TRIAL peak dynamic NI bearing pressure for wedge force equilibrium (Estimate of σ_{ult})

$$\theta := \arccos\left[\frac{(R_s - B_1)}{R_s}\right]$$

$$\theta = 54.071\text{.deg}$$

Angle in horizontal plane

$$X_b := 2 \cdot R_s \cdot \sin(\theta)$$

$$X_b = 117.576\text{.ft}$$

Width of shield building within distance B_1 from passive edge.

Filename: Case_HAR3_BC_W1.xmcd
Date: 2/19/2009.
Page: 1

$$A_{load} := \pi \cdot R_s^2 \cdot \left(2 \cdot \frac{\theta}{360 \text{deg}} \right) - \frac{1}{2} \cdot (R_s - B_1) \cdot X_b$$

Area of shield building within distance B_1 from passive edge

$$A_{load} = 2.47 \times 10^3 \cdot \text{ft}^2$$

$$\text{Elev}_{site} := 260 \text{ft}$$

Site Grade Elevation (ft NGVD 29)

$$\text{Elev}_{basemat} := 221.5 \text{ft}$$

Bottom of NI Basemat Elevation (ft NGVD 29)

$$D_{emb} := \text{Elev}_{site} - \text{Elev}_{basemat}$$

Depth of NI embedment

$$D_{emb} = 38.5 \text{ft}$$

$$H_{conc} := 6 \text{ft}$$

Height of concrete sidewall fill above the bottom of basemat (in contact with rock)

$$D_{s2} := 31 \text{ft}$$

Depth to sound rock below site grade on Passive wedge side

* NOTE: depth to GW is conservatively assigned as zero (at site grade) for all calculations

Discontinuity Set #1 Parameters

$$\beta_1 := 48.6 \text{deg}$$

Dip of discontinuity set #1 from horizontal

$$\phi_{1r} := 45 \text{deg}$$

Friction angle of discont. set #1 in rock

$$c_{1r} := 0 \text{psf}$$

Cohesion of discont. set #1 in rock

$$\phi_{1s} := 30 \text{deg}$$

Friction angle of discont. set #1 in soil

$$c_{1s} := 0 \text{psf}$$

Cohesion of discont. set #1 in soil

Filename: Case_HAR3_BC_W1.xmcd
Date: 2/19/2009.
Page: 2

Discontinuity Set #2 Parameters

$$\beta_2 := 17.8\text{deg}$$

Dip of discontinuity set #2 from horizontal

$$\phi_{2r} := 0\text{deg}$$

Friction angle of discont. set #2 in rock

$$c_{2r.\text{above.NI}} := 1500\text{psf}$$

Cohesion of discont. Set #2 in rock above the NI subgrade elevation

$$c_{2r.\text{below.NI}} := 2200\text{psf}$$

Cohesion of discont. Set #2 in rock below the NI subgrade elevation

$$\phi_{2s} := 0\text{deg}$$

Friction angle of discont. set #2 in soil

$$c_{2s} := 1500\text{psf}$$

Cohesion of discont. set #2 in soil

$$D_1 := B_1 \cdot \tan(\beta_1) \quad D_1 = 34.028 \cdot \text{ft}$$

Depth of Wedge 1 below NI

$$c_{2r} := \frac{[(D_{\text{emb}} - D_{s2}) \cdot c_{2r.\text{above.NI}} + D_1 \cdot c_{2r.\text{below.NI}}]}{[D_{\text{emb}} + (D_1 - D_{s2})]}$$

Average cohesion of discont. Set #2 in rock

$$c_{2r} = 2.074 \times 10^3 \cdot \text{psf}$$

Vertical Discontinuity Parameters

$$\phi_{vr} := 45\text{deg}$$

Friction angle of vertical discont. in rock

$$c_{vr} := 0\text{psf}$$

Cohesion of vertical discont. in rock

$$\phi_{vs} := 30\text{deg}$$

Friction angle of vertical discont. in soil

$$c_{vs} := 0\text{psf}$$

Cohesion of vertical discont. in soil

$$\phi_{vr.1\text{to}3} := 0\text{deg}$$

Friction angle of vertical joint between Wedges 1 and 3

$$c_{vr.1\text{to}3} := 0\text{psf}$$

Cohesion of vertical joint between Wedges 1 and 3

$$K_{hs} := 0.5$$

Lateral earth pressure coefficients in soil and rock along vertical discontinuities in direction perpendicular to section

$$K_{hr} := 0.5$$

Other Parameters:

$$\phi_{\text{geomemb}} := 28.8\text{deg}$$

Controlling interface friction angle at the waterproofing geomembrane

Filename: Case_HAR3_BC_W1.xmcd
Date: 2/19/2009.
Page: 3

Load and Weight Parameters

$W_s := 286387\text{kip}$ Total weight of NI Structure
 $W_b := 76003\text{kip}$ Buoyant force acting on NI
 $W'_s := W_s - W_b$ Effective weight of NI Structure
 $W'_s = 2.104 \times 10^5 \cdot \text{kip}$

Relationship Between Distance B_1 and Peak Bearing Pressure Ratio P_{1b}

Each value in array $P_{1b\text{west}}$ is the ratio of the average applied foundation pressure to σ_{peak} within the corresponding NI foundation dimension B_1 (represented by array B_{westb}). This relationship is based on the shape of the dynamic load profile presented in Figure 2.4-2 of WEC Report APP-GW-GLR-044, R0, scaled by the the areas of NI foundation under various intervals of B_1 .

$B_{\text{westb}} :=$	ft	$P_{1b\text{west}} :=$
0		0.90
3		0.92
6		0.96
8		0.96
10		0.95
15		0.89
20		0.84
25		0.78
30		0.74
35		0.70
40		0.67
45		0.64
50		0.61
55		0.59
60		0.57
65		0.55
70		0.53
75		0.52

$P_{1b} := \text{interp}(B_{\text{westb}}, P_{1b\text{west}}, B_1)$

$P_{1b} = 0.74$

P_{1b} is the ratio of the average applied foundation pressure to σ_{peak} within the NI foundation dimension B_1 .

$\sigma_{\text{struct}} := \sigma_{\text{peak}} \cdot P_{1b}$ $\sigma_{\text{struct}} = 96.94 \cdot \text{ksf}$ Average applied bearing pressure over the NI foundation within dimension B_1

$P_{\text{struct}} := A_{\text{load}} \cdot \sigma_{\text{struct}}$ Dynamic NI bearing load applied over Wedge 1

$$P_{\text{struct}} = 2.394 \times 10^5 \cdot \text{kip}$$

$\sigma_{\text{demand}} := 35 \text{ksf}$ Peak dynamic bearing demand - AP1000 site parameter

A lateral traction force ($F_{\text{lat1.traction}}$) may develop at the top of Wedge 1 under seismic loading due to friction between the NI and the subgrade. This is considered as an additional lateral driving force over Wedge 1. The value of $F_{\text{lat1.traction}}$ is calculated as the total NI sliding load ($F_{\text{lat.struct}}$) multiplied by the ratio P_{lat} .

$F_{\text{lat.struct}} := 60634 \text{kip}$ Lateral seismic inertial structure load

$P_{\text{lat}} := \frac{P_{\text{struct}}}{W_s}$ $P_{\text{lat}} = 0.836$ Fraction of total NI structure weight applied over Wedge 1.

$F_{\text{lat1.traction}} := P_{\text{lat}} \cdot F_{\text{lat.struct}}$

$$F_{\text{lat1.traction}} = 5.069 \times 10^4 \cdot \text{kip}$$

Other Load and Weight Parameters

$\gamma_s := 140 \text{pcf}$ Unit weight of soil (total)

$\gamma_r := 160 \text{pcf}$ Unit weight of rock (total)

$\gamma_w := 62.4 \text{pcf}$ Unit weight of water

Accelerations due to Seismic Loading (fraction of g)

Note: Positive direction is driving (horizontal) or up (vertical)

$a_{rh} := 0.14$	Rock mass acceleration near NI base - horizontal
$a_{rv} := 0.11$	Rock mass acceleration near NI base - vertical (positive is up)
$a_{rhs} := 1.2 \cdot a_{rh} = 0.168$	Soil and weathered rock mass acceleration between site grade and top of sound rock - Horizontal
$a_{rvs} := 1.2 \cdot a_{rv} = 0.132$	Soil and weathered rock mass acceleration between site grade and top of sound rock - vertical (positive is up)

3. Wedge Calculations:

3.1 Wedge 1 - Below NI Width B_1

Wedge #1 represents rock below the NI between the passive edge of the NI and a trial discontinuity that daylight at the NI subgrade a distance B_1 from the edge. The external force F_{lat1} required to act on the passive side of the wedge, for force equilibrium, is calculated.

Wedge 1 Dimensions and Weights

$L_1 := \frac{B_1}{\cos(\beta_1)}$	$L_1 = 45.364 \cdot \text{ft}$	Length of Wedge 1 along discontinuity set #1
$A_1 := L_1 \cdot X_b$	$A_1 = 5.334 \times 10^3 \cdot \text{ft}^2$	Area of Wedge 1 along discontinuity Set #1
$A_{s1} := \frac{B_1 \cdot D_1}{2}$	$A_{s1} = 510.425 \cdot \text{ft}^2$	Side Area of Wedge 1 (parallel to section)
$A_{1to3} := D_1 \cdot X_b$	$A_{1to3} = 371.695 \cdot \text{m}^2$	Area of interface between Wedge 1 and 3
$W_1 := A_{s1} \cdot X_b \cdot \gamma_r$	$W_1 = 9.602 \times 10^3 \cdot \text{kip}$	Total Weight of Wedge 1 Rock
$W'_1 := A_{s1} \cdot X_b \cdot (\gamma_r - \gamma_w)$	$W'_1 = 5.857 \times 10^3 \cdot \text{kip}$	Effective Weight of Wedge 1 Rock

Filename: Case_HAR3_BC_W1.xmcd
Date: 2/19/2009.
Page: 6

$$\sigma_{s1} := K_{hr} \left[D_{s2} \cdot (\gamma_s - \gamma_w) + \left(D_{emb} + \frac{D_1}{3} - D_{s2} \right) \cdot (\gamma_r - \gamma_w) \right]$$

$$\sigma_{s1} = 2.122 \times 10^3 \text{ psf}$$

Average lateral pressure on side of Wedge 1
(at centroid of side area)

Driving Forces - Wedge 1:

$$F_{d1} := (W'_1 - W_1 \cdot a_{rv}) \cdot \sin(\beta_1) + W_1 \cdot a_{rh} \cdot \cos(\beta_1) + P_{struct} \cdot \sin(\beta_1) \dots \\ + F_{lat1} \cdot \text{traction} \cdot \cos(\beta_1)$$

$$F_{d1} = 2.176 \times 10^5 \cdot \text{kip}$$

Driving forces acting down-dip along
discontinuity set #1. Note that a_{svb} is
negative for compressive (down), hence
($1 - a_{svb}$) is greater than 1 if compressive.

Resisting Forces - Wedge 1:

$$F_{r1} := \left[(W'_1 - W_1 \cdot a_{rv}) \cos(\beta_1) - W_1 \cdot a_{rh} \cdot \sin(\beta_1) \right] \cdot \tan(\phi_{1r}) + A_1 \cdot c_{1r} \dots = 5.544 \times 10^8 \text{ N} \\ + A_{s1} \cdot 2 \cdot (c_{vr} + \sigma_{s1} \cdot \tan(\phi_{vr})) + P_{struct} \cos(\beta_1) \cdot \tan(\phi_{1r}) \dots \\ + A_{1to3} \cdot c_{vr.1to3} \cdot (\sin(\beta_1) - \cos(\beta_1) \cdot \tan(\phi_{1r})) \dots \\ + (-1) F_{lat1} \cdot \text{traction} \cdot \sin(\beta_1) \tan(\phi_{1r})$$

$$F_{r1} = 1.246 \times 10^5 \cdot \text{kip}$$

Resisting forces acting up-dip along
discontinuity set #1

Calculate F_{Lat1} , the lateral force required along the passive side of Wedge 1 for static stability:

$$F_{lat1} := \frac{F_{d1} - F_{r1}}{(\cos(\beta_1) + \sin(\beta_1) \cdot \tan(\phi_{1r}) + \tan(\phi_{vr.1to3}) \cdot \sin(\beta_1) - \tan(\phi_{vr.1to3}) \cos(\beta_1) \tan(\phi_{1r}))}$$

$$F_{lat1} = 6.586 \times 10^4 \cdot \text{kip}$$

F_{lat1} acts as a driving force in overall stability
calculations presented later

3.3 Wedge 3 - Passive Wedge

Wedge #3 represents soil and rock on the passive side of the NI to a depth of D_1 below the NI. The base of this wedge is oriented along discontinuity set # 2, passing through depth D_1 on the passive side of the NI.

The total lateral resistance that can be provided by this wedge is calculated as R_{lat3} . This force is available to resist F_{lat1} and to provide additional passive resistance to NI sliding forces.

Filename: Case_HAR3_BC_W1.xmcd
Date: 2/19/2009.
Page: 7

Wedge #3 Dimensions and Weights

$$B_{3a} := \frac{(D_{emb} + D_1 - D_{s2})}{\tan(\beta_2)} \quad B_{3a} = 129.346 \cdot \text{ft} \quad \text{See Sketch}$$

$$L_{3a} := \frac{B_{3a}}{\cos(\beta_2)} \quad L_{3a} = 135.849 \cdot \text{ft}$$

$$B_{3b} := \frac{D_{s2}}{\tan(\beta_2)} \quad B_{3b} = 96.554 \cdot \text{ft}$$

$$L_{3b} := \frac{B_{3b}}{\cos(\beta_2)} \quad L_{3b} = 101.408 \cdot \text{ft}$$

$$A_{3a} := L_{3a} \cdot X_b \quad A_{3a} = 1.597 \times 10^4 \cdot \text{ft}^2 \quad \text{Area of Wedge 3a along discontinuity set \#2}$$

$$A_{s3ar} := \frac{[B_{3a}(D_{emb} + D_1 - D_{s2})]}{2} \quad \text{Side area of Wedge 3a in rock}$$

$$A_{s3ar} = 2.686 \times 10^3 \cdot \text{ft}^2$$

$$A_{s3as} := B_{3a} \cdot D_{s2} \quad A_{s3as} = 4.01 \times 10^3 \cdot \text{ft}^2 \quad \text{Side area of Wedge 3a in soil}$$

$$A_{3b} := L_{3b} \cdot X_b \quad A_{3b} = 1.192 \times 10^4 \cdot \text{ft}^2 \quad \text{Area of Wedge 3b along discontinuity set \#2}$$

$$A_{s3bs} := \frac{B_{3b} \cdot D_{s2}}{2} \quad A_{s3bs} = 1.497 \times 10^3 \cdot \text{ft}^2 \quad \text{Side area of Wedge 3b in soil}$$

$$W_{3ar} := A_{s3ar} \cdot X_b \cdot \gamma_r \quad W_{3ar} = 5.052 \times 10^4 \cdot \text{kip} \quad \text{Total weight of Wedge 3a, rock}$$

$$W_{3as} := A_{s3as} \cdot X_b \cdot \gamma_s \quad W_{3as} = 6.6 \times 10^4 \cdot \text{kip} \quad \text{Total weight of Wedge 3a, soil}$$

$$W'_{3ar} := A_{s3ar} \cdot X_b \cdot (\gamma_r - \gamma_w) \quad W'_{3ar} = 3.082 \times 10^4 \cdot \text{kip} \quad \text{Effective weight of Wedge 3a, rock}$$

$$W'_{3as} := A_{s3as} \cdot X_b \cdot (\gamma_s - \gamma_w) \quad W'_{3as} = 3.658 \times 10^4 \cdot \text{kip} \quad \text{Effective weight of Wedge 3a, soil}$$

$$W_{3b} := A_{s3bs} \cdot X_b \cdot \gamma_s \quad W_{3b} = 2.463 \times 10^4 \cdot \text{kip} \quad \text{Total weight of Wedge 3b}$$

Filename: Case_HAR3_BC_W1.xmcd
Date: 2/19/2009.
Page: 8

$$W'_{3b} := A_{s3bs} \cdot X_b \cdot (\gamma_s - \gamma_w) \quad W'_{3b} = 1.365 \times 10^4 \cdot \text{kip} \quad \text{Effective weight of Wedge 3b}$$

$$\sigma_{s3ar} := K_{hr} \cdot \left[D_{s2} \cdot (\gamma_s - \gamma_w) + \frac{(D_{emb} + D_1 - D_{s2}) \cdot (\gamma_r - \gamma_w)}{3} \right]$$

$$\sigma_{s3ar} = 1.878 \times 10^3 \cdot \text{psf} \quad \text{Average lateral pressure on side of Wedge 3a, rock portion (at centroid of rock side area)}$$

$$\sigma_{s3as} := K_{hs} \cdot \left[\frac{D_{s2} \cdot (\gamma_s - \gamma_w)}{2} \right]$$

$$\sigma_{s3as} = 601.4 \cdot \text{psf} \quad \text{Average lateral pressure on side of Wedge 3a, soil portion (at centroid of soil side area)}$$

$$\sigma_{s3bs} := K_{hs} \cdot \left[\frac{D_{s2} \cdot (\gamma_s - \gamma_w)}{3} \right]$$

$$\sigma_{s3bs} = 400.933 \cdot \text{psf} \quad \text{Average lateral pressure on side of Wedge 3b, soil portion (at centroid of soil side area)}$$

Driving Forces - Wedge #3:

$$F_{d3} := [W_{3ar} \cdot a_{rh} + (W_{3as} + W_{3b}) \cdot a_{rhs}] \cdot \cos(\beta_2)$$

$$F_{d3} = 2.123 \times 10^4 \cdot \text{kip}$$

Resisting Forces - Wedge #3:

$$\begin{aligned} F_{r3} := & (W'_{3ar} - W_{3ar} \cdot a_{rv} + W'_{3as} - W_{3as} \cdot a_{rvs}) \cdot \cos(\beta_2) \cdot \tan(\phi_{2r}) \dots \\ & + (W_{3ar} \cdot a_{rh} + W_{3as} \cdot a_{rhs}) \cdot \sin(\beta_2) \cdot \tan(\phi_{2r}) \dots \\ & + (W'_{3b} - W_{3b} \cdot a_{rvs}) \cdot \cos(\beta_2) \cdot \tan(\phi_{2s}) + W_{3b} \cdot a_{rhs} \cdot \sin(\beta_2) \cdot \tan(\phi_{2s}) \dots \\ & + (W'_{3ar} - W_{3ar} \cdot a_{rv} + W'_{3as} - W_{3as} \cdot a_{rvs}) \cdot \sin(\beta_2) + (W'_{3b} - W_{3b} \cdot a_{rvs}) \cdot \sin(\beta_2) \dots \\ & + A_{3a} \cdot c_{2r} + A_{3b} \cdot c_{2s} \dots \\ & + 2 \cdot \left[A_{s3ar} \cdot (c_{vr} + \sigma_{s3ar} \cdot \tan(\phi_{vr})) + A_{s3as} \cdot (c_{vs} + \sigma_{s3as} \cdot \tan(\phi_{vs})) \dots \right] \dots \\ & + A_{1to3} \cdot \tan(\phi_{vr,1to3}) \cdot (\sin(\beta_2) + \cos(\beta_2) \cdot \tan(\phi_{2r})) \dots \\ & + A_{1to3} \cdot c_{vr,1to3} \cdot (\sin(\beta_2) + \cos(\beta_2) \cdot \tan(\phi_{2r})) \end{aligned}$$

$$F_{r3} = 8.399 \times 10^4 \cdot \text{kip}$$

Filename: Case_HAR3_BC_W1.xmcd
Date: 2/19/2009.
Page: 9

Calculate R_{lat3} , the external lateral force along the NI side of Wedge 3 that can be resisted under force equilibrium:

$$\text{Beta} := (\cos(\beta_2) - \sin(\beta_2) \cdot \tan(\phi_{2r}))$$

$$\text{Beta} = 0.952$$

$$\text{Beta}_{\text{eff}} := \text{if}(\text{Beta} > 0.01, \text{Beta}, 0.01)$$

$$\text{Beta}_{\text{eff}} = 0.952$$

Limit the denominator of the R_{lat3} equation to a minimum of 0.01 (prevent negative number if total net resistance is very high)

$$R_{lat3} := \frac{F_{r3} - F_{d3}}{(\text{Beta}_{\text{eff}})}$$

$$R_{lat3} = 6.592 \times 10^4 \cdot \text{kip}$$

R_{lat3} acts as a resisting force in overall stability calculations presented later.

4. Overall Stability Against Sliding and Bearing Failure

4.1 Wedge Lateral Force Summary:

Driving Forces:

$$F_{lat1} = 6.586 \times 10^4 \cdot \text{kip}$$

Resisting Forces:

$$R_{lat3} = 6.592 \times 10^4 \cdot \text{kip}$$

The above forces are based on a trial σ_{peak} of:

$$\sigma_{\text{peak}} = 131 \cdot \text{ksf}$$

4.2 Net Resistance (R_{net})

For the above trial σ_{peak} , the difference between R_{lat3} and F_{lat1} is the net resistive force against bearing loads. If R_{net} is positive, the actual σ_{ult} is greater than σ_{peak} . If R_{net} is negative, the actual σ_{ult} is less than σ_{peak} .

To calculate the σ_{peak} at equilibrium for distance B_1 , iterate σ_{peak} until R_{net} is approximately zero (variance ratio less than or equal to 0.02). FS_b is then calculated as the ratio of σ_{peak} (estimate of σ_{ult}) to σ_{demand} .

$$R_{net} := R_{lat3} - F_{lat1} \quad R_{net} = 52.557 \cdot \text{kip}$$

$$\text{Variance} := \frac{R_{net}}{F_{lat1}} \quad \text{Variance} = 7.98 \times 10^{-4}$$

$$FS_b := \frac{\sigma_{peak}}{\sigma_{demand}} \quad FS_b = 3.743$$

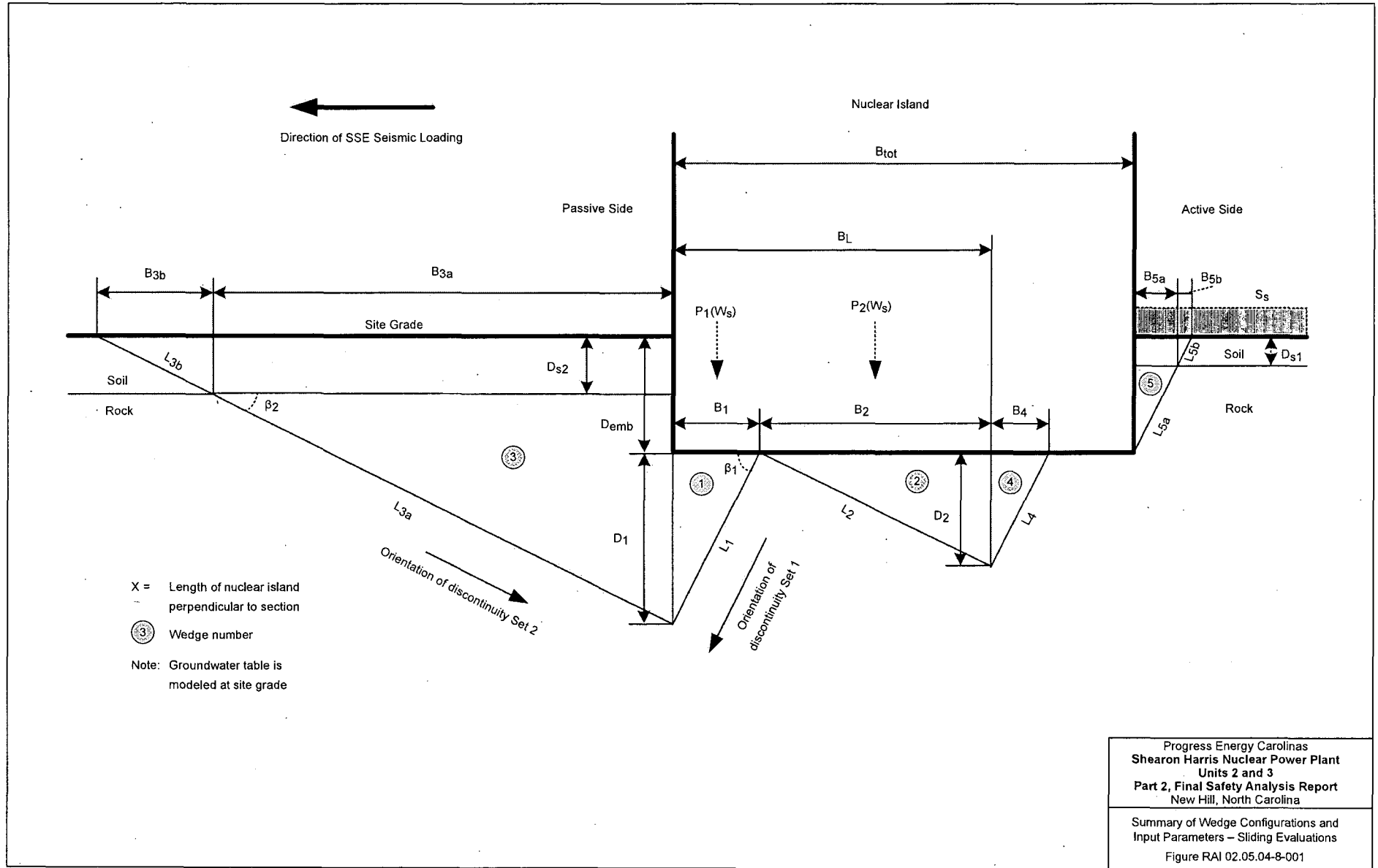
4.3 Summary of Results

$$\text{Results} := \begin{pmatrix} \frac{B_1}{\text{ft}} \\ \frac{\sigma_{peak}}{\text{ksf}} \\ FS_b \\ \frac{F_{lat1}}{\text{kip}} \\ \frac{R_{lat3}}{\text{kip}} \\ \frac{R_{net}}{\text{kip}} \\ \text{Variance} \end{pmatrix}$$

$$\text{Results} = \begin{pmatrix} 30 \\ 131 \\ 3.743 \\ 6.586 \times 10^4 \\ 6.592 \times 10^4 \\ 52.557 \\ 7.98 \times 10^{-4} \end{pmatrix}$$

Parameter Values:

B_1 (ft)
 σ_{peak} (ksf)
 FS_b (kip)
 F_{lat1} (kip)
 R_{lat3} (kip)
 R_{net} (kip)
 Variance (fract)



X = Length of nuclear island perpendicular to section

③ Wedge number

Note: Groundwater table is modeled at site grade

Progress Energy Carolinas
 Shearon Harris Nuclear Power Plant
 Units 2 and 3
 Part 2, Final Safety Analysis Report
 New Hill, North Carolina
 Summary of Wedge Configurations and
 Input Parameters - Sliding Evaluations
 Figure RAI 02.05.04-8-001

Shearon Harris Nuclear Power Plant Units 2 and 3
COL Application
Part 2, Final Safety Analysis Report

Table RAI 02.05.04-8-001
Results of Sliding Stability Evaluations

Case ID	Plant Direction of Seismic Loading	Discontinuity Set 1 Strength Parameters			Discontinuity Set 2 Strength Parameters			Depth to Sound Rock (below site grade)		Adjacent Building Surcharge S_s (psf)	Critical B_1 (ft)	Net Passive Resistance $R_{passive}$ (kips x 10^3)	Net Base Sliding Resistance R_{base} (kips x 10^3)	Inertial Sliding Force $F_{instruct}$ (kips x 10^3)	Net Active Force F_{active} (kips x 10^3)	Resulting FS_{slide}	Net Passive Force Required for $FS_{slide} = 1.1$	
		β_1	ϕ_{1r}	c_{1r}	β_2	ϕ_{2r}	c_{2r}	Active Side D_{s1} (ft)	Passive Side D_{s2} (ft)								Required Passive Force (kips x 10^3)	Percent of $R_{passive}$ (%)
		(deg)	(deg)	(psf)	(deg)	(deg)	(psf)	(ft)	(ft)									
HAR 2																		
HAR2-N1	North	8	0	1500	45.6	45	0	8	11	520	0	946.0	104.4	50.3	8.3	17.9	0.0	0%
HAR2-N2	North	8	0	1500	45.6	45	0	8	11	520	0	946.0	104.4	50.3	8.3	17.9	0.0	0%
HAR2-E1	East	3.9	0	1500	63.4	45	0	15	6	0	0	1073.0	104.4	60.6	14.0	15.8	0.0	0%
HAR2-E2	East	3.9	0	1500	63.4	45	0	15	6	0	0	1073.0	104.4	60.6	14.0	15.8	0.0	0%
HAR2-S1	South	45.6	45	0	8	0	1500	11	8	1700	0	49.4	76.0	50.3	11.7	2.03	0.0	0%
HAR2-S2	South	45.6	45	0	8	0	1500	11	8	1700	0	49.4	76.0	50.3	11.7	2.03	0.0	0%
HAR2-W1	West	63.4	45	0	3.9	0	1500	6	15	1700	0	175.6	62.8	60.6	24.0	2.82	30.2	17%
HAR2-W2	West	63.4	45	0	3.9	0	1500	6	15	1700	0	175.6	62.8	60.6	24.0	2.82	30.2	17%
HAR 3																		
HAR3-N1	North	15.8	0	1500	54.5	45	0	27	17	520	0	652.5	104.4	50.3	8.3	12.9	0.0	0%
HAR3-N2	North	15.8	0	1500	54.5	45	0	27	17	520	0	652.5	104.4	50.3	8.3	12.9	0.0	0%
HAR3-E1	East	17.8	0	1500	48.6	45	0	31	7	0	0	1811.0	104.4	60.6	14.0	25.7	0.0	0%
HAR3-E2	East	17.8	0	1500	48.6	45	0	31	7	0	0	1811.0	104.4	60.6	14.0	25.7	0.0	0%
HAR3-S1	South	54.5	45	0	15.8	0	1500	17	27	1700	15	40.5	86.6	50.3	11.7	2.05	0.0	0%
HAR3-S2	South	54.5	45	0	15.8	0	1500	17	27	1700	0	27.2	104.4	50.3	11.7	2.13	0.0	0%
HAR3-W1	West	48.6	45	0	17.8	0	1500	7	31	1700	15	70.6	77.8	60.6	24.0	1.75	15.3	22%
HAR3-W2	West	48.6	45	0	17.8	0	1500	7	31	1700	0	49.6	104.4	60.6	24.0	1.82	0.0	0%

**Shearon Harris Nuclear Power Plant Units 2 and 3
COL Application
Part 10, License Conditions and ITAAC**

**Table 3.8-3
Concrete Fill Inspections, Tests, Analyses, and Acceptance Criteria**

Design Commitment	Inspections, Tests, Analyses	Acceptance Criteria
Concrete fill will be installed between the NI basemat and adjacent rock excavation, as described in FSAR Subsections 2.5.4.5.3, 2.5.4.10.2, and Table 2.5.4-212.	Construction verification testing and inspection of the concrete fill will be performed to demonstrate that the design commitment has been satisfied.	A report exists which verifies that concrete fill has been installed between the NI basemat and adjacent rock excavation sidewalls, reconciles deviations during construction, and concludes that the as-built concrete fill conforms to the approved design and will sufficiently transfer the required passive resistance to the adjacent rock to prevent sliding as described in FSAR Subsection 2.5.4.10.2.